

Aus der Klinik für Neurologie mit experimenteller Neurologie
der Medizinischen Fakultät Charité – Universitätsmedizin Berlin

DISSERTATION

**Eslicarbazepine acetate effects in a model of *KCNQ2*-
related epilepsy**

–

**Wirkungen von Eslicarbazepinacetat in einem Modell
der *KCNQ2*-bedingten Epilepsie**

zur Erlangung des akademischen Grades
Doctor of Philosophy (PhD)

vorgelegt der Medizinischen Fakultät
Charité – Universitätsmedizin Berlin

Von

Laura Monni

aus Portogruaro, Venedig, Italien

Datum der Promotion: 25.06.2023

Table of contents

Table of contents	3
1. List of Figures	5
2. List of abbreviations	6
3. Abstract	7
4. Zusammenfassung (Abstract in German)	8
5. Introduction	10
5.1. The <i>KCNQ2</i> -related epilepsy syndrome	10
5.2. An animal model to study <i>KCNQ2</i> -related self-limited epilepsy	12
5.3. Eslicarbazepine acetate as a novel ASM to treat childhood onset epilepsies.....	12
5.4. <i>In vitro</i> physiological hippocampal oscillations as biomarker of cognitive function.....	14
5.5. Evaluation of antiseizure efficacy via <i>in vitro</i> and <i>in vivo</i> acute seizure models.....	15
5.6. Hypothesis and aims of the PhD thesis project.....	16
6. Materials and Methods	17
6.1. Animals.....	17
6.2. Chemicals.....	17
6.3. Mouse hippocampal acute slice preparation.....	18
6.4. Electrophysiology.....	18
6.4.1 Physiological neuronal activity	19
6.4.2 Pathological seizure-like events.....	20
6.4.3 Input/Output relationship and fEPSP/PS coupling	21
6.5. <i>In vivo</i> 6 Hz psychomotor seizure model	22
6.5.1 Staircase test.....	22
6.5.2 ESL antiseizure efficacy test.....	23
6.5.3 Rotarod test.....	24
6.6. Pharmacokinetic analysis of S-Lic	24
6.7. Data processing.....	25
6.8. Statistical analysis	26
7. Results	27
7.1. S-Lic effects on <i>in vitro</i> physiological hippocampal oscillations	27
7.2. S-Lic does not affect input/output behavior and intrinsic excitability in CA1	30
7.3. S-Lic effects on <i>in vitro</i> pathological neuronal activity.....	31
7.4. Seizure threshold and ESL antiseizure efficacy in the 6 Hz psychomotor seizure model <i>in vivo</i>	31
7.5. S-Lic concentration positively correlates with its antiseizure efficacy both <i>in vivo</i> and <i>in vitro</i>	34
8. Discussion	35
9. Conclusion	40

10. References	41
11. Statutory declaration	50
12. Affidavit-Declarations of own contributions to the top-journal for a PhD degree	51
13. Print copy of the selected publication	53
14. Curriculum Vitae.....	73
15. Complete list of own publications.....	75
16. Acknowledgments.....	76

1. List of Figures

<u>Figure 1</u> : <i>In vivo</i> experimental protocol.....	24
<u>Figure 2</u> : Concentration-dependent effects of S-Lic on <i>in vitro</i> sharp wave-ripple complexes	28
<u>Figure 3</u> : Effects of S-Lic on gamma oscillations <i>in vitro</i>	29
<u>Figure 4</u> : S-Lic does not affect input / output properties in the CA1 region <i>in vitro</i>	30
<u>Figure 5</u> : Seizure probability analysis in male and female <i>Kcnq2^{+/+}</i> and <i>Kcnq2^{+/-}</i> animals.....	32
<u>Figure 6</u> : S-Lic and ESL antiseizure efficacy <i>in vitro</i> and <i>in vivo</i>	33

2. List of abbreviations

4-AP	4-aminopyridine
aCSF	artificial cerebrospinal fluid
ASM	antiseizure medication
CA1-3	cornu ammonis hippocampal regions 1 and 3
ESL	eslicarbazepine acetate
fEPSP	field excitatory postsynaptic potential
KA	kainic acid (kainate)
KCNQ	potassium channel, voltage-gated, KQT-like subfamily
LFP	local field potential
S-Lic	eslicarbazepine or S-Licarbazepine (active metabolite)
SLE	seizure-like event
SPW-R	sharp-wave ripple
PS	population spike

3. Abstract

KCNQ2-related epilepsies encompass a spectrum of rare childhood epilepsies caused by mutations of the gene encoding for the K_v7.2 subunit of non-inactivating potassium channels. *KCNQ2*-related diseases can be differentiated into two main forms: the benign autosomal dominant neonatal self-limited epilepsy, mainly caused by *KCNQ2* haploinsufficiency, and the severe encephalopathy phenotype caused by missense variants of the *KCNQ2* gene. Most heterozygous patients carrying the latter mutation develop pharmaco-resistant epilepsy, hence there is need of new effective treatments. Eslicarbazepine acetate (ESL), a sodium channel blocker, has shown a good tolerability profile and high efficacy as an antiseizure medication (ASM) in adults. By employing a mouse model of self-limited neonatal epilepsy caused by a heterozygous deletion of the *Kcnq2* gene, I conducted a study on ESL effects as a first effort to estimate the value of this drug in the *KCNQ2* disease spectrum. In more detail, I first investigated effects of the major active metabolite eslicarbazepine (S-Lic) on *in vitro* physiological and pathological hippocampal network activity in mouse brain hippocampal slices: sharp wave-ripples (SPW-Rs), gamma oscillations and seizure-like events (SLEs). S-Lic (10-300 μM) decreased the incidence and increased the amplitude of SPW-Rs in a concentration-dependent manner and marginally reduced gamma oscillations frequency. 4-AP-induced SLEs were completely blocked by the highest S-Lic concentration and considerably decreased in incidence at lower concentrations. No difference was detected between *Kcnq2*^{+/+} and *Kcnq2*^{+/-} genotypes, although the EC₅₀ estimation suggested a higher efficacy in *Kcnq2*^{+/-} mice. Next, I tested ESL antiseizure efficacy in young mice by employing the 6 Hz psychomotor model of acute seizures *in vivo*. Seizure thresholds obtained from the Staircase test were different in male and female animals, resulting inconclusive for the latter. Therefore, I continued the *in vivo* experiments in male animals only. As previously described, *Kcnq2*^{+/-} mice showed a lower threshold for acute seizures when compared to *Kcnq2*^{+/+} littermates. However, ESL revealed a nearly complete protection against seizures in both genotypes. The effect decreased in a dose-dependent manner with lower efficacy of ESL in *Kcnq2*^{+/-} mice. The results of my work suggest that the increased excitability phenotype in *Kcnq2*^{+/-} mice might be efficiently targeted by S-Lic. *In vivo*, the mutation is reflected in an increased sensitivity to epileptogenic stimuli which is sensitive to ESL, albeit with lower efficacy than in *Kcnq2*^{+/+} littermates.

4. Zusammenfassung (Abstract in German)

Unter *KCNQ2*-bedingten Epilepsien wird ein Spektrum von seltenen Formen von Epilepsien im Kindesalter verstanden, welche durch Mutationen des Gens verursacht werden, das für die $K_v7.2$ -Untereinheit der nicht inaktivierenden Kaliumkanäle kodiert. *KCNQ2*-bedingte Erkrankungen reichen von einer gutartigen Form der autosomal-dominanten neonatalen selbstlimitierenden Epilepsie, die häufig durch *KCNQ2*-Haploinsuffizienz verursacht wird, bis hin zu einem schwereren Enzephalopathie-Phänotyp, der Folge von *KCNQ2*-Missense-Varianten ist. Bei den meisten heterozygoten Patienten, die die zweitgenannte Mutation tragen, kommt es zur Entwicklung von schwerer pharmakoresistenter Epilepsie. Deshalb sind neue wirksame Behandlungen erforderlich. Eslicarbazepinacetat (ESL), ein Natriumkanalblocker, hat ein gutes Verträglichkeitsprofil und eine hohe Wirksamkeit als Antiepileptikum bei Erwachsenen. Anhand eines Mausmodells für eine selbstlimitierende neonatale Epilepsie, das eine heterozygote Deletion des *Kcnq2*-Gens trägt, habe ich eine Studie über die Wirkung von ESL durchgeführt und damit einen ersten Schritt unternommen, den Nutzen dieser Substanz für das *KCNQ2*-Krankheitsspektrum zu bewerten. Zunächst untersuchte ich die Wirkung des Hauptmetaboliten Eslicarbazepin (S-Lic) auf physiologische und pathologische neuronale Aktivität im Hippocampus von Mäusen *in vitro*: Sharp Wave-Ripples (SPW-Rs), Gamma-Oszillationen und anfallsartige Ereignisse (seizure-like events, SLEs). S-Lic (10-300 μ M) erhöhte die Amplitude und verringerte die Häufigkeit von SPW-Rs in einer konzentrationsabhängigen Weise und verringerte leicht die Frequenz der Gamma-Oszillationen. Durch 4-AP induzierte SLEs wurden bei hohen S-Lic-Konzentrationen blockiert und bei niedrigeren Konzentrationen in ihrer Häufigkeit erheblich reduziert. Diese Ergebnisse unterschieden sich bei *Kcnq2^{+/+}* und *Kcnq2^{+/-}* Mäusen nicht, obwohl die Bestimmung der EC_{50} eine höhere Wirksamkeit bei *Kcnq2^{+/-}* Tieren zeigte. Anschließend testete ich die Wirksamkeit von ESL bei jugendlichen Mäusen *in vivo* im psychomotorischen 6-Hz-Modell für akute epileptische Anfälle. Die beim Staircase-Test ermittelten Schwellenwerte für Krampfanfälle waren bei männlichen und weiblichen Tieren unterschiedlich, so dass die Ergebnisse für letztere nicht schlüssig waren. Daher setzte ich die In-vivo-Versuche nur mit männlichen Tieren fort. Wie bereits beschrieben, hatten *Kcnq2^{+/-}*-Mäuse im Vergleich zu *Kcnq2^{+/+}*-Mäusen eine niedrigere Anfallsschwelle. Bei beiden Genotypen zeigte ESL einen nahezu vollständigen Schutz vor epileptischen Anfällen. Die Wirkung nahm dosisabhängig ab, wobei die Wirksamkeit von ESL bei *Kcnq2^{+/-}* Mäusen geringer war. Die Ergebnisse meiner Arbeit zeigen, dass der Phänotyp der erhöhten Erregbarkeit in *Kcnq2^{+/-}* Mäusen durch hohe Konzentrationen von S-Lic, das Natriumkanäle blockiert, wirksam bekämpft werden kann. *In vivo* führt die Mutation zu einer erhöhten Empfindlichkeit gegenüber epileptogenen Reizen, welche durch

ESL reduziert werden kann, wenn auch mit geringerer Wirksamkeit als bei *Kcnq2*^{+/-}-Geschwistern des gleichen Wurfs.

5. Introduction

5.1. The *KCNQ2*-related epilepsy syndrome

Epilepsy is one of the most common neurological disorders accompanied by stigma and life-changing consequences and affecting up to 1% of the population (Fiest et al., 2017; Hirtz et al., 2007). This disease has a prevalence of 7.6 per 1,000 individuals with a higher incidence (>60 per 100,000 individuals) in children and older patients (>60 years) (Fiest et al., 2017; Symonds et al., 2019). Despite the availability of a great variety of antiseizure medications (ASMs) and treatments such as dietary therapies, deep-brain stimulation or surgical resection of the seizure focus, >30% of patients still continue to experience seizures and their comorbidities (Chen et al., 2019; Kwan & Brodie, 2000; Lozano et al., 2019). There are many different types of epilepsy, characterized by a number of differences in terms of seizure types (generalized, focal, or combined), age at onset, or causes, either genetic or structural, to name a few (Fisher et al., 2017; Scheffer et al., 2017). Moreover, the presence of a cluster of features including seizure type, specific EEG pattern, age at onset and others, leads to the diagnosis of an epilepsy syndrome (Scheffer et al., 2017). Frequently, these syndromes are associated with childhood-onset epilepsies, that may be characterized also by developmental, intellectual and psychiatric comorbidities (Pearl, 2018). One of the most recurrent causes leading to pediatric epilepsy syndromes is the presence of mutations in genes controlling neuronal excitability and therefore resulting in a disruption of normal brain development, e.g. *SCN1A* (Dravet syndrome), *ARX* and *CDKL5* (West syndrome), or *KCNQ2* (López-Rivera et al., 2020; Mirzaa et al., 2013; Wheless et al., 2020). In this thesis, I have focused on the *KCNQ2*-related epilepsy syndrome. The clinical spectrum of *KCNQ2*-related diseases ranges from a rather benign form called self-limited familial neonatal epilepsy (BFNE) to the more severe phenotype referred to as *KCNQ2* epileptic encephalopathy. Different pathogenic variants of the *KCNQ2* gene seem to underlie the broad variety of this syndrome, by causing different levels of functional impairment (Goto et al., 2019; Miceli et al., 2013; Weckhuysen et al., 2012; for review see Nappi et al., 2020). Stop-gain mutations in *KCNQ2* gene usually represent the main cause of BFNE and the principal pathogenic mechanism is due to the gene haploinsufficiency (Goto et al., 2019; Miceli et al., 2013). Clinically, BFNE is characterized by seizures occurring in the very first days of life (4-7), and resolves within 4-6 months, usually accompanied by a normal neurological and cognitive development (International League Against Epilepsy, ILAE; *EpilepsyDiagnosis.Org*). In contrast, *de novo* occurring *KCNQ2* gene missense variants are one of the main causes of the severe phenotype *KCNQ2* epileptic encephalopathy (Goto et al., 2019; Kato et al., 2013). These mutations usually lead to a dominant-negative suppression of the M-current (Jentsch, 2000; Miceli et al., 2013). The resulting clinical phenotype is

characterized mainly by pharmaco-resistant epilepsy. Although seizure frequency decreases over time, the patients display also varying degrees of neurocognitive and developmental impairment (Kato et al., 2013). Recently, López-Rivera and colleagues have reported a predicted incidence for *KCNQ2* epileptic encephalopathy of 2.9–3.6 per 100,000 neonates (2020).

The *KCNQ2* gene encodes for a particular non-inactivating voltage-gated potassium channel subunit called $K_v7.2$, which belongs to the $K_v7/KNCQ$ potassium channel family. Overall, five subunits of this family are known to constitute functional, so-called M-type channels that are expressed differently within the body. $K_v7.1$ assemblies have been shown to be present in the heart and epithelia, while $K_v7.4$ ones are mostly expressed in the auditory system. $K_v7.2$, $K_v7.3$ and $K_v7.5$ represent the most abundant subunits in the central nervous system (Jentsch, 2000; J Robbins, 2001; Schroeder et al., 1998; Wang et al., 1998). Specifically, four subunits of $K_v7.2$ along with $K_v7.3$ and $K_v7.5$, assemble to form the functional non-inactivating potassium channel. All subunits present in the central nervous system can form homomeric channels or combine with each other in restricted combinations to form heteromeric assemblies (Schroeder et al., 2000; Schroeder et al., 1998). The resulting M-type potassium channel is a slowly activating and non-inactivating voltage-dependent potassium channel which mediates the M-current, so called due to the ability of the cholinergic blocker muscarine (M) to inhibit the channel activity (Brown & Passmore, 2009; Delmas & Brown, 2005; Wang et al., 1998). M-type currents are present in several neuronal subtypes and localized in numerous cell compartments, including nodes of Ranvier and axonal initial segment (Devaux et al., 2004), somatodendritic compartment (Shah et al., 2002), as well as postsynaptic and presynaptic terminals (Fidzinski et al., 2015; Martire et al., 2004). Alongside membrane depolarization, the M-current is activated and reduces neuronal excitability (Brown & Adams, 1980; Delmas & Brown, 2005; Jentsch, 2000).

The great variability of *KCNQ2*-related epilepsy resides on a variety of mechanisms. Different *KCNQ2* loss-of-function mutations lead to different levels of M-current decrease (Jentsch, 2000; Miceli et al., 2013) while alterations in network interactions are thought to be induced by *KCNQ2* gain-of-function mutations (Miceli et al., 2015; Millichap et al., 2017). Other mechanisms such as altered subcellular distribution or reduced sensitivity to phosphatidylinositol 4,5-bisphosphate (PIP₂) have been shown to be involved in modulating *KCNQ2*-related diseases severity (Abidi et al., 2015; Soldovieri et al., 2016).

At onset, the primary and most effective treatments for patients showing the mild BFNE phenotype are diverse types of ASMs such as the GABA_A receptor agonist phenobarbital or

the sodium channel blocker carbamazepine (Grinton et al., 2015; Sands et al., 2016). On the other hand, despite our increasing knowledge of the underlying molecular mechanisms and the availability of different ASMs, *KCNQ2* encephalopathy continues to cause pharmaco-resistant epilepsy and related cognitive impairments (Goto et al., 2019; Miceli et al., 2013; Weckhuysen et al., 2012; for review see Nappi et al., 2020).

5.2. An animal model to study *KCNQ2*-related self-limited epilepsy

The mouse model of *KCNQ2*-related self-limited epilepsy carries a deletion from exon 3 to exon 5 in the *Kcnq2* gene, which generates a loss of 429 base pairs in a region encoding for a critical portion of the resulting potassium channel subunit (Watanabe et al., 2000). Homozygous (*Kcnq2*^{-/-}) mice show a complete absence of *KCNQ2* protein expression and die shortly after birth as a result of pulmonary atelectasis, apparently not related to brain impairments. The heterozygous littermates (*Kcnq2*^{+/-}) show a 50% reduction of the *KCNQ2* protein expression compared to the wild types (*Kcnq2*^{+/+}) and, phenotypically, a normal lifespan, no behavioral abnormalities and absence of spontaneous epileptic seizures (Watanabe et al., 2000). Nevertheless, these animals have shown an increased sensitivity to epileptogenic stimuli, likely caused by the reduced expression of the *KCNQ2* protein in the heterozygous phenotype. This augmented sensitivity was demonstrated in both chemically- and electrically-induced seizure models, such as the pentylenetetrazol (PTZ) or 6 Hz corneal stimulation, respectively (Otto et al., 2009; Watanabe et al., 2000). The main characteristic of *Kcnq2*^{+/-} mice not showing spontaneous seizures but an increased susceptibility to epileptogenic stimuli has been associated with the clinical phenotype exhibited by pediatric patients showing *KCNQ2*-related self-limited epilepsy (Otto et al., 2009; Watanabe et al., 2000). Indeed, an intriguing aspect of this disease is the remission of seizures after the first few months from the disease onset without any associated cognitive damage. However, these patients show also an increased risk for the development of epilepsy later in life (Ronen et al., 1993). Therefore, this mouse model might be a good candidate to evaluate the antiseizure potential of a novel ASM against refractory seizures given by an increased epileptogenic sensitivity of the brain tissue.

5.3. Eslicarbazepine acetate as a novel ASM to treat childhood onset epilepsies

Eslicarbazepine acetate (ESL) is a substance that was developed in the early 2000s by the Portuguese pharmaceutical company Bial (Almeida & Soares-da-Silva, 2007; Bonifácio et al., 2001; Parada & Soares-Da-Silva, 2002). ESL is a third-generation compound belonging to the

dibenzoazepine family of ASMs and acting via the blocking of sodium channels, similarly to the other ASM family members carbamazepine and oxcarbazepine (Benes et al., 1999; Soares-da-Silva et al., 2015). ESL has been approved as mono- and adjunctive therapy in adult patients diagnosed with focal-onset seizures by the European Medicines Agency (EMA) in 2009, the Food and Drug Administration (FDA) in 2013, and Health Canada in 2014 (Trinka et al., 2018). Since 2017, ESL has been additionally approved for the treatment of partial-onset seizures in children aged between 4 and 17 years old (*Sunovion Pharmaceuticals Inc.*, 2017).

The chemical structure of ESL slightly differs from the one of carbamazepine and oxcarbazepine at the 10,11-position, but it is characterized by the same dibenzoazepine nucleus with a 5-carboxamide substituent (Benes et al., 1999). The variation in the molecular structure of ESL results in a different drug metabolism. ESL is a prodrug that is metabolized into active compounds R-licarbazepine and S-licarbazepine at a ratio of 1:20 (Hainzl et al., 2001). Both enantiomers possess antiseizure effects but R-licarbazepine undergoes rapid inactivation (Hainzl et al., 2001). ESL dose is given once-daily and after the oral intake, it is quickly metabolized by hydrolysis in its circulating major active metabolite, S-licarbazepine (S-Lic). The half-life of ESL is 13-20 h and its peak plasma concentration is reached after 2 h in patients with epilepsy (Almeida et al., 2008). Differently from carbamazepine and oxcarbazepine that principally act on the fast inactivation of the channels, ESL's main mechanism of action is the block of voltage-gated sodium channels by prolonging their slow inactivation state (Hebeisen et al., 2015; Soares-da-Silva et al., 2015). The affinity of ESL for the inactivated state of the sodium channel is 5-15-fold lower than that of carbamazepine and oxcarbazepine. This makes the compound more selective for the inhibition of rapidly firing neurons typically present in the epileptic brain tissue, over normally behaving neurons (Bonifácio et al., 2001). Moreover, in contrast to carbamazepine, oxcarbazepine and R-licarbazepine, S-Lic effectively inhibits both high and low affinity $Ca_v3.2$ T-type calcium channels, an ability that likely implies a potential protective effect against epileptogenesis (Doeser et al., 2015). Regarding the tolerability and safety of ESL, several trials have been conducted since its approval in Europe in 2009. As an example, Gama and colleagues in 2017 analyzed pooled data from different clinical trials in order to review the safety profile of ESL after 6 years of post-marketing surveillance. Their study showed that $\geq 10\%$ of patients reported the most common dose-dependent adverse events after ESL administration, namely dizziness, somnolence, headache, and nausea (Gama et al., 2017). Furthermore, due to a long half-life, ESL has the advantage of being a once-daily therapy compared to the commonly used twice-daily carbamazepine treatment. In a phase III clinical trial, ESL administered in monotherapy has been demonstrated to have a non-inferior antiseizure efficacy versus carbamazepine for newly diagnosed epilepsy and focal-onset seizures (Trinka et al., 2018). In a phase-II trial by

Jóźwiak and colleagues, ESL has shown encouraging effects for the treatment as adjunctive therapy in children aged 6–16 years – the compound was able to reduce the frequency of seizures without impacting cognitive and behavioral functions (Jóźwiak et al., 2018).

5.4. *In vitro* physiological hippocampal oscillations as biomarker of cognitive function

In vitro electrophysiological measurements of physiological hippocampal oscillations can be used to gain indirect insight on the effects of an ASM on cognitive functions. An essential characteristic of hippocampal neuronal populations is their ability to fire in a synchronized and oscillatory manner at certain frequencies, either individually or together as a unique network (Buzsáki, 1986; Klausberger & Somogyi, 2008). The mechanism underlying this collective activity is often associated to the balance of excitatory and inhibitory synaptic activities and gap junctions providing electrical coupling, or single neuron influences, such as the pacemaker-behaving cells (Blankenship & Feller, 2010; Maier et al., 2003; Penn et al., 2016). Network oscillations such as sharp wave-ripples (SPW-Rs) and gamma oscillations are modulated by network connectivity but also by the intrinsic excitability of both presynaptic and postsynaptic neurons (Cohen & Miles, 2000). These different oscillatory patterns occurring at specific frequencies are associated with distinct stages of memory consolidation. SPW-R complexes are characterized by two main spectral components: fast ripples occurring at a frequency of 120-200 Hz, which are superimposed on slow sharp waves having a frequency of 5-15 Hz (Buzsáki, 1986; Buzsáki et al., 1992). SPW-R represent the main synchronized population activity during “off-line” states of immobility and non-REM sleep and are supposed to play a pivotal role during the “consummatory” brain states (Buzsáki, 1986, 2015). The actions of animals, comprising humans, are defined by a first state of planning an action and a second phase during which the action is completed and the memory trace is consolidated. These two actions have been referred to as preparatory and consummatory, respectively (Buzsáki, 2015). The role of SPW-Rs during consummatory behavioral states, specifically consolidation of memory, has been demonstrated also by their frequency enhancement after training and learning in rats and humans (Axmacher et al., 2008; Pangalos et al., 2013; Ponomarenko et al., 2008). The disruption of these events has been shown to impair the spatial learning and memory in rodents and might contribute to the cognitive decline associate with childhood onset epilepsy syndromes (Cheah et al., 2019; Ego-Stengel & Wilson, 2010). On the other hand, gamma oscillations are believed to represent mainly memory encoding and retrieval. Compared to SPW-Rs, gamma rhythms vary considerably in frequencies and amplitudes and cannot be clearly associated to a specific behavioral state (Buzsáki et al., 1983; Colgin, 2015). Indeed, there are two distinct gamma rhythms, fast (~100 Hz) and slow (~25-50 Hz) which have been shown to be driven by different inputs coming from the entorhinal

cortex and hippocampal CA3 projecting to CA1, respectively (Colgin et al., 2009; Montgomery & Buzsáki, 2007). Moreover, these two oscillations seem to have different functions. The most attractive and reliable hypothesis is that slow gamma may be associated with retrieval of stored memory, while fast gamma may promote memory encoding, for example during novel objects or spatial recognition (Bieri et al., 2014; Colgin, 2015; Colgin et al., 2009; Yamamoto et al., 2014). As for SPW-Rs, the impairment of gamma oscillations is likely associated with cognitive deficits including impaired learning and memory (Nakazono et al., 2018). Thus, investigating the modulation of the physiological hippocampal network oscillations by an antiseizure compound allows evaluating its possible impact on the neuronal mechanisms behind complex behaviors, such as consolidation of memory or episodic memory retrieval and spatial memory.

5.5. Evaluation of antiseizure efficacy using *in vitro* and *in vivo* acute seizure models

The preclinical evaluation of an ASM for the treatment of an age-specific epilepsy syndrome as the *KCNQ2*-related hyperexcitability includes the investigation of its antiseizure efficacy. *In vitro* seizure-like events (SLEs) represent a disinhibited synchronous epileptiform activity, resembling seizures in *in vivo* condition. SLEs can be evoked by ionic or pharmacological manipulations applied on brain slices. In my thesis project, I used the well-established 4-aminopyridine (4-AP) model of SLEs, already optimized in our lab for rat and human hippocampal slices, which acts by non-selectively blocking potassium channels (Avoli et al., 1993; Perreault & Avoli, 1992). Advantages of this model include the possibility to perform several experiments in tissue from one animal and the possibility to evoke stable SLEs and a concomitant low occurrence of spreading depolarization, often seen in other *in vitro* models such as low magnesium or electrical stimulation (Heuzeroth et al., 2019). A number of commonly used classical as well as new generation ASMs have been screened via the 4-AP *in vitro* model, such as carbamazepine and phenytoin, or lacosamide and zonisamide, respectively (D'Antuono et al., 2010; Fueta & Avoli, 1992; Heuzeroth et al., 2019).

After an *in vitro* assessment of antiseizure effects of a novel ASM, it is critical to validate the findings in an *in vivo* condition. A number of *in vivo* models of acute and chronic seizures have been developed over the past years of epilepsy research (Löscher, 2017). One valuable paradigm to study refractory seizures in particular is the 6 Hz psychomotor seizure model. This model was firstly developed in the 1950s as an attempt to find an alternative method to the previous approaches of electrically- (maximal electroshock stimulation, MES) or chemically- (pentylenetetrazol, PTZ) induced acute seizures (Barton et al., 2001; Brown et al., 1953). These two traditional screening models have long been successfully employed, leading to the discovery and approval of a number of ASMs currently in use for the treatment of epilepsy

(Löscher, 2011). However, MES and PTZ models showed a low sensitivity to novel compounds with a high potential for the treatment of pharmacoresistant epilepsies, for example levetiracetam. Levetiracetam was ineffective in MES and PTZ models, even at high doses (Klitgaard et al., 1998; Löscher & Hönack, 1993). This example shows the importance of alternative screening methods resembling more the human condition of refractory seizures. The paradigm of the 6 Hz psychomotor seizure model is characterized by low frequency and long duration of the current stimulus (6 Hz and 3 s, respectively), which leads to a different behavioral response compared to the higher frequency and faster pulse of the MES (50 Hz for 0.2 s). The paradigm of the 6 Hz model has been shown to induce acute seizures characterized by a clonic phase followed by a stereotypical behavior reminiscent of focal automotor seizures in human temporal lobe epilepsy (Brown et al., 1953). After being at first abandoned for the lack of sensitivity to phenytoin, Barton and colleagues conducted an exhaustive characterization of the 6 Hz model, by screening a number of first and second generation ASMs (Barton et al., 2001). Their results showed that by increasing the current stimulations (i.e. 1.5x and 2x of the current intensity needed to evoke seizures in 97% of the animals), this model can mimic pharmacoresistant limbic seizures and can therefore be successfully employed for the testing of novel compounds (Barton et al., 2001).

5.6. Hypothesis and aims of the PhD thesis project

Given the therapeutic potential and the tolerability of ESL for childhood epilepsies, the aim of my PhD project was to investigate its efficacy in the mouse model of *KCNQ2*-related self-limited epilepsy. The principal goal was to assess the antiseizure efficacy and therapeutic value of ESL in the treatment of the *KCNQ2*-related diseases.

The main hypothesis of my thesis is that by prolonging the slow inactivation state of sodium channels, ESL might be efficacious in dampening the increased excitability causing seizures in *KCNQ2*-related epilepsy. Based on this hypothesis, I pursued three main aims:

- 1) Assessing the *in vitro* effects of the main metabolite of ESL, S-Lic, on physiological hippocampal neuronal activities, namely SPW-Rs and gamma oscillations;
- 2) Screening of S-Lic antiseizure potential on the 4-AP *in vitro* model of SLEs evoked in mouse brain slice preparations;
- 3) Testing ESL antiseizure efficacy in an *in vivo* approach of refractory seizures, namely the 6 Hz psychomotor seizures model.

For all these purposes, I used juvenile mice carrying a heterozygous deletion of *Kcnq2* gene, which resemble most of the clinical features of the human condition, comprising an increased sensitivity to epileptogenic stimuli.

6. Materials and Methods

6.1. Animals

All animal experiments aimed at achieving the goals of this PhD project were conducted in agreement with the German Animal Welfare Act for animal experiments and the European Directive 2010/63/EU and approval was given by the Institutional Animal Welfare Officer and the local authorities in charge (Landesamt für Gesundheit und Soziales Berlin, license numbers: T0265/17, G0078/18). All animal experiments performed and reported in this thesis comply with the directions of the ARRIVE guidelines (Pierce du Sert et al., 2020). Remarkable care was taken in order to reduce animal suffering and the number of animals needed and used. Wild type (*Kcnq2^{+/+}*) and heterozygous (*Kcnq2^{+/-}*) mice with C57BL/6J background were crossed in order to circumvent homozygous animals birth (*Kcnq2^{-/-}*) animals that have been shown to die shortly after birth (Watanabe et al., 2000). Wild type littermates obtained from the crossing with heterozygous were considered as control for all experiments. Animals were kept under controlled environmental conditions, with 12h light/dark cycle (6:00 h/18:00 h). Cages were enriched and supplied with wooden litter. Cages were individually ventilated and contained up to 9 mice of the same sex. All animals had *ab libitum* access to food and water.

6.2. Chemicals

Eslicarbazepine acetate [(–)-(S)-10-acetoxy-10,11-dihydro-5H-dibenzo[b,f]azepine-5-carboxamide] (ESL) and its active metabolite eslicarbazepine ([S]-licarbazepine, S-Lic) [(+)-(S)-10,11-dihydro-10-hydroxy-5H-dibenzo[b,f]azepine-5-carboxamide] were manufactured with purities >99.5% and tested by BIAL Portela & Ca, S.A., both prior to the beginning of the project and after 2 years. Kainic acid (kainate) was obtained from Cayman Chemical Company, Ann Arbor, MI, USA and was employed to evoke *in vitro* gamma oscillations. 4-aminopyridine (4-AP) was purchased from Sigma, Munich, Germany. 4-AP is a non-selective potassium channel blocker and was employed as *in vitro* seizure model to induce acute seizure-like events (SLEs). Dimethyl sulfoxide (DMSO,) and hydroxypropylmethylcellulose (HPMC) were obtained from Sigma. For *in vitro* experiments, 0.12% DMSO served to dissolve S-Lic to a stock concentration of 250 mM. 0.2% HPMC was dissolved in distilled water and used as solvent for ESL to obtain the solution for oral administration during *in vivo* experiments.

6.3. Mouse hippocampal acute slice preparation

Acute mouse brain hippocampal slices were used in all *in vitro* experiments for electrophysiological recordings and analysis of S-Lic tissue concentration. Slices were obtained from juvenile (4 weeks, P27-34) *Kcnq2^{+/+}* and *Kcnq2^{+/-}* mice having a weight range of 20-25 g. Dissection and preparation of the slices was conducted similar to established procedures to obtain rat hippocampal slices (Heuzeroth et al., 2019). Mice were anesthetized with isoflurane at 2% volume for 2 min and euthanized through decapitation. The brain was quickly surgically taken out and kept in carbogenated (95% O₂, 5% CO₂) ice cold (4 °C) artificial cerebrospinal fluid (aCSF). aCSF contained in mM: NaCl 125.0, KCl 2.0, MgCl₂ 1.0, CaCl₂ 2.0, NaH₂PO₄ 1.25, NaHCO₃ 25.0, and glucose 10.0. The solution had a final pH of 7.4 and an osmolarity of 300 ±10 mOsm, which was monitored by an osmometer at the beginning of each experimental day. After extraction of the brain and removal of the cerebellum and the forebrain, the hemispheres were separated and glued to a refrigerated vibratome holder, which was immediately immersed in semi-frozen aCSF contained in the vibratome reservoir. Hippocampal 400 µm-thick horizontal slices were obtained from cutting both hemispheres at the same time, by using a vibratome (Leica VT1200S, Wetzlar, Germany). Slices were chosen for electrophysiological recordings according to the presence of: the entorhinal cortex (EC), the subiculum (SUB), the dentate gyrus (DG) and the cornu ammonis regions 1 and 3 (CA1, CA3). During cutting process, the chosen slices were put on three layers of filter paper laid on the slice-holding compartment of an Haas-type interface chamber (Haas et al., 1979). The chamber compartment was constantly perfused with prewarmed (35 °C) and carbogenated aCSF at a speed 1.6 ml/min. The three layers of filter paper are needed to ensure the continuous occurrence of a sufficient amount of solution below the slices (Kraus et al., 2020). Before each electrophysiological experiment, the slices were allowed to recover in the interface chamber for at least 1 h.

6.4. Electrophysiology

Local field potential (LFP) recordings denote an electrophysiological approach by which it is possible to measure the activity of a local population of neurons. Specifically, a small-sized electrode, as I employed for this method, is placed in the extracellular space of a specific brain slice region and allows the recording of field potentials giving rise to neuronal oscillations. These oscillations represent the synchronous activation of the neuronal population (Buzsáki et al., 2012). Differently from intracellular recordings of action potential or synaptic currents, LFP recordings can differ depending on the methodological approaches and details of

application (Kajikawa & Schroeder, 2011). For my thesis project, I applied two different methods of LFP recordings: (1) direct recordings of ongoing neuronal oscillations, either spontaneous (SPW-Rs) or chemically-induced (gamma oscillations and SLEs); and (2) in response to a stimulus (input-output recordings of field excitatory postsynaptic potentials, fEPSPs; and population spikes, PS). LFP recordings do not measure the intracellular, single-neuron activity but rather indicate the temporal synchrony of the entire neuronal network under consideration and allow to discover and investigate the changes happening in the local circuits, for example during the application of a drug (Montgomery & Buzsáki, 2007).

Therefore, I employed this electrophysiological approach to record physiological and pathological hippocampal network oscillations. In particular, spontaneous SPW-Rs and gamma oscillations induced by kainate were recorded to investigate the effects of S-Lic on hippocampal physiological network synchronization. Seizure-like events (SLEs) were instead evoked by application of 4-AP to test the antiseizure efficacy of S-Lic *in vitro*. In addition, the highest concentration of S-Lic (300 μ M) was used to evaluate effects on synaptic transmission and neuronal population excitability, via the input/output recordings of fEPSPs and fEPSPs/PS coupling, respectively, evoked by electrical stimulation. A vertical puller (PC-10, Narishige, Tokyo, Japan) was used to pull borosilicate pipettes, filled with 154 mM NaCl (Science Products, Hofheim, Germany; 1.5 mm outer diameter) and having an electrode resistance of 1–2 M Ω , optimal for extracellular recordings. The use of borosilicate glass for electrophysiological recordings ensures a low level of electric noise during the measurements, thanks to the low dissipation factor and dielectric constant of the material (0.002-0.005 and 4.5-6, respectively) (The Axon Guide, 2020). A sample size of five-nine animals was calculated on the basis of previous studies or control experiments in order to obtain a statistical power of 80% with an effect size of 20-25% (Maier et al., 2009, 2012).

6.4.1 Physiological neuronal activity

SPW-R spontaneous events were recorded from CA1 pyramidal layer of ventral hippocampal slices (Kubota et al., 2003; Maier et al., 2003, 2009; Papatheodoropoulos & Kostopoulos, 2002). Only ventral hippocampal slices were chosen for spontaneous SPW-Rs recording for the following reasons: (1) previous work by Papatheodoropoulos and Kostopoulos has demonstrated that ventral hippocampal slices generate persistent spontaneous activity when perfused with normal aCSF (2002), and (2) during the first preliminary experiments, I noticed a difference in the occurrence of SPW-R complexes between dorsal and ventral slices, with dorsal slices often not displaying spontaneous activity.

SPW-Rs recordings were done in an improved submerged-type recording chamber characterized by a high flow rate (10-13 ml/min) (Hill & Greenfield, 2011; Kraus et al., 2020). Hippocampal slices were put in a semipermeable membrane glued to a plastic ring and placed inside the submerged chamber. The inflow and outflow of the membrane chamber are both connected to tubes for the supply of solution. These tubes are secured in a peristaltic pump in a way that the inflow and outflow move in opposite directions (Kraus et al., 2020). During baseline activity in which only aCSF was perfused, spontaneous SPW-R events were recorded for ≥ 30 min, during which SPW-Rs showed an incidence of ~ 1 Hz. Subsequently, aCSF containing S-Lic at a concentration of 0 (0.12% DMSO as vehicle control), 10, 30, 100 or 300 μM was applied and spontaneous activity was recorded for ≥ 30 min. The solution containing different drug concentrations was assigned randomly to one slice per each mouse. The drug was finally washed out with aCSF for ≥ 30 min.

Gamma oscillations were simultaneously recorded from CA3 and CA1 pyramidal layers of both ventral and dorsal hippocampal slices and were chemically-induced by adding kainate at 100 nM (Schneider et al., 2015; Wójtowicz et al., 2009). I chose a concentration of 100 nM after a period where I optimized the protocol. I conducted a testing of different kainate concentrations ranging 100-400 nM in order to determine the adequate concentration for induction of gamma oscillations without initiating irreversible bursting activity (data not shown or published). In pilot experiments, I also tested which type of electrophysiological set-up is most suitable to record gamma oscillations. In the submerged chamber used to record SPW-Rs, most of the recordings showed that gamma activity was either not detectable or displaying insufficient frequency. Therefore, gamma hippocampal oscillations were recorded in an interface chamber electrophysiological set-up in which slices were placed on a transparent and semipermeable membrane (culture plate inserts 0.4 μm Millicell; Millipore, Bedford, MA, United States) located inside one of the slice-holding compartments. Baseline gamma oscillations were recorded for ≥ 60 min to achieve stable frequency. aCSF containing S-Lic at a concentration of 0 (0.12% DMSO as vehicle control) and 300 μM was randomly applied to one slice per each mouse. Upon application of vehicle control or S-Lic, gamma oscillations were recorded for ≥ 30 min. Finally, the drug was washed out and substituted with aCSF containing kainate and the activity was recorded for further ≥ 30 min.

6.4.2 Pathological seizure-like events

SLEs were recorded in the submerged-type chamber. SLEs were evoked using an *in vitro* model previously reported and used in our lab (Heuzeroth et al., 2019; Kraus et al., 2020). Acute SLEs were evoked by applying 100 μM 4-AP, a compound acting by non-selectively

blocking potassium channels (Avoli et al., 1993; Perreault & Avoli, 1992). I then recorded the resulting field potentials from the entorhinal cortex (Lopantsev & Avoli, 1998). 4-AP evoked *in vitro* SLEs are characterized by an initial negative field potential depolarization showing low-amplitude gamma-activity, which is followed by constant tonic events. A typical SLE usually terminates with rhythmic bursting decreasing in frequency and increasing in amplitude (Avoli et al., 1996). SLEs were visually detected during the ongoing recording and were identified through some typical electrographic features. The duration of the negative field potential shift usually exceeds 10 s, the field potential decreases of at least 0.5 mV, and I considered a single spike preceding the negative shift as the starting of a SLE, while ending when the rhythmic bursting terminates (for an example trace see Fig. 5A). Baseline epileptiform activity was recorded for ≥ 30 min. S-Lic was subsequently added to the aCSF containing 4-AP. S-Lic at a concentration of 0 (0.12% DMSO as vehicle control), 30, 100 and 300 μM was assigned randomly to one slice per mouse each and the resulting activity was recorded for ≥ 30 min. Finally, the drug solution was washed out with aCSF containing 4-AP for further ≥ 30 min.

6.4.3 Input/Output relationship and fEPSP/PS coupling

Evoked neuronal population responses were measured in the submerged-type chamber set-up upon application of 300 μM S-Lic as described in the publication Monni et al., 2022. Specifically, input/output (I/O) curves and fEPSP/PS coupling were determined from electrophysiological field responses in order to detect potential effects of S-Lic (300 μM) on synaptic transmission and neuronal excitability, respectively. In addition to the recording electrodes made as described in previous paragraphs, a bipolar stimulating electrode having a resistance of 1–2 $\text{M}\Omega$ was positioned in the stratum (st.) radiatum of CA1. The stimulating electrode was necessary to evoke and record the fEPSPs at more distal locations of CA1 st. radiatum. Three independent measurements were selected for each stimulus intensity that was progressively increased and adjusted to get the chosen amplitude of the fiber volley, which denotes the presynaptic action potential arriving at the recording site and the fEPSP itself (Fidzinski et al., 2015). In all I/O curve experiments, fiber volley amplitude was used as reference for the detection of the change of fEPSPs (20–80% of the maximum) due to increasing stimulus. Indeed, plotting the fiber volley against the fEPSP amplitude allows the evaluation of postsynaptic response as opposed to presynaptic response in the hippocampal slice (Hawkins et al., 2017). Similarly, one stimulation electrode and two recording electrodes were used to measure fEPSP/PS coupling. Recording electrodes were placed (1) in CA1 pyramidal cell layer to record PS and (2) in the CA1 st. radiatum to record fEPSPs. In this paradigm, the intensity of the stimulus was adjusted to achieve the maximal fEPSP slope suitable for every slice used ($\sim 1.6\text{-}2$ mV/ms) and then the change of PS due to fEPSP slope

increase was examined. fEPSP slopes were detected as occurring 1 ms prior to the PS and PS amplitude was calculated as the absolute difference between PS peak and anti-peak.

6.5. *In vivo* 6 Hz psychomotor seizure model

After *in vitro* electrophysiological measurements, I sought to test the antiseizure efficacy of ESL *in vivo*. To this end, I employed the 6 Hz psychomotor seizure model. This model has been very often used in epilepsy research to electrically induce *in vivo* acute seizures in rodents, which are thought to mimic seizures occurring in pharmacoresistant epilepsy (Barton et al., 2001; Brown et al., 1953). For my PhD project, I used juvenile *Kcnq2^{+/+}* and *Kcnq2^{+/-}* mice aged P21–P28 to test the potential protective effect of ESL against acute seizures evoked by the corneal stimulation. I started the animals handling one week before the stimulation experiments in order to obtain a complete acclimatization of all animals to the experimenter and to the restrain technique. Moreover, animals were kept in the experiment room for ≥ 1 h before the experiment started, in order to provide a further acclimatization process. A 0.5 ml drop of local anesthetic (0.4% oxybuprocaine hydrochloride, Omnivision GmbH, Puchheim, Germany) was applied to both eyes of the mouse and was allowed to act for 3 min. Subsequently, each mouse was stimulated via corneal electrodes connected to a constant current pulse generator (Electro-Convulsive-Therapy, ECT Unit 5780, Ugo Basile, Comerio, Italy). The stimulation parameters were: 0.2 ms rectangular current pulses for 3 s at 6 Hz. 0.9% saline was used to wet the two electrodes before being placed over the eyes, allowing securing a sufficient electrical contact between the electrode and the cornea. This technique is quite peculiar and it is currently employed only in few laboratories. I therefore visited the laboratory of Prof. Wolfgang Löscher in the Department of Pharmacology, Toxicology and Pharmacy at the University of Veterinary medicine, Hannover (Germany) and here I could learn the basics of the MES technique, which I then applied to the 6 Hz model.

6.5.1 Staircase test

Before testing antiseizure efficacy in the 6 Hz psychomotor model, it is considered good scientific practice to establish the model for the mouse strain used because of the potential differences that might be present due to genetic background, age and sex of the animals (Barker-Haliski et al., 2018). Therefore, for the present project, by using the “staircase test” technique (Barton et al., 2001) and a total of 40 animals (four subgroups with 10 animals each: male *Kcnq2^{+/+}*, male *Kcnq2^{+/-}*, female *Kcnq2^{+/+}*, female *Kcnq2^{+/-}*), I determined the mean convulsion current (CC_{50} denoting 50% of animals and CC_{97} referring to 97% of animals showing a seizure) required for the induction of acute seizures in both genotypes separately.

In the staircase procedure, animals were stimulated two or three times every 48 h with current intensities ranging between a minimum of 8 and a maximum of 24 mA. The intensity was increased by 2 mA for the subsequent stimulation when a given stimulation did not result in a seizure, and the intensity was decreased by 2 mA for the subsequent stimulation when the animal did show a seizure response.

6.5.2 ESL antiseizure efficacy test

ESL antiseizure efficacy was investigated in 20 *Kcnq2^{+/+}* and 20 *Kcnq2^{+/-}* male mice by stimulating them with the genotype-specific CC₉₇ multiplied by a factor of 1.5. Additional 20 *Kcnq2^{+/-}* mice were stimulated with 1.5-fold *Kcnq2^{+/+}*-CC₉₇ in order to control that the effectiveness was actually due to ESL effect on the genotype and not to a genotype-specific CC₉₇. Groups' size was previously estimated and approved in agreement with previous studies showing that a minimum number of five-nine events per predictor variable is sufficient to assure statistic certainty with a probability of type II error <20% (Vittinghoff & McCulloch, 2007). Following the 3Rs approach, I decided to use the lowest possible numbers with five animals per ESL dose. Each animal was stimulated twice every 72 h, achieving a number of 10 independent values for each group. The interval of 72 h was chosen in order to assure complete clearance of the drug, which has been shown to occur at a rate of 20-30 ml/min (Almeida & Soares-da-Silva, 2007). Every day of the experiment, animal welfare and potential signs of stress were monitored according to the score sheet of humane endpoints (Morton, 1999). Vehicle control (0.2% HPMC, 0 mg/kg ESL) and three different ESL doses (10, 30, 100 mg/kg) were administrated via oral gavage (10 ml/kg solution volume) approximately 60 min before the stimulation. Directly after the stimulation, each mouse was placed in an open small cage (dimensions: 25x20x14 cm) for observation and scoring. I chose to use a modified Racine's scale for scoring seizure intensity as described in Monni et al., 2022: "0, no behavioral changes; 1, sudden arrest with orofacial automatism; 2, sudden arrest with head nodding; 3, forelimb clonus; 4, forelimb clonus with rearing and possibly falling; 5, generalized tonic-clonic activity with loss of postural tone and sporadic wild jumping (Racine, 1972)". The protocol for *in vivo* experiments is illustrated in figure 1. I was blinded for mice genotype during the whole experiment and for both ESL doses and genotypes during the following scoring process, as described in the section 6.8 "Statistical analysis". Blindness for ESL doses during the experiments was not possible due to the different aspects of the drug solution, which changed to become more milky-white as the drug concentration increased. All mice were sacrificed by decapitation under isoflurane anesthesia on the day of the second stimulation. Whole brain was weighted and plasma was separated from the blood solid components by two centrifugation rounds at 20,000 g for 5 min. Brain and plasma were then immediately snap-

frozen with liquid nitrogen and stored at -80 °C. After the conclusion of all *in vitro* and *in vivo* experiments, the frozen samples were sent to our collaborators at the BIAL-Portela Pharmaceutical Company laboratories in Porto (Portugal) for the analysis of S-Lic tissue concentration (described in section 6.6).

6.5.3 Rotarod test

Between ESL oral administration and the electrical stimulation, I employed the Rotarod test as a screening for ESL side effects with regard to motor coordination (Dunham & Miya, 1957). The main advantage of this test is the possibility to create a continuous measurable variable, namely the latency to fall from the rotating rod, which can be employed to quantify subtle toxic effects of the drug. The obtained parameter of this test is not subjected to judgments of ability, thus representing a perfectly reliable dataset (Rustay et al., 2003). Despite ESL showed a median toxic dose for motor impairment at high doses of >300 mg/kg (Doeser et al., 2015), I tested the lower concentrations used here in order to validate my results. Moreover, the Rotarod test can be used to test the motor coordination of genetically modified epileptic mice, which may show severe motor impairment (Doeser et al., 2015). Thus, after oral administration of the ESL, mice were placed on a rotating rod (Ugo Basile, model 47600) at a constant speed of 15 rpm for 2 min. The time during which the mouse was able to rotate without grasping onto the drum or falling while rotating was measured and analyzed. Each mouse was subjected to two Rotarod trials, interrupted by a 5 min break. I excluded all trials in which the mouse was unable to maintain balance while rotating for at least 10 s. Upon falling, the mouse was put back on the rod for a maximum of three times.

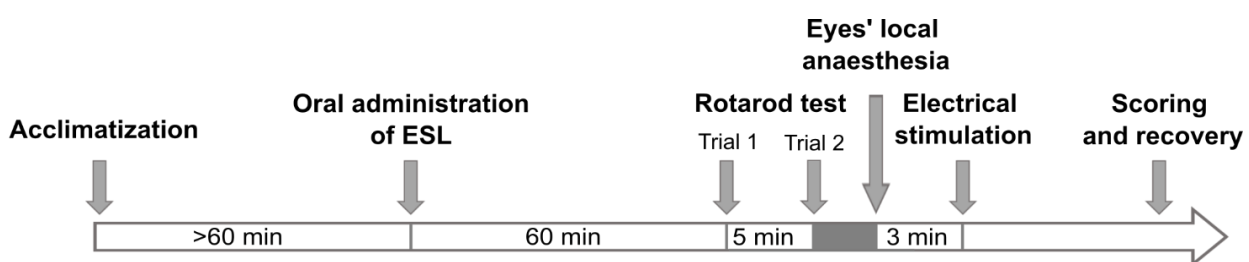


Figure 1: *in vivo* experimental protocol. Graphical visualization of the timeline for the 6 Hz psychomotor test. Arrows indicate time points of each step of the protocol. (Figure taken from Monni et al., 2022, Fig. 5A).

6.6. Pharmacokinetic analysis of S-Lic

Analysis of S-Lic concentration was performed in whole brains, hippocampal slices and blood plasma samples, which were sent as frozen samples to our collaborators (laboratory of Prof.

Patricio Soares-da-Silva, BIAL-Portela, Portugal). S-Lic concentration was determined using an enantioselective LC-MS/MS assay (6470, Triple Quad LC-MS Agilent Technologies, Santa Clara, CA, USA). For details of the protocol see Loureiro et al., 2011 and Monni et al., 2022. In brief, samples were thawed, weighted and added to 100 μ l of internal standard working solution (ISTD; 2,000 ng/ml of 10,11-dihydrocarbamazepine in phosphate buffer pH 5.6). The resulting solution was vortexed and centrifuged at 20,000 *g* for 10 min. The supernatant was finally filtered and put into HPLC vials/plates that were injected into the LC-MS/MS. Samples were measured with the analytical calibration range of 10.0 to 5,000.0 ng/ml and the limit of quantification was set to 10.0 ng/ml.

6.7. Data processing

Electrophysiological recordings performed in the submerged-type chamber setup, were sampled at 20 kHz (SPW-Rs) or 10 kHz (SLEs, stimulation experiments), low-pass filtered at 2 kHz and digitized by a Digidata1550 interface. Digital signal was then displayed and processed by PClamp10 software (Molecular Devices, Sunnyvale, CA, USA). For gamma oscillations experiments recorded through an interface-type chamber setup, signals were sampled at 10 kHz and acquired by custom-made amplifiers (10 \times) connected to an AD converter (Micro 1401 mk II, Cambridge Electronic Design Limited, Cambridge, United Kingdom). Data were then showed and processed with Spike2 and Signal software (versions 7.00 and 3.07, respectively; Cambridge Electronic Design Limited, Cambridge, United Kingdom). Custom-written MATLAB scripts (R2014b, R2016b, R2020b MathWorks, Natick, MA, United States) were developed to analyze the raw data of SPW-Rs, gamma oscillations and SLEs. Details regarding MATLAB parameters and thresholds employed for the analysis are described in Monni et al., 2022. Briefly, SPW-R components were analyzed by first low-pass filtering the events at 50 Hz and by setting the threshold at 3.5 times the standard deviation (SD) in order to isolate the slower sharp waves. Then the raw data were further filtered at 80-600 Hz with the same threshold of 3.5 times the SD, a range that allows the detection of the faster components, namely the ripples. Finally, in order to perform the correlation analysis between the sharp waves and the ripples, the correlation coefficient of their peak amplitudes was calculated by the MATLAB script. Gamma oscillation frequency was calculated using the raw data divided in smaller vectors of 10 s. Subsequently, the vectors were processed with fast Fourier transformation in the 30-48 Hz frequency band, which is the frequency range of the low gamma oscillations generated in CA3. Another MATLAB script was used for the analysis of CA3-CA1 temporal relationship and cross-correlation, the gamma phase and the time lag between the two hippocampal regions. In this case, I took into consideration the last 5 min of each condition recorded from both CA3 and CA1 (baseline,

treatment, washout). The raw data were firstly notch-filtered at 50 Hz, down-sampled to 5 kHz and finally band-pass filtered at 1-100 Hz. 5 s stretches from CA3 and CA1 filtered data were cross-correlated by the MATLAB function “xcorr” and the peaks of cross-correlation, as well as time lag, were averaged.

CC₅₀ and CC₉₇ ± 95% confidence intervals specific for each genotype were determined by analyzing the data from *in vivo* staircase tests in the 6 Hz psychomotor seizure model with the probit analysis procedure (Finney, 1971). Stimulation values were not considered for statistical analysis if it was not possible to certainly detect the occurrence of a seizure, either because of a change in electrodes' conductance detected by the pulse generator or the absence of a sufficiently distinct response from the mouse. Therefore, a value of “+” was given if the mouse showed a seizure, “-“ if the seizure was not induced and “0” if the stimulation had to be excluded. For the subsequent *in vivo* seizure scoring during ESL antiseizure efficacy test, Dr. Larissa Kraus (a former researcher in our working group) and I blindly assigned a score to each individual mouse response to the current stimulus, recorded in a video during the experiment days. The two independent scores were then averaged and their mean was considered for the following statistical analysis.

6.8. Statistical analysis

All *in vitro* and *in vivo* data were analyzed with GraphPad Prism 5 (GraphPad Software Inc., San Diego, CA, USA). Statistical analysis was performed on groups with a sample size of independent values ≥ 5. Power calculations of the statistical tests were performed *a priori*, with the exception of the analysis of CA3-CA1 cross-correlation. Sample size was therefore estimated to reach a power of at least 80% and an effect size of 20-25%. Before statistical evaluation, D'Agostino and Pearson omnibus normality test or Kolmogorov-Smirnov normality test (when n < 8) were applied to all data in order to test for normal distribution. Data were then further analyzed accordingly with one way ANOVA or Friedman for non-parametric data and parametric or non-parametric *post-hoc* test (Tukey's or Dunnett's test for multiple comparisons, respectively). Data across genotypes were tested by using Two-way ANOVA and Bonferroni's test for multiple comparisons. Importantly, *post-hoc* tests were run only if the F value of ANOVA was statistically significant and if there was no inhomogeneity detected between the variance tested with the Bartlett's test for equal variance. Analysis of correlation coefficients with either Pearson or Spearman coefficients for parametric or non-parametric data, respectively, was performed to test the relationship between (1) sharp waves and ripples amplitude, and (2) S-Lic concentration in plasma and whole brain and seizure score. Simple linear regression analysis was applied to investigate potential differences between the coefficient of

determination (r^2) of the *in vitro* and *in vivo* results regarding ESL antiseizure efficacy, related to the subsequent measurements of S-Lic concentration in hippocampal slices and whole brain, respectively. The estimation of EC_{50} and ED_{50} values was calculated with AAT Bioquest web software (*EC₅₀ Calculator | AAT Bioquest*). Statistical differences were considered significant if the p -value was ≤ 0.05 . Data are shown as mean \pm SD and normalized data are always expressed as ratio between treatment with ESL/S-Lic and baseline only for illustrative purposes.

7. Results

7.1. S-Lic effects on *in vitro* physiological hippocampal oscillations

I first examined the *in vitro* effects of four concentrations of S-Lic (10, 30, 100, 300 μ M) on physiological hippocampal SPW-Rs and gamma oscillations. This evaluation is useful during the investigation of an antiseizure compound for a potential novel use and in the animal model chosen to mimic the disease. SPW-Rs and gamma oscillations particularly allow evaluating the effect of the ASM on hippocampal functional synchronization (Buhl et al., 1998; Kubota et al., 2003; Maier et al., 2003; Papatheodoropoulos & Kostopoulos, 2002). To this aim, I recorded spontaneous SPW-Rs from CA1 pyramidal layer (Fig. 2A), while kainate-evoked gamma oscillations from both CA3 and CA1 pyramidal layers (Fig. 3A). SPW-Rs are usually generated from the synchronous discharge of CA3 neuronal network, propagating then to CA1 (Buzsáki, 1986). However, spontaneous SPW-Rs have been shown to occur at similar rate of incidence in both the regions (Maier et al., 2003). A recent study has shown that SPW-Rs are also independently generated in the subiculum (Imbrosci et al., 2021). As these were the first experiments I conducted for my thesis, I performed most of the recordings solely from CA1, from which SPW-Rs appeared to occur and be recorded more frequently.

In the local field potential recordings, SPW-Rs are defined by two components: fast, high frequency (~ 200 Hz) “ripple” oscillations that are superimposed on slow waves (~ 5 -10 Hz, called sharp waves) (Fig. 2B). As explained in the introduction, SPW-Rs occur mostly during immobility and non-REM sleep and are involved in the consolidation of memory. Gamma oscillations occur at a higher frequency range compared to SPW-Rs (30-100 Hz, Fig. 3B) (Buzsáki & Wang, 2012; Freeman, 2007) and play an important role in other cognitive functions, such as episodic memory retrieval and during exploratory behavior (Csicsvari et al., 2003; Montgomery & Buzsáki, 2007).

In order to first assess the functional synchronization during SPW-Rs oscillations and whether the highest concentration of S-Lic had an impact on it, I performed a correlation analysis between the amplitude of the two components: sharp waves and ripples. The result showed

that the two activities were strongly and positively correlated, even when the S-Lic was applied (Fig. 2C). Upon application of S-Lic, SPW-R incidence was significantly and reversibly reduced (Fig. 2D), while increasing in amplitude (Fig. 2E), in a concentration-dependent manner. Moreover, the results were not different between *Kcnq2^{+/+}* and *Kcnq2^{+/-}* mice.

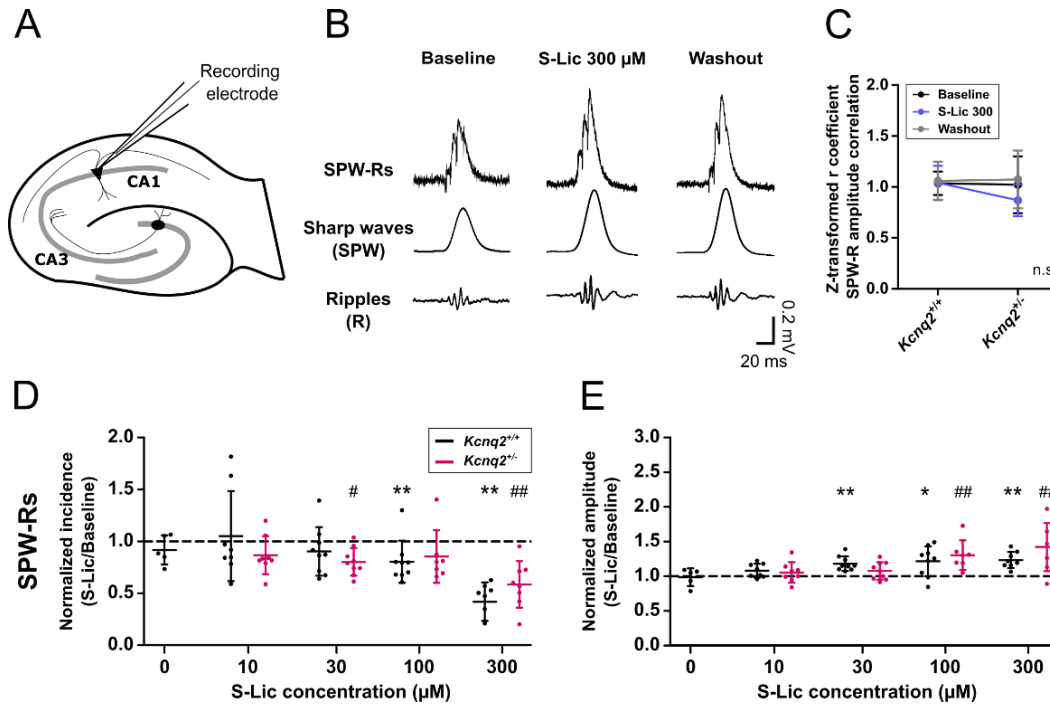


Figure 2: Concentration-dependent effects of S-Lic on *in vitro* sharp wave-ripple complexes. (A) Scheme of a mouse hippocampal slice showing CA3 and CA1 pyramidal layers and the electrode position during LFP recordings of SPW-Rs. (B) Examples of the events during baseline, S-Lic 300 μM and washout. Top events represent unfiltered SPW-Rs; middle events were low-pass filtered at 30 Hz showing the sharp wave component, and bottom events were band-pass filtered at 80-250 Hz to obtain the ripple component. (C) Plot depicting the correlation analysis between sharp waves (SPW) and ripples (R). (D, E) Scatter plots showing the normalized values of SPW-R complexes incidence (D) and amplitude (E) recorded in the hippocampal CA1 pyramidal layer during the application of four increasing concentrations of S-Lic. *Kcnq2^{+/+}* data are depicted in black, *Kcnq2^{+/-}* in dark pink. Each dot refers to one slice obtained from one animal, data are shown as mean ± standard deviation. Asterisks and number signs indicate statistically significant differences as assessed by one-way ANOVA or Friedman test and Tukey's or Dunnett's *post-hoc* test for multiple comparisons on raw data, respectively (* or #: p-value ≤ 0.05; ** or ##: p-value ≤ 0.01, n.s.: not significant.). (Figure modified from Monni et al., 2022, Fig. 1)

Differently from SPW-Rs, which occur spontaneously, *in vitro* gamma oscillations need to be chemically evoked. To this end, I employed 100 nM kainate, a substance that activates ionotropic glutamate receptors (Buhl et al., 1998). In order to look at possible effects of S-Lic and given its concentration-dependent impact on the SPW-Rs, I focused on the investigation of the highest concentration of the drug. As mentioned in the introduction, *in vitro* recordings of gamma oscillations from the CA3-CA1 network showed a low frequency range of 30-40 Hz

during baseline activity (Fig. 3C). Application of 300 μM S-Lic significantly reduced gamma oscillations frequency in both CA3 and CA1, equally in *Kcng2*^{+/+} and *Kcng2*^{+/-} mice, while during recordings conducted with the vehicle control (S-Lic 0 μM), gamma frequency remained stable (Fig. 3C). Moreover, hippocampal oscillations did not show any difference between the genotypes, during either SPW-Rs or gamma activity. Taking advantage of simultaneously recorded gamma oscillations from CA3 and CA1, I could get insights on the synchronization and temporal relationship between these two regions, both during baseline activity and during S-Lic application. To do so, a specific MATLAB script generously provided by Dr. Nikolaus Maier was applied in order to analyze the time delay between the activity recorded from the two regions, as well as their functional cross-correlation and phase of the oscillations. The datasets revealed that: (1) the difference in the gamma oscillation phase recorded during the propagation from CA3 to CA1 (depicted in the figure as delta, Δ) was unaltered by S-Lic (Fig. 3C); (2) gamma rhythms cross-correlation between CA3 and CA1 networks decreased upon application of S-Lic (Fig. 3D); and (3) S-Lic significantly increased the time lag/delay from CA3 to CA1 (Fig. 3E). These results provide insight into the oscillations' mechanism during the application of antiseizure medication *per se*.

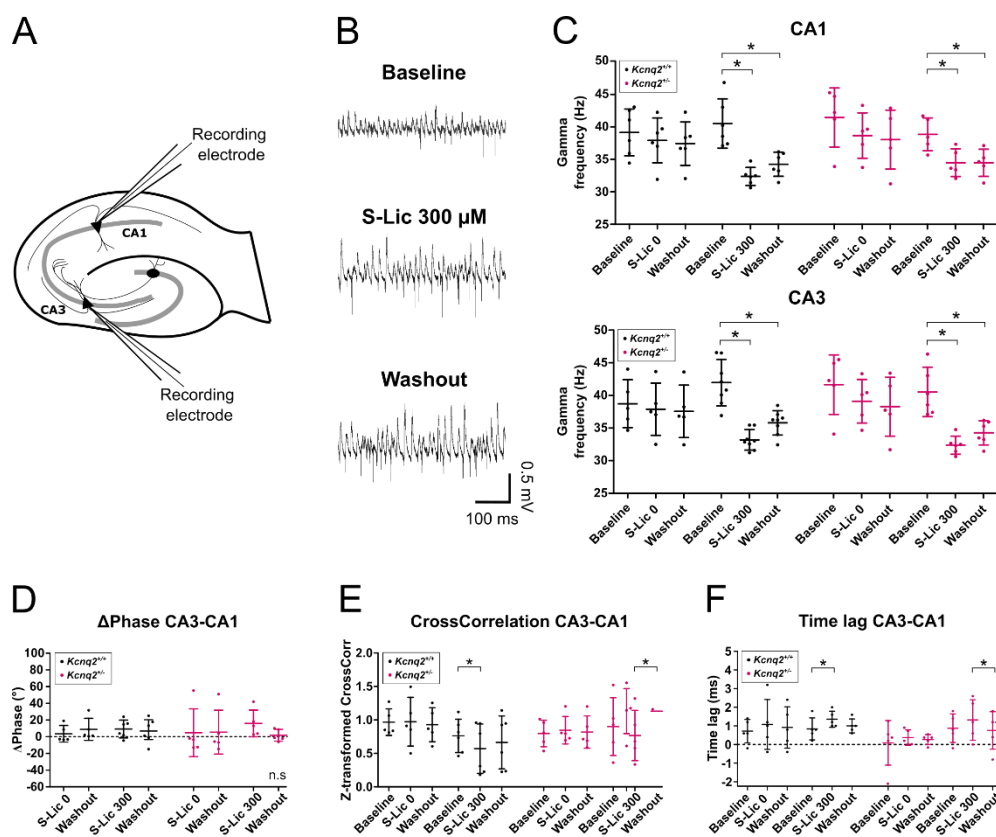


Figure 3: Effects of S-Lic on gamma oscillations *in vitro*. (A) Scheme of a mouse hippocampal slice showing CA3 and CA1 pyramidal layers and electrode positions during LFP recordings. (B) Examples of gamma rhythms during baseline, S-Lic application (300 μM) and washout. (C) Scatter plots showing the raw values of gamma frequency during baseline, S-Lic 0 μM or 300 μM , and washout. Top plot: data recorded from CA1, bottom plot: s

data recorded from CA3. **(D, E, F)** Scatter plot of the temporal and synchronization analyses between gamma rhythms in CA3 and CA1. **(D)** Delta (Δ) phase, **(E)** cross-correlation, **(F)** time lag. *Kcnq2^{+/+}* data are depicted in black, *Kcnq2^{+/-}* in dark pink. Each dot refers to one slice obtained from one animal, data are shown as mean \pm standard deviation. Asterisks indicate statistically significant differences as assessed by one-way ANOVA or Friedman test and Tukey's or Dunnett's *post-hoc* test for multiple comparisons on raw data, respectively (* or #: p-value \leq 0.05, n.s.: not significant.). (Figure modified from Monni et al., 2022, Fig. 2 and Suppl. Fig. 2).

7.2. S-Lic does not affect input/output behavior and intrinsic excitability in CA1

In order to better understand S-Lic effects on *in vitro* physiological hippocampal oscillations, I decided to investigate network properties critical for hippocampal network activity, such as the interplay between synaptic excitation and inhibition (Atallah & Scanziani, 2009; Buzsáki, 2015; Kubota et al., 2003; Maier et al., 2003). More specifically, input/output (I/O) and fEPSP/PS coupling can give insights on synaptic transmission basal properties and excitation-inhibition balance in the recorded region, respectively. I conducted I/O and fEPSP/PS extracellular recordings in CA1 region (Fig. 4A) in control conditions (S-Lic 0) and when applying the highest concentration of S-Lic (300 μ M). Surprisingly, both post-synaptic fEPSP slopes, and PS amplitude were not affected by S-Lic (Fig. 4B-C). Of note, I did not detect any difference between genotypes.

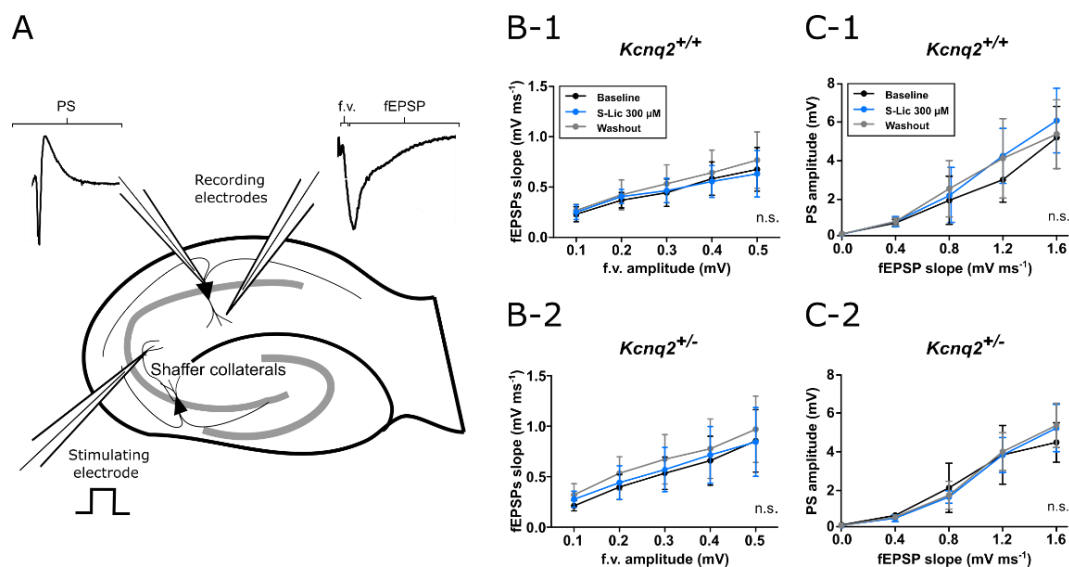


Figure 4: S-Lic does not affect input / output properties in the CA1 region *in vitro*. **(A)** Scheme of a mouse hippocampal slice showing CA3 Schaffer collaterals in which the stimulating electrode is positioned to provide electrical stimulation for the induction of fEPSPs and PS, recorder by two recording electrodes placed either at the st. radiatum or pyramidale, respectively. Note that the fEPSP is preceded by the fiber volley (f.v.). **(B-1, B-2)** Line graphs showing recorded fEPSPs slopes in relation to f.v. amplitudes, recorded in slices from *Kcnq2^{+/+}* **(B-1)** or *Kcnq2^{+/-}* **(B-2)** mice. Dots and lines represent mean fEPSPs slopes \pm SD for a given fiber volley amplitude. **(C-1, C-2)** Line graphs showing recorded PS amplitudes in relation to fEPSP slopes, recorded in slices from *Kcnq2^{+/+}* **(C-1)**

or *Kcnq2^{+/-}* (C-2) mice. Dots and lines represent mean PS amplitude \pm SD for a given fEPSP slope. For all the plots, black lines refer to baseline, blue lines to S-Lic 300 μ M and grey lines show washout values. n.s.: not significant. (Figure modified from Monni et al., 2022, Fig. 3).

7.3. S-Lic effects on *in vitro* pathological neuronal activity

The 4-AP acute model of seizure-like events (SLEs) is widely used to study synaptic foundations of network synchronization in pathological conditions (Avoli et al., 1993; Losi et al., 2016; Perreault & Avoli, 1992). In our lab, we have established this model both in interface chamber setup for experiments using rat brain slices (Heuzeroth et al., 2019) and in the submerged chamber by using human hippocampal slices (Kraus et al., 2020). I applied the same method for mouse hippocampal slices, optimizing it for the employment of the submerged chamber. Stable SLEs recorded from entorhinal cortex in brain slices obtained from both *Kcnq2^{+/+}* and *Kcnq2^{+/-}* mice were evoked upon bath-application of 100 μ M 4-AP (Fig. 6A). S-Lic effectively blocked SLE activity in a concentration-dependent manner, in both genotypes (Fig. 6B). Moreover, it has to be noted that at a submaximal concentration of 100 μ M, S-Lic reduced SLE incidence in all slices from *Kcnq2^{+/-}* mice but only in half of the slices from the wild type littermates. I calculated an estimate of S-Lic EC₅₀ to a value of 55.3 μ M for slices from *Kcnq2^{+/-}* mice and a value of 73.8 μ M for slices from *Kcnq2^{+/+}* mice. A statistical analysis of the EC₅₀ values according to pharmacological standards was not possible due to the requirement of at least three independent sets of experiments (Jiang & Kopp-Schneider, 2015) – for this thesis, I used one independent set of experiments to keep the number of used animals as low as possible according to 3Rs requirements.

7.4. Seizure threshold and ESL antiseizure efficacy in the 6 Hz psychomotor seizure model *in vivo*

Next, I expanded the study to an *in vivo* approach by establishing the 6 Hz psychomotor seizure procedure for our mouse model and subsequently testing the antiseizure efficacy of 4 doses of ESL. The 6 Hz psychomotor seizure test represents a model of seizures occurring in pharmacoresistant epilepsy and has been widely used to investigate the antiseizure efficacy of a variety of ASMs (Barker-Haliski et al., 2018; Barton et al., 2001). Firstly, I employed the staircase method optimized by Barton and colleagues (2001), to set the seizure threshold (referred to as CC₅₀), namely the current necessary to induce acute seizures in 50% of the mice. To this end, I used animals from both sexes and both genotypes and I stimulated them with increasing current intensities from a minimal value of 8 to a max of 24 mA. By performing the probit analysis, I found that the seizure threshold for male *Kcnq2^{+/-}* mice was decreased

when compared to the *Kcnq2^{+/+}* littermates, and this was in line with previous results (*Kcnq2^{+/+}*: CC₅₀=17.1 mA, 95% CI 16.2–17.9 mA; *Kcnq2^{+/-}*: CC₅₀=14.5 mA, 95% CI 13.6–15.5 mA). Results from female mice showed high variability of responses, particularly in the *Kcnq2^{+/+}* group (Fig. 5). We did not expect this result, as one of the planned analysis of the thesis was to investigate whether differences between sexes were present and to plan the following experiments accordingly. In particular, if no difference was found, we would have aimed to use both sexes randomly. Nevertheless, as no consistent result was obtained from female animals' data, we decided to carry out probit analysis and the following investigation of ESL antiseizure efficacy only in male animals.

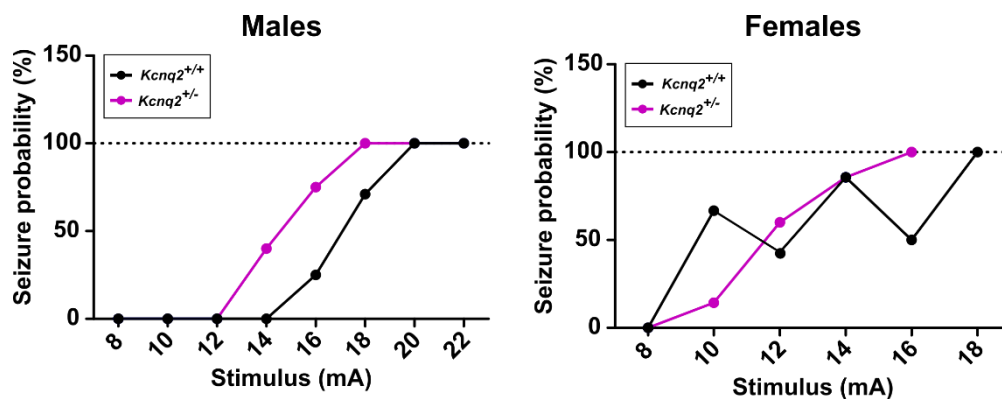
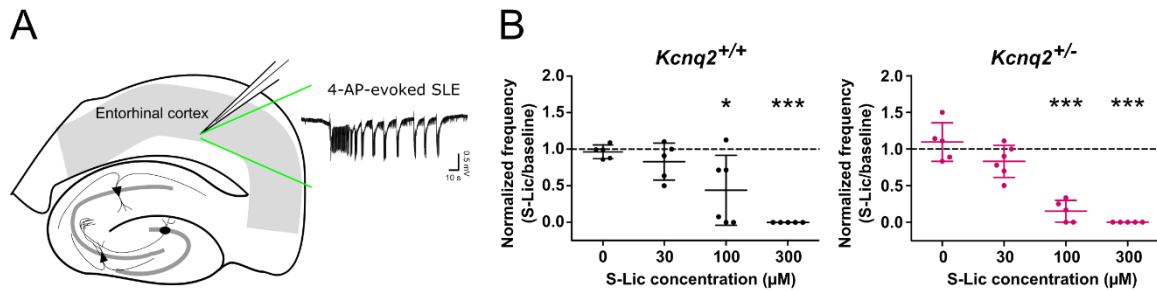


Figure 5: Seizure probability analysis in male and female *Kcnq2^{+/+}* and *Kcnq2^{+/-}* animals. Seizure probability for each stimulation intensity shown as line and points graphs calculated with the probit analysis. Black and dark pink points represent percentage ratios of stimulated and responding animals of *Kcnq2^{+/+}* and *Kcnq2^{+/-}* genotypes, respectively. The graphs show male data on the left (n=23 *Kcnq2^{+/+}*; n=16 *Kcnq2^{+/-}*) and female data on the right (n=25 *Kcnq2^{+/+}*; n=27 *Kcnq2^{+/-}*). (Figure partially modified from Monni et al., 2022, Fig. 5B).

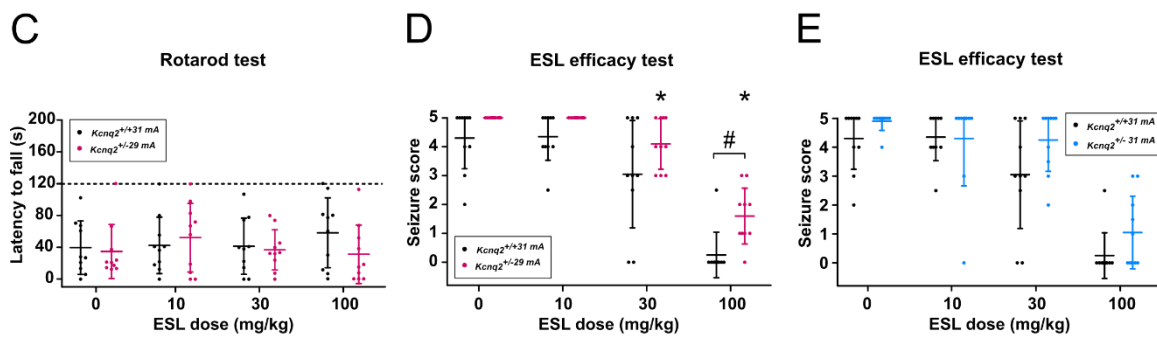
The *in vivo* antiseizure efficacy of ESL was tested by stimulating male animals with a current intensity of 1.5-fold CC₉₇, demonstrated to be suitable for the screening of ASMs' efficacy (Barker-Haliski et al., 2018; Barton et al., 2001). The resulting 1.5-fold CC₉₇ current intensities obtained from the staircase procedure were 31 mA for *Kcnq2^{+/+}* and 29 mA for *Kcnq2^{+/-}* mice. A Rotarod test performed immediately before the stimulation revealed no difference in latency to fall from the rotating rod between mice administered ESL and mice receiving vehicle control, and also between genotypes (Fig. 6C). ESL exerted antiseizure effects in a dose-dependent manner in both genotypes with higher efficacy in *Kcnq2^{+/+}* mice upon administration of ESL at 100 mg/kg (Fig. 6D). Data obtained after administration of vehicle control showed a trend of *Kcnq2^{+/-}* mice to exhibit a higher seizure score, observation confirmed also by the estimation of a higher ED₅₀ for *Kcnq2^{+/-}* mice compared to *Kcnq2^{+/+}* mice (67.4 vs 33.0 μ M, respectively). Finally, I replicated the tests in an additional group of *Kcnq2^{+/-}* mice by stimulating them with the 1.5-fold CC₉₇ specific for *Kcnq2^{+/+}* animals (31 mA) in order to exclude that the results were solely attributable to the different genotype-specific current intensities stimulation. I found that

the difference in seizure score were unchanged (Fig. 6E). Taken together, the results confirmed that *Kcnq2*^{+/-} mice displayed a lower seizure threshold compared to wild types and revealed the efficacy of ESL as a protecting compound against acute, electrically-induced seizures.

In vitro S-Lic antiseizure efficacy



In vivo ESL antiseizure efficacy



In vitro VS *In vivo* effectiveness

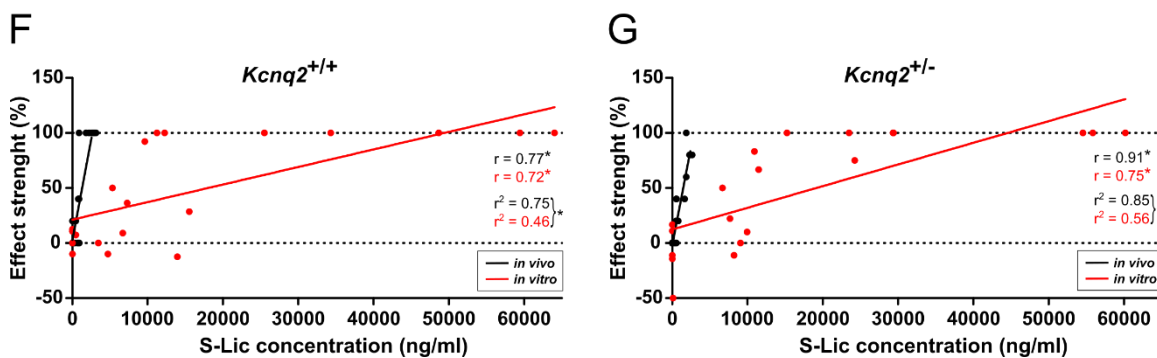


Figure 6: S-Lic and ESL antiseizure efficacy *in vitro* and *in vivo*. (A) Scheme of a mouse brain slice including hippocampus and the entorhinal cortex, where the electrode is positioned in order to record SLEs. (B) Scatter plots showing normalized *in vitro* SLEs frequency during application of vehicle control (0) and three increasing concentrations of S-Lic recorded in *Kcnq2*^{+/+} (left) and *Kcnq2*^{+/-} (right) mouse slices. (C) Scatter plots showing *in vivo* rotarod test results expressed as latency time to fall after oral injection of different ESL doses including vehicle control. Black dots (mean of 2 trials) and lines (\pm SD of all experiments): *Kcnq2*^{+/+} mice; pink dots (mean of 2 trials) and lines (\pm standard deviation of all experiments): *Kcnq2*^{+/-} mice. (C, D) Seizure scores (0-5) at different ESL

doses. **(D, E)** Scatter plots depicting ESL efficacy test expressed as seizure scores for each genotype-specific CC₉₇. Black color indicates *Kcnq2^{+/+}* mice, while pink color denotes *Kcnq2^{+/-}* mice **(D)**, blue color in **(E)** indicates *Kcnq2^{+/-}* mice stimulated with 1.5 x CC₉₇ of *Kcnq2^{+/+}* mice (31 mA). Data are depicted as mean ± SD and each dot refers to one slice obtained from one animal (*in vitro*) or one animal stimulated twice (*in vivo*). Asterisks indicate statistically significant differences as assessed by one-way ANOVA and Dunnett's *post-hoc* test for multiple comparisons or repeated measurements non-parametric Friedman test and Dunnett's *post-hoc* test for multiple comparisons. Number signs mark statistically significant differences between genotypes (*in vivo*) assessed by two-way ANOVA and Bonferroni's *post-hoc* test. **(F, G)** Dot plots showing the relationship between S-Lic concentration and antiseizure efficacy expressed as effect strength given in % for the experiments performed *in vitro* (SLEs, red) and *in vivo* (6 Hz-induced seizures, black). Right: *Kcnq2^{+/+}* mice, Left: *Kcnq2^{+/-}* mice. Each dot refers to one hippocampal slice or whole brain sample obtained from one animal. Statistically significant differences between black and red best-fit lines were assessed by linear regression analysis and asterisks indicate statistical significance. (Figure partially modified from Monni et al., 2022, Fig. 4, 5 and 6).

7.5. S-Lic concentration positively correlates with its antiseizure efficacy both *in vivo* and *in vitro*

In collaboration with BIAL laboratories in Porto (Portugal), we obtained the pharmacokinetic analysis of the main metabolite of ESL (S-Lic) from whole brain and plasma samples taken from mice that underwent 6 Hz psychomotor seizure procedure. In addition, S-Lic concentration was determined from hippocampal slices in which S-Lic was applied *in vitro*. I used these data to perform a correlation analysis between S-Lic tissue concentration and ESL antiseizure activity *in vitro* and *in vivo*. In line with previously demonstrated efficacy of ESL against seizures, S-Lic concentration found in plasma and brain was significantly and negatively correlated to the *in vivo* seizure score, in both genotypes (data shown in Fig. 6A-B of the publication Monni et al., 2022). Correlation and linear regression analyses were then conducted to compare S-Lic tissue concentrations from *in vitro* and *in vivo* experiments with the corresponding effect strength. The effect strength was defined as the relative drug efficacy in suppressing seizure-like activity. For the *in vitro* experiments, effect strength was considered as [(1 – SLE frequency drug/SLE frequency baseline) x100]. Instead, the *in vivo* experiments effect strength corresponded to the seizure scores, as follows: 5 = 0%; 4 = 20%; 3 = 40%; 2 = 60%; 1 = 80%; 0 = 100%. S-Lic concentration measured in brain tissues from both *in vitro* and *in vivo* experiments correlated significantly and positively with its effect strength, in either genotype. In addition, simple linear regression analysis revealed a statistically significant difference between *in vitro* and *in vivo* correlation data from both genotypes (Fig. 6F-G). Interestingly, the estimation of EC₅₀ values, as well as the results on the linear regression comparing *in vitro* and *in vivo* effectiveness, revealed that compared to ED₅₀ for *in vivo* antiseizure efficacy considerably higher concentrations of S-Lic are necessary to effectively reduce seizure-like activity *in vitro* (41 µM *in vitro* vs 4-6 µM *in vivo*).

8. Discussion

The *KCNQ2*-related epilepsy syndrome is a rare form of epilepsy with onset at the very first days of life. This syndrome presents two main phenotypes: (1) the self-limited familial neonatal epilepsy and (2) the epileptic encephalopathy. The self-limited epilepsy form represents the mild phenotype, usually treated with common ASMs such as valproate, phenytoin or carbamazepine, and spontaneously resolving within 4-6 months, often carrying an increased risk of developing epilepsy later in life. On the other hand, the sporadically occurring severe encephalopathy phenotype is characterized by the presence of pharmacoresistant epilepsy accompanied by severe neurodevelopmental impairment in neonates and children. Despite the presence of more than 20 different types of potent ASMs, pharmacoresistance continues to represent one of the main challenges.

In the present thesis, I investigated the *in vitro* and *in vivo* effects of ESL and its major active metabolite S-Lic in a mouse model resembling the features of self-limited *KCNQ2*-related epilepsy (Watanabe et al., 2000) as a first endeavor to evaluate the potential role of ESL in the treatment of the *KCNQ2* disease spectrum.

Firstly, I successfully established all three types of local field potential extracellular recordings of *in vitro* hippocampal oscillations. Physiological SPW-R and gamma oscillations, and pathological seizure-like events recordings were optimized by using either a submerged chamber or a Haas-type interface chamber, such that an investigation on S-Lic effects was reliably achievable. In addition, I established input/output and fEPSP/PS coupling stimulation experiments in the submerged chamber electrophysiology setup of our lab, in order to be able to test S-Lic effects on synaptic activity and intrinsic excitability of CA1 neuronal population, respectively. *In vitro*, S-Lic (1) decreased SPW-Rs incidence while increasing their amplitude, (2) decreased the frequency of gamma oscillations and possibly CA3-CA1 cross-correlation during these oscillations, and (3) did not exert major effects on synaptic activity and intrinsic excitability as investigated in extracellular stimulation recordings in CA1. Moreover, (4) S-Lic effectively reduced 4-AP-induced pathological seizure-like events. The effects of S-Lic on *in vitro* neuronal oscillations may be associated with cognitive side effects often observed with high doses of ESL (Andermann et al., 2018). However, the therapeutic concentrations of S-Lic measured in plasma samples from patients are lower by a magnitude of ~10 when compared to the ones I used in the *in vitro* condition (Hebeisen et al., 2015). Although I did not find substantial differences between the genotypes *in vitro*, the phenomenon is likely related to the chosen mouse model. In fact, heterozygous mice for *Kcnq2* gene have been shown to carry a suppression of the M-current of almost 60% in neurons, which was accompanied by a

reduction in *Kcnq2* mRNA expression of about 30% (Robbins et al., 2013; Watanabe et al., 2000). On the other hand, the model has demonstrated that the same current appeared to be fully maintained in neurons from adult (≥ 6 weeks) *Kcnq2* heterozygous mice (Robbins et al., 2013). Robbins et al. proposed that this phenomenon might be caused by an increased *Kcnq2* mRNA transcription generated by hyperexcitable neurons. In my thesis, I employed juvenile mice (≤ 4 weeks). Given that the M-current is involved in shaping the network synchronization underlying hippocampal physiological oscillations (such as SPW-Rs and gamma neuronal activities) (Cooper et al., 2001; Fidzinski et al., 2015; Trompoukis et al., 2020), it is likely that the “compensatory” mechanism shown by Robbins and colleagues was perhaps already affecting the regulation of neuronal oscillations. This phenomenon might clarify the lack of differences between the genotypes upon application of S-Lic during physiological hippocampal oscillations. S-Lic effects on physiological hippocampal oscillations may point to an impact of the drug on rhythm generators. Given the decreased SPW-Rs incidence but also the decreased gamma oscillations frequency accompanied by a likely decreased CA3-CA1 cross-correlation, it is possible that S-Lic affects the temporal relationship between CA3 and CA1, potentially by causing a less precise spiking of the neuronal populations involved. As discussed in the publication, through the inhibition of the voltage-gated sodium channels, S-Lic might affect the feedback regulation between interneurons and pyramidal neurons, which plays a critical role in the synchronization of hippocampal oscillations (Fisahn et al., 1998; Monni et al., 2022). It has to be noted, however, that we decided to perform the follow-up analysis on the cross-correlation between CA3 and CA1 during gamma oscillations in a second moment compared to the data collection. The sample size calculation revealed to be too low, being it slightly underpowered due to the *post-hoc* nature of the setting. In this specific case, I performed a *post-hoc* calculation in order to check for the appropriate sample size calculated *a priori* for the analysis of the CA3-CA1 cross-correlation, even though the power and sample size calculations must be performed while planning the experiments and not while interpreting results (Goodman & Berlin, 1994).

The slow restoration of the M-current in our animal model might have also affected pathological *in vitro* seizure-like events, even if to a lower extent. Clinically, this phenomenon might resemble the transitory epilepsy caused by the *KCNQ2* gene mutation underlying the mild phenotype in patients experiencing the self-limited phenotype (Robbins et al., 2013; Watanabe et al., 2000). The age of the animal model used here represents a limitation of the study but at the same time, it was necessary in order to be able to establish and apply the 6 Hz psychomotor seizure model *in vivo*. As we discuss in the published work (Monni et al., 2022), acute epilepsy models present limitations *per se* and chronic models of spontaneous seizures represent a more suitable choice to study pharmaco-resistant epilepsy in general. However, at

the time of the experiments performed for my thesis, no adequate chronic animal model was present to investigate ESL effects in *KCNQ2* childhood epilepsy. Only in 2020, Milh and colleagues developed a knock-out mouse model carrying the p.(Thr274Met) variant, resembling most of the pathophysiological features of the *KCNQ2* severe form epileptic encephalopathy (Milh et al., 2020). Therefore, future investigation on ESL antiseizure efficacy against pharmacoresistant *KCNQ2* epilepsy by using the *Kcnq2*^{p.(Thr274Met)/+} mouse model would be a helpful and valuable additional pre-clinical data collection for a possible novel treatment.

In addition to S-Lic effects on *in vitro* physiological hippocampal oscillations, I was able to show that S-Lic substantially reduced and even blocked pathological SLEs *in vitro*. These effects were present in both genotypes but, curiously, at the submaximal concentration of 100 μ M, S-Lic effectiveness against SLEs was higher in hippocampal slices from heterozygous mice than those from the wild type littermates (see Fig. 6B). This observation was confirmed by the estimation of a higher EC₅₀ in wild type mice compared to the heterozygous (73.8 μ M vs 55.3 μ M, respectively). However, it has to be noted that induction of *in vitro* SLEs through the inhibition of potassium channels by 4-AP is a strong pro-epileptic stimulus that impacts the physiological network of the hippocampus and its equilibrium (Heuzeroth et al., 2019; Perreault & Avoli, 1992). This might also represent a possible explanation for the big difference between S-Lic effective concentrations *in vitro* and those measured from *in vivo* experiments (almost a magnitude of ~10). In order to clarify whether S-Lic effect against *in vitro* SLEs is specific, other models of *in vitro* SLEs should be tested. In our lab, we have tried to establish other models of acute seizure-like activity, such as the reduction of magnesium ion concentration (which unblocks NMDA receptors) or the application of the GABAergic blocker bicuculline. However, these methods are less consistent than the application of 4-AP and evoke SLEs in only 50% of slices (Kraus et al., 2020). In addition, the low magnesium model of acute SLEs has been shown to display unstable epileptiform activity that is quickly substituted by a continuous rhythmic activity, often accompanied by spreading depolarization, which precludes a proper analysis of drug effects (Anderson et al., 1986; Dulla et al., 2018; Mody et al., 1987). The 4-AP model was already established in our lab for stable SLEs recorded from rat hippocampal slices in the interface chamber setup (Heuzeroth et al., 2019). Therefore, I combined the same model and the advantages of the modified submerged chamber in order to be able to evoke stable SLEs in hippocampal slices from the *Kcnq2* mouse model. Furthermore, I decided to use juvenile mice (P21-28) for S-Lic and ESL antiseizure efficacy testing as well, for several reasons. My main interest resided on whether ESL would have been able to counteract the increased susceptibility and sensibility to epileptogenic stimuli showed by this mouse model at a juvenile age range and resembling the human clinical phenotype. Besides translational reasons, the mice age-range was chosen also for the specific technical requirements needed

in order to be able to evoke *in vitro* SLEs in brain slice preparations and acute seizures *in vivo* induced by the 6 Hz psychomotor seizure model (Barton et al., 2001; Raimondo et al., 2017). Moreover, the emergence and patterns of SLEs is strongly impacted by the age of the animals from which the brain slices are prepared. This is mainly due to the complex differences in neuronal excitability and changing of signaling pathways during development (Raimondo et al., 2017). To name the most important, the role of the inhibitory neurotransmitter GABA being depolarizing instead of hyperpolarizing during gestation and first postnatal days (until P13 in rats and P8 in mice), mechanistically due to an increased intracellular chloride concentration (Ben-Ari, 2002; Khazipov et al., 2004; Valeeva et al., 2016). This initial dual action of GABA considerably influences the degree of seizure susceptibility of the brain tissue, both *in vitro* and *in vivo* (Isaev et al., 2005; Khazipov et al., 2004). Thus, I chose to use P21-28 mice for *in vitro* SLEs induction in order to be able to compare and test the effect of S-Lic, without the influence of neuronal networks excitation developmental changes.

Nevertheless, a critical limitation of *in vitro* acute models of SLEs that differentiate them from epileptic animals is the unavailability of the epileptic network *per se* (Heuzeroth et al., 2019). In fact, *in vitro* SLEs reproduce only the electrographic features of the epileptogenic activity but not seizures as experienced by a living animal. Therefore, given S-Lic efficacy *in vitro*, I further investigated its antiseizure potential in the 6 Hz psychomotor model of acute seizures *in vivo* and was able to demonstrate that: (1) *Kcnq2*^{+/-} mice have a lower seizure threshold compared to wild types littermates, (2) ESL effectively reduces seizure incidence and strength in the 6 Hz psychomotor seizure model, (3) *Kcnq2*^{+/-} mice show a decreased sensitivity to ESL compared to *Kcnq2*^{+/+} mice and (4) no effects of ESL on motor coordination tested with Rotarod test are detected at the doses used for this thesis. Moreover, pharmacokinetic analysis of S-Lic concentration in brain tissue and plasma confirms that (5) S-Lic concentration negatively correlates with seizure score and reveals (6) differences between *in vitro* and *in vivo* effective S-Lic concentrations.

The results on the decreased seizure threshold shown by the *Kcnq2* heterozygous mice are in line with previous studies conducted by using both chemically and electrically-evoked acute seizures *in vivo* (Otto et al., 2009; Watanabe et al., 2000). In contrast with these studies, my results on female animals represent a weakness of this work. In fact, the data I collected during the staircase test, which are needed to calculate the CC₉₇, were very variable particularly for the wild type genotype and did not allow a proper and consistent probit analysis. The high variability of seizure susceptibility seen in female animals is likely caused by the hormonal cycle effects on neuronal excitability and, consequently, on the seizure threshold itself (Scharfman & MacLusky, 2006). To clarify this point, an additional study of ESL efficacy in

female mice taking into account both age and the hormonal cycle would have been necessary. Given that during the planning of my project the sample size of the animals was calculated *a priori*, I did not have the possibility to conduct the test on an additional group of female animals of both genotypes in order to obtain data by taking into account the hormonal cycle. Consequently, I could perform the following 6 Hz psychomotor seizure model to test ESL antiseizure efficacy only on male animals. However, in the following experiments ESL protected the animals from both genotypes against electrically-evoked acute seizures. The protection was higher in wild type compared to heterozygous animals, further confirming the presence of more resistant seizures in the *Kcnq2*^{+/-} genotype. The estimation of the ESL-ED₅₀ further reinforced this finding (33 mg/kg vs 67 mg/kg in *Kcnq2*^{+/+} and *Kcnq2*^{+/-} respectively). Another intriguing aspect arises from control experiments: *Kcnq2*^{+/-} showed higher seizure scores compared to *Kcnq2*^{+/+} even when the drug was not administered. This result is in line with the increased excitability caused by the heterozygous deletion of the *Kcnq2* gene, which is perhaps easier to detect *in vivo* than in *in vitro* preparations, where the network connectivity is moderately but inevitably compromised. Finally, all used doses of ESL did not affect motor coordination when examined with the Rotarod test. This finding is in line with previous *in vivo* studies on ESL, where it has been demonstrated that ESL median toxic dose was 300 mg/kg and no motor impairment was present up to 150 mg/kg (Doeser et al., 2015). Overall, the results of the *in vivo* experiments point to a strong antiseizure efficacy of ESL tested with the 6 Hz psychomotor seizure model and confirm a higher drug resistance in the *Kcnq2* heterozygous mice.

The antiseizure efficacy of ESL at the doses used for my thesis has shown comparable effects also in previous studies, in different *in vitro* and *in vivo* epilepsy models. ESL at dose range of 100-300 mg/kg has been demonstrated to prevent both acute and chronic seizures and also epileptogenesis in mouse and rat models of epilepsy (Doeser et al., 2015; Sierra-Paredes et al., 2014). ESL antiseizure efficacy has been demonstrated also at lower doses (30-100 mg/kg). At this range, ESL exerted its protecting efficacy against chronic seizures induced by corneal and amygdala kindling *in vivo* models (Potschka et al., 2014). Moreover, ESL at 50-150 mg/kg was effective in both MES and 6 Hz psychomotor procedures applied to NMRI adult wild type mice (Hebeisen et al., 2015). *In vitro*, the metabolite S-Lic at concentrations of 30-300 µM has shown to reduce intracellular epileptic activity induced by magnesium free aCSF and 4-AP application in hippocampal slices from wild type CD1 mice (Hebeisen et al., 2015). In slight contrast with the results of my thesis, Hebeisen and colleagues have shown that measurements of S-Lic from plasma and whole brain result in comparable values between S-Lic concentrations used for the *in vitro* studies and ESL doses employed for *in vivo* experiments (2015). Conversely, I observed a difference between the effective doses needed to exert

antiseizure efficacy *in vivo*, which was ~10 times lower than the effective concentration *in vitro* (Monni et al., 2022). Given the limited number of doses used in this thesis, I was able to calculate only estimations of the effective concentrations and doses and a reliable statistical analysis agreeing with the standards of pharmacology (Jiang & Kopp-Schneider, 2015) was not possible. Nevertheless, the considerations that arose from the estimated values underlie the importance of an extreme caution that is necessary when interpreting results of a drug's effects in *in vitro* and *in vivo* disease models.

ESL has undergone various clinical trials for other epilepsy types in children and adults. ESL showed good tolerability in patients and good efficacy against seizures in epilepsy pharmacoresistant to other sodium channel blockers, such as carbamazepine and oxcarbazepine (Almeida et al., 2008; Elger et al., 2009; Galiana et al., 2017; Halász et al., 2010; Rocamora, 2015; Trinká et al., 2018). Therefore, the focus of my thesis indirectly addressed one of the most rare and severe epilepsy syndromes, namely the *KCNQ2* encephalopathy, characterized by epilepsy refractory towards the most commonly used and potent ASMs such as phenytoin and carbamazepine (Kuersten et al., 2020). One of the advantages of ESL over other ASMs in terms of antiseizure efficacy and safety, likely resides on its slightly different molecular mechanisms of action. Indeed, several differences have been shown between ESL and carbamazepine, oxcarbazepine and phenytoin: ESL has a lower affinity for the resting state of voltage-gated sodium channels, has been proven to prolong the slow inactivation of these channels, and does not display the classical fast inactivation phenomenon common with other sodium channel blockers. In addition to sodium channel block, ESL inhibits Ca_v3.2 T-type calcium channels (Doeser et al., 2015; Hebeisen et al., 2015; Soares-da-Silva et al., 2015). These molecular mechanisms might reveal a role of ESL as a potential treatment to prevent seizures in *KCNQ2* epilepsy syndrome, especially the severe encephalopathy phenotype.

9. Conclusion

Taken together, the results of my PhD thesis verified our initial hypothesis. In fact, overall the data show that the reduced expression of *KCNQ2* potassium channels in a mouse model causes neuronal hyperexcitability, which can be efficiently targeted by an antiseizure medication as ESL, acting primarily by inhibiting voltage-gated sodium channels. Moreover, the thesis confirms the increased seizure susceptibility of the mouse model employed and demonstrates the antiseizure efficacy of eslicarbazepine acetate in the 6 Hz psychomotor seizure model *in vivo*. Finally, the thesis work underpins considerable differences between *in vitro* and *in vivo* pharmacological studies in acute seizure and epilepsy models.

10. References

- Abidi, A., Devaux, J. J., Molinari, F., Alcaraz, G., Michon, F. X., Sutera-Sardo, J., Becq, H., Lacoste, C., Altuzarra, C., Afenjar, A., Mignot, C., Doummar, D., Isidor, B., Guyen, S. N., Colin, E., De La Vaissière, S., Haye, D., Trauffer, A., Badens, C., Prieur, F., Lesca, G., Villard, L., Milh, M., & Aniksztejn, L. (2015). A recurrent KCNQ2 pore mutation causing early onset epileptic encephalopathy has a moderate effect on M current but alters subcellular localization of Kv7 channels. *Neurobiology of Disease*, *80*, 80–92. <https://doi.org/10.1016/j.nbd.2015.04.017>
- Almeida, L., Minciu, I., Nunes, T., Butoianu, N., Falcão, A., Magureanu, S. A., & Soares-Da-Silva, P. (2008). Pharmacokinetics, efficacy, and tolerability of eslicarbazepine acetate in children and adolescents with epilepsy. *Journal of Clinical Pharmacology*, *48*(8), 966–977. <https://doi.org/10.1177/0091270008319706>
- Almeida, L., & Soares-da-Silva, P. (2007). Eslicarbazepine acetate (BIA 2-093). *Neurotherapeutics: The Journal of the American Society for Experimental NeuroTherapeutics*, *4*(1), 88–96. <https://doi.org/10.1016/J.NURT.2006.10.005>
- Andermann, E., Biton, V., Benbadis, S. R., Shneker, B., Shah, A. K., Carreño, M., Trinkka, E., Ben-Menachem, E., Biraben, A., Rocha, F., Gama, H., Cheng, H., & Blum, D. (2018). Psychiatric and cognitive adverse events: A pooled analysis of three phase III trials of adjunctive eslicarbazepine acetate for partial-onset seizures. *Epilepsy & Behavior: E&B*, *82*, 119–127. <https://doi.org/10.1016/J.YEBEH.2017.12.017>
- Anderson, W., Lewis, D., Swartzwelder, H., & Wilson, W. (1986). Magnesium-free medium activates seizure-like events in the rat hippocampal slice. *Brain Research*, *398*(1), 215–219. [https://doi.org/10.1016/0006-8993\(86\)91274-6](https://doi.org/10.1016/0006-8993(86)91274-6)
- Atallah, B. V., & Scanziani, M. (2009). Instantaneous Modulation of Gamma Oscillation Frequency by Balancing Excitation with Inhibition. *Neuron*, *62*(4), 566–577. <https://doi.org/10.1016/j.neuron.2009.04.027>
- Avoli, M., Psarropoulou, C., Tancredi, V., & Fueta, Y. (1993). On the Synchronous Activity Induced by 4-Aminopyridine Subfield of Juvenile Rat Hippocampus in the CA3 subfield of juvenile rat hippocampus. *Journal of Neurophysiology*, *70*(3), 1018–1029.
- Avoli, M., Barbarosle, M., Lücke, A., Nagao, T., Lopantsev, V., & Köhling, R. (1996). Synchronous GABA-mediated potentials and epileptiform discharges in the rat limbic system in vitro. *Journal of Neuroscience*, *16*(12), 3912–3924. <https://doi.org/10.1523/jneurosci.16-12-03912.1996>
- Axmacher, N., Elger, C. E., & Fell, J. (2008). Ripples in the medial temporal lobe are relevant for human memory consolidation. *Brain*, *131*(7), 1806–1817. <https://doi.org/10.1093/brain/awn103>
- Axon Guide - Electrophysiology and Biophysics Laboratory Techniques | Molecular Devices*. Retrieved from <http://www.moleculardevices.com/patents>
- Barker-Haliski, M., Löscher, W., Xiao, B., Brandt, C., Ravizza, T., Smolders, I., & Harte-Hargrove, L. C. (2018). A companion to the preclinical common data elements for pharmacologic studies in animal models of seizures and epilepsy. A Report of the TASK3 Pharmacology Working Group of the ILAE/AES Joint Translational Task Force. *Epilepsia Open*, *3*, 53–68. <https://doi.org/10.1002/epi4.12254>
- Barton, M. E., Klein, B. D., Wolf, H. H., & White, H. S. (2001). Pharmacological characterization of the 6 Hz psychomotor seizure model of partial epilepsy. In *Epilepsy Research* (Vol. 47). www.elsevier.com/locate/epilepsyres
- Ben-Ari, Y. (2002). Excitatory actions of gaba during development: the nature of the nurture. *Nature Reviews Neuroscience* *2002* *3*:9, *3*(9), 728–739. <https://doi.org/10.1038/nrn920>
- Benes, J., Parada, A., Figueiredo, A. A., Alves, P. C., Freitas, A. P., Learmonth, D. A., Cunha, R. A., Garrett, J., & Soares-Da-Silva, P. (1999). Anticonvulsant and sodium channel-blocking properties of novel 10,11-dihydro-5H-dibenz[b,f]azepine-5-carboxamide derivatives. *Journal of Medicinal Chemistry*, *42*(14), 2582–2587. <https://doi.org/10.1021/jm980627g>
- Bieri, K. W., Bobbitt, K. N., & Colgin, L. L. (2014). Slow and fast γ rhythms coordinate different spatial coding modes in hippocampal place cells. *Neuron*, *82*(3), 670–681. <https://doi.org/10.1016/J.NEURON.2014.03.013>

- Blankenship, A. G., & Feller, M. B. (2010). Mechanisms underlying spontaneous patterned activity in developing neural circuits. *Nature Reviews. Neuroscience*, *11*(1), 18–29. <https://doi.org/10.1038/NRN2759>
- Bonifácio, M. J., Sheridan, R. D., Parada, A., Cunha, R. A., Patmore, L., & Soares-Da-Silva, P. (2001). Interaction of the novel anticonvulsant, BIA 2-093, with voltage-gated sodium channels: comparison with carbamazepine. *Epilepsia*, *42*(5), 600–608. <https://doi.org/10.1046/J.1528-1157.2001.43600.X>
- Brown, D. A., & Adams, P. R. (1980). Muscarinic suppression of a novel voltage-sensitive K⁺ current in a vertebrate neurone [18]. In *Nature* (Vol. 283, Issue 5748, pp. 673–676). <https://doi.org/10.1038/283673a0>
- Brown, David A., & Passmore, G. M. (2009). Neural KCNQ (Kv7) channels. In *British Journal of Pharmacology* (Vol. 156, Issue 8, pp. 1185–1195). John Wiley & Sons, Ltd. <https://doi.org/10.1111/j.1476-5381.2009.00111.x>
- Brown, W. C., Schiffman, D. O., Swinyard, E. A., & Goodman, L. S. (1953). Comparative assay of an antiepileptic drugs by psychomotor seizure test and minimal electroshock threshold test. *The Journal of Pharmacology and Experimental Therapeutics*, *107*(3), 273–283. <http://www.ncbi.nlm.nih.gov/pubmed/13035666>
- Buhl, E. H., Tamás, G., & Fisahn, A. (1998). Cholinergic activation and tonic excitation induce persistent gamma oscillations in mouse somatosensory cortex in vitro. *Journal of Physiology*, *513*(1), 117–126. <https://doi.org/10.1111/j.1469-7793.1998.117by.x>
- Buzsáki, G. (1986). Hippocampal sharp waves: Their origin and significance. *Brain Research*, *398*(2), 242–252. [https://doi.org/10.1016/0006-8993\(86\)91483-6](https://doi.org/10.1016/0006-8993(86)91483-6)
- Buzsáki, G. (2015). Hippocampal sharp wave-ripple: A cognitive biomarker for episodic memory and planning. *Hippocampus*, *25*(10), 1073–1188. <https://doi.org/10.1002/hipo.22488>
- Buzsáki, G., Anastassiou, C. A., & Koch, C. (2012). The origin of extracellular fields and currents — EEG, ECoG, LFP and spikes. *Nature Reviews Neuroscience* *2012* *13*:6, *13*(6), 407–420. <https://doi.org/10.1038/nrn3241>
- Buzsáki, G., Horváth, Z., Urioste, R., Hetke, J., & Wise, K. (1992). High-frequency network oscillation in the hippocampus. *Science (New York, N.Y.)*, *256*(5059), 1025–1027. <https://doi.org/10.1126/SCIENCE.1589772>
- Buzsáki, G., Lai-Wo S., L., & Vanderwolf, C. H. (1983). Cellular bases of hippocampal EEG in the behaving rat. *Brain Research*, *287*(2), 139–171. [https://doi.org/10.1016/0165-0173\(83\)90037-1](https://doi.org/10.1016/0165-0173(83)90037-1)
- Buzsáki, G., & Wang, X.-J. (2012). Mechanisms of Gamma Oscillations. *Annual Review of Neuroscience*, *35*(1), 203–225. <https://doi.org/10.1146/annurev-neuro-062111-150444>
- Cheah, C. S., Lundstrom, B. N., Catteral, W. A., & Oakley, J. C. (2019). Impairment of Sharp-Wave Ripples in a Murine Model of Dravet Syndrome. *Journal of Neuroscience*, *39*(46), 9251–9260. <https://doi.org/10.1523/JNEUROSCI.0890-19.2019>
- Chen, Z., Brodie, M. J., Liew, D., & Kwan, P. (2018). Treatment outcomes in patients with newly diagnosed epilepsy treated with established and new antiepileptic drugs a 30-year longitudinal cohort study. *JAMA Neurology*, *75*(3), 279–286. <https://doi.org/10.1001/jamaneurol.2017.3949>
- Cohen, I., & Miles, R. (2000). Contributions of intrinsic and synaptic activities to the generation of neuronal discharges in in vitro hippocampus. *The Journal of Physiology*, *524 Pt 2*(Pt 2), 485–502. <https://doi.org/10.1111/J.1469-7793.2000.00485.X>
- Colgin, L. L. (2015). Do slow and fast gamma rhythms correspond to distinct functional states in the hippocampal network? *Brain Research*, *1621*, 309. <https://doi.org/10.1016/J.BRAINRES.2015.01.005>
- Colgin, L. L., Denninger, T., Fyhn, M., Hafting, T., Bonnevie, T., Jensen, O., Moser, M. B., & Moser, E. I. (2009). Frequency of gamma oscillations routes flow of information in the hippocampus. *Nature*, *462*(7271), 353–357. <https://doi.org/10.1038/nature08573>
- Cooper, E. C., Harrington, E., Jan, Y. N., & Jan, L. Y. (2001). M channel KCNQ2 subunits are localized to key sites for control of neuronal network oscillations and synchronization in mouse brain. *Journal of Neuroscience*, *21*(24), 9529–9540. <https://doi.org/10.1523/jneurosci.21-24-09529.2001>
- Csicsvari, J., Jamieson, B., Wise, K. D., & Buzsáki, G. (2003). Mechanisms of gamma oscillations in the hippocampus of the behaving rat. *Neuron*, *37*(2), 311–322. [https://doi.org/10.1016/S0896-6273\(02\)01169-8](https://doi.org/10.1016/S0896-6273(02)01169-8)
- D’Antuono, M., Köhling, R., Ricalzone, S., Gotman, J., Biagini, G., & Avoli, M. (2010). Antiepileptic drugs abolish

ictal but not interictal epileptiform discharges in vitro. *Epilepsia*, 51(3), 423–431. <https://doi.org/10.1111/j.1528-1167.2009.02273.x>

- Delmas, P., & Brown, D. A. (2005). Pathways modulating neural KCNQ/M (Kv7) potassium channels. In *Nature Reviews Neuroscience* (Vol. 6, Issue 11, pp. 850–862). Nature Publishing Group. <https://doi.org/10.1038/nrn1785>
- Devaux, J. J., Kleopa, K. A., Cooper, E. C., & Scherer, S. S. (2004). KCNQ2 Is a Nodal K⁺ Channel. *Journal of Neuroscience*, 24(5), 1236–1244. <https://doi.org/10.1523/JNEUROSCI.4512-03.2004>
- Doeser, A., Dickhof, G., Reitze, M., Uebachs, M., Schaub, C., Pires, N. M., Bonifácio, M. J., Soares-Da-Silva, P., & Beck, H. (2015). Targeting pharmacoresistant epilepsy and epileptogenesis with a dual-purpose antiepileptic drug. *Brain*, 138(2), 371–387. <https://doi.org/10.1093/brain/awu339>
- Dulla, C. G., Janigro, D., Jiruska, P., Raimondo, J. V., Ikeda, A., Lin, C.-C. K., Goodkin, H. P., Galanopoulou, A. S., Bernard, C., & de Curtis, M. (2018). How do we use in vitro models to understand epileptiform and ictal activity? A report of the TASK1-WG4 group of the ILAE/AES Joint Translational Task Force. *Epilepsia Open*, 3(4), 460–473. <https://doi.org/10.1002/epi4.12277>
- Dunham, N. W., & Miya, T. S. (1957). A Note on a Simple Apparatus for Detecting Neurological Deficit in Rats and Mice**College of Pharmacy, University of Nebraska, Lincoln 8. *Journal of the American Pharmaceutical Association (Scientific Ed.)*, 46(3), 208–209. <https://doi.org/10.1002/jps.3030460322>
- EC50 Calculator | AAT Bioquest. Retrieved November 24, 2020, from <https://www.aatbio.com/tools/ec50-calculator>
- Ego-Stengel, V., & Wilson, M. A. (2010). Disruption of ripple-associated hippocampal activity during rest impairs spatial learning in the rat. *Hippocampus*, 20(1), 1. <https://doi.org/10.1002/HIPO.20707>
- Elger, C., Halász, P., Maia, J., Almeida, L., & Soares-Da-Silva, P. (2009). Efficacy and safety of eslicarbazepine acetate as adjunctive treatment in adults with refractory partial-onset seizures: A randomized, double-blind, placebo-controlled, parallel-group phase III study. *Epilepsia*, 50(3), 454–463. <https://doi.org/10.1111/j.1528-1167.2008.01946.x>
- EpilepsyDiagnosis.org*. Retrieved April 28, 2021, from <https://www.epilepsydiagnosis.org/>
- Falco-Walter, J. J., Roehl, K., Ouyang, B., & Balabanov, A. (2019). Do certain subpopulations of adults with drug-resistant epilepsy respond better to modified ketogenic diet treatments? Evaluation based on prior resective surgery, type of epilepsy, imaging abnormalities, and vagal nerve stimulation. *Epilepsy and Behavior*, 93, 119–124. <https://doi.org/10.1016/j.yebeh.2019.01.010>
- Fidzinski, P., Korotkova, T., Heidenreich, M., Maier, N., Schuetze, S., Kobler, O., Zuschratter, W., Schmitz, D., Ponomarenko, A., & Jentsch, T. J. (2015). KCNQ5 K⁺ channels control hippocampal synaptic inhibition and fast network oscillations. *Nature Communications*, 6, 6254. <https://doi.org/10.1038/ncomms7254>
- Fiest, K. M., Sauro, K. M., Wiebe, S., Patten, S. B., Kwon, C. S., Dykeman, J., Pringsheim, T., Lorenzetti, D. L., & Jetté, N. (2017). Prevalence and incidence of epilepsy. In *Neurology* (Vol. 88, Issue 3, pp. 296–303). Lippincott Williams and Wilkins. <https://doi.org/10.1212/WNL.0000000000003509>
- Finney, D. J. (1971). Probit Analysis. *Journal of Pharmaceutical Sciences*, 60(9), 1432. <https://doi.org/10.1002/jps.2600600940>
- Fisahn, A., Pike, F. G., Buhl, E. H., & Paulsen, O. (1998). Cholinergic induction of network oscillations at 40 Hz in the hippocampus in vitro. *Nature*, 394(6689), 186–189. <https://doi.org/10.1038/28179>
- Fisher, R. S., Cross, J. H., French, J. A., Higurashi, N., Hirsch, E., Jansen, F. E., Lagae, L., Moshé, S. L., Peltola, J., Roulet Perez, E., Scheffer, I. E., & Zuberi, S. M. (2017). Operational classification of seizure types by the International League Against Epilepsy: Position Paper of the ILAE Commission for Classification and Terminology. *Epilepsia*, 58(4), 522–530. <https://doi.org/10.1111/epi.13670>
- Freeman, W. J. (2007). Definitions of state variables and state space for brain-computer interface: Part 1. Multiple hierarchical levels of brain function. *Cognitive Neurodynamics*, 1(1), 3–14. <https://doi.org/10.1007/s11571-006-9001-x>
- Fueta, Y., & Avoli, M. (1992). Effects of antiepileptic drugs on 4-aminopyridine-induced epileptiform activity in young and adult rat hippocampus. *Epilepsy Research*, 12(3), 207–215. <https://doi.org/10.1016/0920->

- Galiana, G. L., Gauthier, A. C., & Mattson, R. H. (2017). Eslicarbazepine Acetate: A New Improvement on a Classic Drug Family for the Treatment of Partial-Onset Seizures. In *Drugs in R and D* (Vol. 17, Issue 3, pp. 329–339). Springer International Publishing. <https://doi.org/10.1007/s40268-017-0197-5>
- Gama, H., Vieira, M., Costa, R., Graça, J., Magalhães, L. M., & Soares-da-Silva, P. (2017). Safety Profile of Eslicarbazepine Acetate as Add-On Therapy in Adults with Refractory Focal-Onset Seizures: From Clinical Studies to 6 Years of Post-Marketing Experience. *Drug Safety*, *40*(12), 1231–1240. <https://doi.org/10.1007/S40264-017-0576-4>
- Goodman, S. N., & Berlin, J. A. (1994). The use of predicted confidence intervals when planning experiments and the misuse of power when interpreting results. *Annals of Internal Medicine*, *121*(3), 200–206. <https://doi.org/10.7326/0003-4819-121-3-199408010-00008>
- Goto, A., Ishii, A., Shibata, M., Ihara, Y., Cooper, E. C., & Hirose, S. (2019). Characteristics of KCNQ2 variants causing either benign neonatal epilepsy or developmental and epileptic encephalopathy. *Epilepsia*, *60*(9), 1870–1880. <https://doi.org/10.1111/epi.16314>
- Grinton, B. E., Heron, S. E., Pelekanos, J. T., Zuberi, S. M., Kivity, S., Afawi, Z., Williams, T. C., Casalaz, D. M., Yendle, S., Linder, I., Lev, D., Lerman-Sagie, T., Malone, S., Bassan, H., Goldberg-Stern, H., Stanley, T., Hayman, M., Calvert, S., Korczyn, A. D., Shevell M., Scheffer I.E., Mulley J.C., & Berkovic, S. F. (2015). Familial neonatal seizures in 36 families: Clinical and genetic features correlate with outcome. *Epilepsia*, *56*(7), 1071–1080. <https://doi.org/10.1111/epi.13020>
- Haas, H. L., Schaerer, B., & Vosmansky, M. (1979). A simple perfusion chamber for the study of nervous tissue slices in vitro. *Journal of Neuroscience Methods*, *1*(4), 323–325. [https://doi.org/10.1016/0165-0270\(79\)90021-9](https://doi.org/10.1016/0165-0270(79)90021-9)
- Hainzl, D., Parada, A., & Soares-Da-Silva, P. (2001). Metabolism of two new antiepileptic drugs and their principal metabolites S(+) and R(-)-10,11-dihydro-10-hydroxy carbamazepine. *Epilepsy Research*, *44*(2–3), 197–206. [https://doi.org/10.1016/S0920-1211\(01\)00231-5](https://doi.org/10.1016/S0920-1211(01)00231-5)
- Halász, P., Cramer, J. A., Hodoba, D., Czåonkowska, A., Guekht, A., Maia, J., Elger, C., Almeida, L., & Soares-Da-Silva, P. (2010). Long-term efficacy and safety of eslicarbazepine acetate: Results of a 1-year open-label extension study in partial-onset seizures in adults with epilepsy. *Epilepsia*, *51*(10), 1963–1969. <https://doi.org/10.1111/j.1528-1167.2010.02660.x>
- Hawkins, K. E., Gavin, C. F., & Sweatt, D. (2017). Long-Term Potentiation: A Candidate Cellular Mechanism for Information Storage in the CNS. *The Curated Reference Collection in Neuroscience and Biobehavioral Psychology*, 33–64. <https://doi.org/10.1016/B978-0-12-809324-5.21103-6>
- Hebeisen, S., Pires, N., Loureiro, A. I., Bonifácio, M. J., Palma, N., Whyment, A., Spanswick, D., & Soares-Da-Silva, P. (2015). Eslicarbazepine and the enhancement of slow inactivation of voltage-gated sodium channels: A comparison with carbamazepine, oxcarbazepine and lacosamide. *Neuropharmacology*, *89*, 122–135. <https://doi.org/10.1016/j.neuropharm.2014.09.008>
- Heuzeroth, H., Wawra, M., Fidzinski, P., Dag, R., & Holtkamp, M. (2019). The 4-aminopyridine model of acute seizures in vitro elucidates efficacy of new antiepileptic drugs. *Frontiers in Neuroscience*, *13*(JUN), 1–12. <https://doi.org/10.3389/fnins.2019.00677>
- Hill, M. R. H., & Greenfield, S. A. (2011). The membrane chamber: A new type of in vitro recording chamber. *Journal of Neuroscience Methods*, *195*(1), 15–23. <https://doi.org/10.1016/j.jneumeth.2010.10.024>
- Hirtz, D., Thurman, D. J., Gwinn-Hardy, K., Mohamed, M., Chaudhuri, A. R., & Zalutsky, R. (2007). How common are the “common” neurologic disorders? In *Neurology* (Vol. 68, Issue 5, pp. 326–337). <https://doi.org/10.1212/01.wnl.0000252807.38124.a3>
- Imbrosci, B., Nitzan, N., McKenzie, S., Donoso, J. R., Swaminathan, A., Böhm, C., Maier, N., & Schmitz, D. (2021). Subiculum as a generator of sharp wave-ripples in the rodent hippocampus. *Cell Reports*, *35*(3), 109021. <https://doi.org/10.1016/J.CELREP.2021.109021>
- Isaev, D., Isaeva, E., Khazipov, R., & Holmes, G. L. (2005). Anticonvulsant Action of GABA in the High Potassium-Low Magnesium Model of Ictogenesis in the Neonatal Rat Hippocampus In Vivo and In Vitro. *J Neurophysiol* (4), 2987-2992. <https://doi.org/10.1152/jn.00138.2005>

- Jentsch, T. J. (2000). Neuronal KCNQ potassium channels: physiology and role in disease. *Nature Reviews Neuroscience*, 1(October), 21–30. <https://doi.org/10.1038/35036198>
- Jiang, X., & Kopp-Schneider, A. (2015). Statistical strategies for averaging EC50 from multiple dose–response experiments. *Archives of Toxicology*, 89(11), 2119–2127. <https://doi.org/10.1007/s00204-014-1350-3>
- Jóźwiak, S., Veggiotti, P., Moreira, J., Gama, H., Rocha, F., & Soares-da-Silva, P. (2018). Effects of adjunctive eslicarbazepine acetate on neurocognitive functioning in children with refractory focal-onset seizures. *Epilepsy and Behavior*, 81, 1–11. <https://doi.org/10.1016/j.yebeh.2018.01.029>
- Kajikawa, Y., & Schroeder, C. E. (2011). How local is the local field potential? *Neuron*, 72(5), 847. <https://doi.org/10.1016/j.NEURON.2011.09.029>
- Kato, M., Yamagata, T., Kubota, M., Arai, H., Yamashita, S., Nakagawa, T., Fujii, T., Sugai, K., Imai, K., Uster, T., Chitayat, D., Weiss, S., Kashii, H., Kusano, R., Matsumoto, A., Nakamura, K., Oyazato, Y., Maeno, M., Nishiyama, K., Kodera, H., Nakashima, M., Tsurusaki, Y., Miyake, N., Saito, K., Hayasaka, K., Matsumoto, N., & Saitsu, H. (2013). Clinical spectrum of early onset epileptic encephalopathies caused by KCNQ2 mutation. *Epilepsia*, 54(7), 1282–1287. <https://doi.org/10.1111/epi.12200>
- Khazipov, R., Khalilov, I., Tyzio, R., Morozova, E., Ben-Ari, Y., & Holmes, G. L. (2004). Developmental changes in GABAergic actions and seizure susceptibility in the rat hippocampus. *The European Journal of Neuroscience*, 19(3), 590–600. <https://doi.org/10.1111/J.0953-816X.2003.03152.X>
- Klausberger, T., & Somogyi, P. (2008). Neuronal Diversity and Temporal Dynamics: The Unity of Hippocampal Circuit Operations. *Science (New York, N.Y.)*, 321(5885), 53. <https://doi.org/10.1126/SCIENCE.1149381>
- Klitgaard, H., Matagne, A., Gobert, J., & Wülfert, E. (1998). Evidence for a unique profile of levetiracetam in rodent models of seizures and epilepsy. *European Journal of Pharmacology*, 353(2–3), 191–206. [https://doi.org/10.1016/S0014-2999\(98\)00410-5](https://doi.org/10.1016/S0014-2999(98)00410-5)
- Kraus, L., Monni, L., Schneider, U. C., Onken, J., Spindler, P., Holtkamp, M., & Fidzinski, P. (2020). Preparation of Acute Human Hippocampal Slices for Electrophysiological Recordings. *J. Vis. Exp*, 159, 61085. <https://doi.org/10.3791/61085>
- Kubota, D., Colgin, L. L., Casale, M., Brucher, F. A., & Lynch, G. (2003). Endogenous waves in hippocampal slices. *Journal of Neurophysiology*, 89(1), 81–89. <https://doi.org/10.1152/jn.00542.2002>
- Kuersten, M., Tacke, M., Gerstl, L., Hoelz, H., Stülpnagel, C. V., & Borggraefe, I. (2020). Antiepileptic therapy approaches in KCNQ2 related epilepsy: A systematic review. In *European Journal of Medical Genetics* (Vol. 63, Issue 1). Elsevier Masson SAS. <https://doi.org/10.1016/j.ejmg.2019.02.001>
- Kwan, P., & Brodie, M. J. (2000). Early Identification of Refractory Epilepsy. *New England Journal of Medicine*, 342(5), 314–319. <https://doi.org/10.1056/NEJM200002033420503>
- Lopantsev, V., & Avoli, M. (1998). Laminar organization of epileptiform discharges in the rat entorhinal cortex in vitro. *Journal of Physiology*, 509(3), 785–796. <https://doi.org/10.1111/j.1469-7793.1998.785bm.x>
- López-Rivera, J. A., Pérez-Palma, E., Symonds, J., Lindy, A. S., McKnight, D. A., Leu, C., Zuberi, S., Brunklaus, A., Møller, R. S., & Lal, D. (2020). A catalogue of new incidence estimates of monogenic neurodevelopmental disorders caused by de novo variants. *Brain*. <https://doi.org/10.1093/brain/awaa051>
- Löscher, W. (2011). Critical review of current animal models of seizures and epilepsy used in the discovery and development of new antiepileptic drugs. *Seizure*, 20(5), 359–368. <https://doi.org/10.1016/j.seizure.2011.01.003>
- Löscher, W. (2017). Animal Models of Seizures and Epilepsy: Past, Present, and Future Role for the Discovery of Antiseizure Drugs. *Neurochemical Research*, 42(7), 1873–1888. <https://doi.org/10.1007/s11064-017-2222-z>
- Löscher, W., & Hönack, D. (1993). Profile of ucb L059, a novel anticonvulsant drug, in models of partial and generalized epilepsy in mice and rats. *European Journal of Pharmacology*, 232(2–3), 147–158. [https://doi.org/10.1016/0014-2999\(93\)90768-D](https://doi.org/10.1016/0014-2999(93)90768-D)
- Losi, G., Marcon, I., Mariotti, L., Sessolo, M., Chiavegato, A., & Carmignoto, G. (2016). A brain slice experimental model to study the generation and the propagation of focally-induced epileptiform activity. *Journal of Neuroscience Methods*, 260, 125–131. <https://doi.org/10.1016/j.jneumeth.2015.04.001>

- Loureiro, A. I., Fernandes-Lopes, C., Wright, L. C., & Soares-da-Silva, P. (2011). Development and validation of an enantioselective liquid-chromatography/tandem mass spectrometry method for the separation and quantification of eslicarbazepine acetate, eslicarbazepine, R-licarbazepine and oxcarbazepine in human plasma. *Journal of Chromatography B: Analytical Technologies in the Biomedical and Life Sciences*, *879*(25), 2611–2618. <https://doi.org/10.1016/j.jchromb.2011.07.019>
- Lozano, A. M., Lipsman, N., Bergman, H., Brown, P., Chabardes, S., Chang, J. W., Matthews, K., McIntyre, C. C., Schlaepfer, T. E., Schulner, M., Temel, Y., Volkmann, J., & Krauss, J. K. (2019). Deep brain stimulation: current challenges and future directions. In *Nature Reviews Neurology*, *15*(3), 148–160. Nature Publishing Group. <https://doi.org/10.1038/s41582-018-0128-2>
- Maier, N., Morris, G., Johenning, F. W., & Schmitz, D. (2009). An approach for reliably investigating hippocampal sharpwave-ripples in vitro. *PLoS ONE*, *4*(9), e6925. <https://doi.org/10.1371/journal.pone.0006925>
- Maier, N., Morris, G., Schuchmann, S., Korotkova, T., Ponomarenko, A., Böhm, C., Wozny, C., & Schmitz, D. (2012). Cannabinoids disrupt hippocampal sharp wave-ripples via inhibition of glutamate release. *Hippocampus*, *22*(6), 1350–1362. <https://doi.org/10.1002/hipo.20971>
- Maier, N., Nimrich, V., & Draguhn, A. (2003). Cellular and network mechanisms underlying spontaneous sharp wave-ripple complexes in mouse hippocampal slices. *The Journal of Physiology*, *550*(Pt 3), 873–887. <https://doi.org/10.1113/jphysiol.2003.044602>
- Martire, M., Castaldo, P., D'Amico, M., Preziosi, P., Annunziato, L., & Tagliatela, M. (2004). M Channels Containing KCNQ2 Subunits Modulate Norepinephrine, Aspartate, and GABA Release from Hippocampal Nerve Terminals. *Journal of Neuroscience*, *24*(3), 592–597. <https://doi.org/10.1523/JNEUROSCI.3143-03.2004>
- Miceli, F., Soldovieri, M. V., Ambrosino, P., Barrese, V., Migliore, M., Cilio, M. R., & Tagliatela, M. (2013). Genotype-phenotype correlations in neonatal epilepsies caused by mutations in the voltage sensor of *Kv7.2* potassium channel subunits. *110*(11). <https://doi.org/10.1073/pnas.1216867110>
- Miceli, F., Soldovieri, M. V., Ambrosino, P., De Maria, M., Migliore, M., Migliore, R., & Tagliatela, M. (2015). Early-onset epileptic encephalopathy caused by gain-of-function mutations in the voltage sensor of *Kv7.2* and *Kv7.3* potassium channel subunits. *Journal of Neuroscience*, *35*(9), 3782–3793. <https://doi.org/10.1523/JNEUROSCI.4423-14.2015>
- Milh, M., Roubertoux, P., Biba, N., Chavany, J., Spiga Ghata, A., Fulachier, C., Collins, S. C., Wagner, C., Roux, J. C., Yalcin, B., Félix, M. S., Molinari, F., Lenck-Santini, P. P., & Villard, L. (2020). A knock-in mouse model for KCNQ2-related epileptic encephalopathy displays spontaneous generalized seizures and cognitive impairment. *Epilepsia*, *61*(5), 868–878. <https://doi.org/10.1111/epi.16494>
- Millichap, J. J., Miceli, F., De Maria, M., Keator, C., Joshi, N., Tran, B., Soldovieri, M. V., Ambrosino, P., Shashi, V., Mikati, M. A., Cooper, E. C., & Tagliatela, M. (2017). Infantile spasms and encephalopathy without preceding neonatal seizures caused by KCNQ2 R198Q, a gain-of-function variant. *Epilepsia*, *58*(1), e10–e15. <https://doi.org/10.1111/epi.13601>
- Mirzaa, G. M., Paciorkowski, A. R., Marsh, E. D., Berry-Kravis, E. M., Medne, L., Alkhateeb, A., Grix, A., Wirrell, E. C., Powell, B. R., Nickels, K. C., Burton, B., Paras, A., Kim, K., Chung, W., Dobyns, W. B., & Das, S. (2013). CDKL5 and ARX mutations in males with early-onset epilepsy. *Pediatric Neurology*, *48*(5), 367–377. <https://doi.org/10.1016/j.pediatrneurol.2012.12.030>
- Mody, I., Lambert, J. D. C., & Heinemann, U. (1987). Low extracellular magnesium induces epileptiform activity and spreading depression in rat hippocampal slices. *Journal of Neurophysiology*, *57*(3), 869–888. <https://doi.org/10.1152/jn.1987.57.3.869>
- Monni, L., Kraus, L., Dipper-Wawra, M., Soares-da-Silva, P., Maier, N., Schmitz, D., Holtkamp, M., & Fidzinski, P. (2022). In vitro and in vivo anti-epileptic efficacy of eslicarbazepine acetate in a mouse model of KCNQ2-related self-limited epilepsy. *British Journal of Pharmacology*, *179*(1), 84–102. <https://doi.org/10.1111/BPH.15689>
- Montgomery, S. M., & Buzsáki, G. (2007). Gamma oscillations dynamically couple hippocampal CA3 and CA1 regions during memory task performance. *Proceedings of the National Academy of Sciences of the United States of America*, *104*(36), 14495–14500. <https://doi.org/10.1073/pnas.0701826104>
- Morton, D. B. (1999). Humane endpoints in animal experimentation for biomedical research: ethical, legal and

practical aspects. *London: Royal Society of Medicine Press*, 5–12.

- Nakazono, T., Jun, H., Blurton-Jones, M., Green, K. N., & Igarashi, K. M. (2018). Gamma oscillations in the entorhinal-hippocampal circuit underlying memory and dementia. *Neuroscience Research*, *129*, 40–46. <https://doi.org/10.1016/J.NEURES.2018.02.002>
- Nappi, P., Miceli, F., Soldovieri, M. V., Ambrosino, P., Barrese, V., & Tagliatela, M. (2020). Epileptic channelopathies caused by neuronal Kv7 (KCNQ) channel dysfunction. In *Pflugers Archiv European Journal of Physiology* (Vol. 472, Issue 7, pp. 881–898). Springer. <https://doi.org/10.1007/s00424-020-02404-2>
- Otto, J. F., Singh, N. A., Dahle, E. J., Leppert, M. F., Pappas, C. M., Pruess, T. H., Wilcox, K. S., & White, H. S. (2009). Electroconvulsive seizure thresholds and kindling acquisition rates are altered in mouse models of human KCNQ2 and KCNQ3 mutations for benign familial neonatal convulsions. *Epilepsia*, *50*(7), 1752–1759. <https://doi.org/10.1111/j.1528-1167.2009.02100.x>
- Pangalos, M., Donoso, J. R., Winterer, J., Zivkovic, A. R., Kempter, R., Maier, N., & Schmitz, D. (2013). Recruitment of oriens-lacunosum-moleculare interneurons during hippocampal ripples. *Proceedings of the National Academy of Sciences of the United States of America*, *110*(11), 4398–4403. <https://doi.org/10.1073/pnas.1215496110>
- Papathodoropoulos, C., & Kostopoulos, G. (2002). Spontaneous, low frequency (~2-3 Hz) field activity generated in rat ventral hippocampal slices perfused with normal medium. *Brain Research Bulletin*, *57*(2), 187–193. [https://doi.org/10.1016/S0361-9230\(01\)00738-9](https://doi.org/10.1016/S0361-9230(01)00738-9)
- Parada, A., & Soares-Da-Silva, P. (2002). The novel anticonvulsant BIA 2-093 inhibits transmitter release during opening of voltage-gated sodium channels: a comparison with carbamazepine and oxcarbazepine. *Neurochemistry International*, *40*(5), 435–440. [https://doi.org/10.1016/S0197-0186\(01\)00101-2](https://doi.org/10.1016/S0197-0186(01)00101-2)
- Pearl, P. L. (2018). Epilepsy Syndromes in Childhood. In *CONTINUUM Lifelong Learning in Neurology*, *24*(1), Child Neurology, 186–209. Lippincott Williams and Wilkins. <https://doi.org/10.1212/CON.0000000000000568>
- Penn, Y., Segal, M., & Moses, E. (2016). Network synchronization in hippocampal neurons. *Proceedings of the National Academy of Sciences of the United States of America*, *113*(12), 3341–3346. https://doi.org/10.1073/PNAS.1515105113/SUPPL_FILE/PNAS.1515105113.SM04.MOV
- Perreault, P., & Avoli, M. (1992). 4-Aminopyridine-induced epileptiform activity and a GABA-mediated long-lasting depolarization in the rat hippocampus. *Journal of Neuroscience*, *12*(1), 104–115. <https://doi.org/10.1523/jneurosci.12-01-00104.1992>
- Pierce du Sert, N., Hurst, V., Ahluwalia, A., Alam, S., Avey, M. T., Baker, M., Browne, W. J., Clark, A., Cuthill, I. C., Dirnagl, U., Emerson, M., Garner, P., Holgate, S. T., Howells, D. W., Karp, N. A., Lazic, S. E., Lidster, K., MacCallum, C. J., Macleod, M., Pearl E.J., Petersen O.H., Rawle, F., Reynolds, P., Rooney, K., Sena, E.S., Silberberg, S.D., Steckler, T., & Würbel, H. (2020). The ARRIVE guidelines 2.0: Updated guidelines for reporting animal research. *Experimental Physiology*, *105*(9), 1459–1466. <https://doi.org/10.1113/EP088870>
- Potschka, H., Soerensen, J., Pekcec, A., Loureiro, A., & Soares-da-Silva, P. (2014). Effect of eslicarbazepine acetate in the corneal kindling progression and the amygdala kindling model of temporal lobe epilepsy. *Epilepsy Research*, *108*(2), 212–222. <https://doi.org/10.1016/j.eplepsyres.2013.11.017>
- Racine, R. J. (1972). Modification of seizure activity by electrical stimulation: II. Motor seizure. *Electroencephalography and Clinical Neurophysiology*, *32*(3), 281–294. [https://doi.org/10.1016/0013-4694\(72\)90177-0](https://doi.org/10.1016/0013-4694(72)90177-0)
- Raimondo, J. V., Heinemann, U., de Curtis, M., Goodkin, H. P., Dulla, C. G., Janigro, D., Ikeda, A., Lin, C. C. K., Jiruska, P., Galanopoulou, A. S., & Bernard, C. (2017). Methodological standards for in vitro models of epilepsy and epileptic seizures. A TASK1-WG4 report of the AES/ILAE Translational Task Force of the ILAE. *Epilepsia*, *58*(Suppl 4), 40–52. <https://doi.org/10.1111/epi.13901>
- Robbins, J. (2001). KCNQ potassium channels: physiology, pathophysiology, and pharmacology. *Pharmacology & Therapeutics*, *90*(1), 1–19. <http://www.ncbi.nlm.nih.gov/pubmed/11448722>
- Robbins, J., Passmore, G. M., Abogadie, F. C., Reilly, J. M., & Brown, D. A. (2013). Effects of KCNQ2 Gene Truncation on M-Type Kv7 Potassium Currents. *PLoS ONE*, *8*(8), 71809. <https://doi.org/10.1371/journal.pone.0071809>

- Rocamora, R. (2015). A review of the efficacy and safety of eslicarbazepine acetate in the management of partial-onset seizures. In *Therapeutic Advances in Neurological Disorders* (Vol. 8, Issue 4, pp. 178–186). SAGE Publications. <https://doi.org/10.1177/1756285615589711>
- Ronen, G. M., Rosales, T. O., Connolly, M., Anderson, V. E., & Leppert, M. (1993). Seizure characteristics in chromosome 20 benign familial neonatal convulsions. *Neurology*, *43*(7), 1355–1360. <http://www.ncbi.nlm.nih.gov/pubmed/8327138>
- Rustay, N. R., Wahlsten, D., & Crabbe, J. C. (2003). Assessment of genetic susceptibility to ethanol intoxication in mice. *Proceedings of the National Academy of Sciences of the United States of America*, *100*(5), 2917–2922. https://doi.org/10.1073/PNAS.0437273100/SUPPL_FILE/7273SUPPORTINGTEXT.HTML
- Sands, T. T., Balestri, M., Bellini, G., Mulkey, S. B., Danhaive, O., Bakken, E. H., Tagliatela, M., Oldham, M. S., Vigeveno, F., Holmes, G. L., & Cilio, M. R. (2016). Rapid and safe response to low-dose carbamazepine in neonatal epilepsy. *Epilepsia*, *57*(12), 2019–2030. <https://doi.org/10.1111/epi.13596>
- Scharfman, H. E., & MacLusky, N. J. (2006). The influence of gonadal hormones on neuronal excitability, seizures, and epilepsy in the female. In *Epilepsia* (Vol. 47, Issue 9, pp. 1423–1440). NIH Public Access. <https://doi.org/10.1111/j.1528-1167.2006.00672.x>
- Scheffer, I. E., Berkovic, S., Capovilla, G., Connolly, M. B., French, J., Guilhoto, L., Hirsch, E., Jain, S., Mathern, G. W., Moshé, S. L., Nordli, D. R., Perucca, E., Tomson, T., Wiebe, S., Zhang, Y. H., & Zuberi, S. M. (2017). ILAE classification of the epilepsies: Position paper of the ILAE Commission for Classification and Terminology. *Epilepsia*, *58*(4), 512–521. <https://doi.org/10.1111/epi.13709>
- Schneider, J., Lewen, A., Ta, T. T., Galow, L. V., Isola, R., Papageorgiou, I. E., & Kann, O. (2015). A reliable model for gamma oscillations in hippocampal tissue. *Journal of Neuroscience Research*, *93*(7), 1067–1078. <https://doi.org/10.1002/jnr.23590>
- Schroeder, B. C., Hechenberger, M., Weinreich, F., Kubisch, C., & Jentsch, T. J. (2000). KCNQ5, a Novel Potassium Channel Broadly Expressed in Brain, Mediates M-type Currents. *Journal of Biological Chemistry*, *275*(31), 24089–24095. <https://doi.org/10.1074/jbc.M003245200>
- Schroeder, B. C., Kubisch, C., Stein, V., & Jentsch, T. J. (1998). Moderate loss of function of cyclic-AMP-modulated KCNQ2/KCNQ3 K⁺ channels causes epilepsy. *Nature*, *396*(6712), 687–690. <https://doi.org/10.1038/25367>
- Shah, M. M., Mistry, M., Marsh, S. J., Brown, D. A., & Delmas, P. (2002). Molecular correlates of the M-current in cultured rat hippocampal neurons. *Journal of Physiology*, *544*(1), 29–37. <https://doi.org/10.1113/jphysiol.2002.028571>
- Sierra-Paredes, G., Loureiro, A. I., Wright, L. C., Sierra-Marñido, G., & Soares-da-Silva, P. (2014). Effects of eslicarbazepine acetate on acute and chronic latrunculin A-induced seizures and extracellular amino acid levels in the mouse hippocampus. *BMC Neuroscience*, *15*(1). <https://doi.org/10.1186/s12868-014-0134-2>
- Soares-da-Silva, P., Pires, N., Bonifácio, M. J., Loureiro, A. I., Palma, N., & Wright, L. C. (2015). Eslicarbazepine acetate for the treatment of focal epilepsy: an update on its proposed mechanisms of action. *Pharmacology Research & Perspectives*, *3*(2), e00124. <https://doi.org/10.1002/prp2.124>
- Soldovieri, M. V., Ambrosino, P., Mosca, I., De Maria, M., Moretto, E., Miceli, F., Alaimo, A., Iraci, N., Manocchio, L., Medoro, A., Passafaro, M., & Tagliatela, M. (2016). Early-onset epileptic encephalopathy caused by a reduced sensitivity of Kv7.2 potassium channels to phosphatidylinositol 4,5-bisphosphate. *Scientific Reports*, *6*(1), 1–12. <https://doi.org/10.1038/srep38167>
- Sunovion Pharmaceuticals Inc. - Sunovion's Aptiom® (eslicarbazepine acetate) receives FDA approval for expanded indication to treat partial-onset seizures in children and adolescents 4 years of age and older. Retrieved from <https://news.sunovion.com/press-releases/press-releases-details/2017/Sunovions-Aptiom-eslicarbazepine-acetate-Receives-FDA-Approval-for-Expanded-Indication-to-Treat-Partial-Onset-Seizures-in-Children-and-Adolescents-4-Years-of-Age-and-Older/default.aspx>
- Symonds, J. D., Zuberi, S. M., Stewart, K., McLellan, A., O'Regan, M., MacLeod, S., Jollands, A., Joss, S., Kirkpatrick, M., Brunklaus, A., Pilz, D. T., Shetty, J., Dorris, L., Abu-Arafeh, I., Andrew, J., Brink, P., Callaghan, M., Cruden, J., Diver, L. A., Findlay, C., Gardiner, S., Grattan, R., Lang, B., MacDonnell, J., McKnight, J., Morrison, C.A., Nairn, L., Slean, M.M., Stephen, E., Webb, A., Vincent, A., & Wilson, M. (2019). Incidence and phenotypes of childhood-onset genetic epilepsies: a prospective population-based national cohort. *Brain: A Journal of Neurology*, *142*(8), 2303–2318. <https://doi.org/10.1093/brain/awz195>

- Trinka, E., Ben-Menachem, E., Kowacs, P. A., Elger, C., Keller, B., Löffler, K., Rocha, J. F., & Soares-da-Silva, P. (2018). Efficacy and safety of eslicarbazepine acetate versus controlled-release carbamazepine monotherapy in newly diagnosed epilepsy: A phase III double-blind, randomized, parallel-group, multicenter study. *Epilepsia*, *59*(2), 479–491. <https://doi.org/10.1111/epi.13993>
- Trompoukis, G., Rigas, P., Leontiadis, L. J., & Papatheodoropoulos, C. (2020). Ih, GIRK, and KCNQ/Kv7 channels differently modulate sharp wave - ripples in the dorsal and ventral hippocampus. *Molecular and Cellular Neuroscience*, *107*, 103531. <https://doi.org/10.1016/j.mcn.2020.103531>
- Valeeva, G., Tressard, T., Mukhtarov, M., Baude, A., & Khazipov, R. (2016). *Systems/Circuits An Optogenetic Approach for Investigation of Excitatory and Inhibitory Network GABA Actions in Mice Expressing Channelrhodopsin-2 in GABAergic Neurons*. <https://doi.org/10.1523/JNEUROSCI.3482-15.2016>
- Vittinghoff, E., & McCulloch, C. E. (2007). Relaxing the Rule of Ten Events per Variable in Logistic and Cox Regression. *American Journal of Epidemiology*, *165*(6), 710–718. <https://doi.org/10.1093/aje/kwk052>
- Wang, H. S., Pan, Z., Shi, W., Brown, B. S., Wymore, R. S., Cohen, I. S., Dixon, J. E., & McKinnon, D. (1998). KCNQ2 and KCNQ3 potassium channel subunits: Molecular correlates of the M-channel. *Science*, *282*(5395), 1890–1893. <https://doi.org/10.1126/science.282.5395.1890>
- Watanabe, H., Nagata, E., Kosakai, A., Nakamura, M., Yokoyama, M., Tanaka, K., & Sasai, H. (2000). Disruption of the epilepsy KCNQ2 gene results in neural hyperexcitability. *Journal of Neurochemistry*, *75*(1), 28–33. <https://doi.org/10.1046/j.1471-4159.2000.0750028.x>
- Weckhuysen, S., Mandelstam, S., Suls, A., Audenaert, D., Deconinck, T., Claes, L. R. F., Deprez, L., Smets, K., Hristova, D., Yordanova, I., Jordanova, A., Ceulemans, B., Jansen, A., Hasaerts, D., Roelens, F., Lagae, L., Yendle, S., Stanley, T., Heron, S. E., Mulley, J. C., Berkovic, S. F., Scheffer, I. E., & De Jonghe, P. (2012). KCNQ2 encephalopathy: Emerging phenotype of a neonatal epileptic encephalopathy. *Annals of Neurology*, *71*(1), 15–25. <https://doi.org/10.1002/ana.22644>
- Wheless, J. W., Fulton, S. P., & Mudigoudar, B. D. (2020). Dravet Syndrome: A Review of Current Management. In *Pediatric Neurology*. Elsevier Inc. <https://doi.org/10.1016/j.pediatrneurol.2020.01.005>
- Wójtowicz, A. M., Van Boom, L. Den, Chakrabarty, A., Maggio, N., Haq, R. U., Behrens, C. J., & Heinemann, U. (2009). Monoamines block kainate- And carbachol-induced. γ -oscillations but augment stimulus-induced γ -oscillations in rat hippocampus in vitro. *Hippocampus*, *19*(3), 273–288. <https://doi.org/10.1002/hipo.20508>
- Yamamoto, J., Suh, J., Takeuchi, D., & Tonegawa, S. (2014). Successful execution of working memory linked to synchronized high-frequency gamma oscillations. *Cell*, *157*(4), 845–857. <https://doi.org/10.1016/j.cell.2014.04.009>

11. Statutory declaration

I, Laura Monni, by personally signing this document in lieu of an oath, hereby affirm that I prepared the submitted dissertation on the topic: “Eslicarbazepine acetate effects in a model of *KCNQ2*-related epilepsy” (“Wirkungen von Eslicarbazepinacetat in einem Modell der *KCNQ2*-bedingten Epilepsie”), independently and without the support of third parties, and that I used no other sources and aids than those stated. All parts which are based on the publications or presentations of other authors, either in letter or in spirit, are specified as such in accordance with the citing guidelines. The sections on methodology (in particular regarding practical work, laboratory regulations, statistical processing) and results (in particular regarding figures, charts and tables) are exclusively my responsibility.

Furthermore, I declare that I have correctly marked all of the data, the analyses, and the conclusions generated from data obtained in collaboration with other persons, and that I have correctly marked my own contribution and the contributions of other persons (cf. declaration of contribution). I have correctly marked all texts or parts of texts that were generated in collaboration with other persons.

My contributions to any publications to this dissertation correspond to those stated in the below joint declaration made together with the supervisor. All publications created within the scope of the dissertation comply with the guidelines of the ICMJE (International Committee of Medical Journal Editors; www.icmje.org) on authorship. In addition, I declare that I shall comply with the regulations of Charité – Universitätsmedizin Berlin on ensuring good scientific practice.

I declare that I have not yet submitted this dissertation in identical or similar form to another Faculty.

The significance of this statutory declaration and the consequences of a false statutory declaration under criminal law (Sections 156, 161 of the German Criminal Code) are known to me.

Date

Signature

12. Affidavit-Declarations of own contributions to the top-journal for a PhD degree

Laura Monni contributed the following to the below listed publication:

Monni L., Kraus L., Dipper-Wawra M., Soares-da-Silva P., Maier N., Schmitz D., Holtkamp M., and Fidzinski P.

In vitro and *in vivo* antiepileptic efficacy of eslicarbazepine acetate in a mouse model of KCNQ2-related self-limited epilepsy. *British Journal of Pharmacology*, 2022 Jan;179(1):84-102. doi: 10.1111/bph.15689. Epub 2021 Oct 4.

Contributions in detail:

Conceptualization of the study and experiments:

Laura Monni, Matthias Dipper-Wawra, Patricio Soares-da-Silva, Martin Holtkamp and Pawel Fidzinski.

Execution of experiments:

In vitro experiments on physiological hippocampal oscillations, SLEs recordings, input/output and fEPSP/PS coupling experiments were performed by Laura Monni.

In vivo experiments, including Staircase test, Rotarod test and 6 Hz psychomotor seizure model were performed by Laura Monni, with the occasional assistance of Larissa Kraus for the organization of the cages and breeding strategy.

Raw data regarding pharmacokinetic analysis of S-Lic through the LC-MS/MS assay were obtained and sent by Patricio Soares-da-Silvia Bial laboratory in Porto, Portugal.

Data Analysis:

All data and statistical analysis were performed by Laura Monni. Matthias Dipper-Wawra and Nikolaus Maier helped and assisted with the use of custom-made MATLAB scripts for the analysis of SPW-Rs and gamma oscillations and SLEs.

Preparation of figures:

Laura Monni

Writing and revisions of the manuscript:

Laura Monni and Pawel Fidzinski

Editing of the manuscript:

All authors.

Signature, date and stamp of first supervising university professor / lecturer

Signature of doctoral candidate

13. Print copy of the selected publication








Monni L, Kraus L, Dipper-Wawra M, Soares-da-Silva P, Maier N, Schmitz D, Holtkamp M, Fidzinski P. *In vitro* and *in vivo* antiepileptic efficacy of eslicarbazepine acetate in a mouse model of *KCNQ2*-related self-limited epilepsy. *British Journal of Pharmacology*, 2021.

Extract from the Journal Summary List:

Journal Data Filtered By: Selected JCR Year: 2019 Selected Editions: SCIE,SSCI
 Selected Categories: "PHARMACOLOGY and PHARMACY" Selected Category
 Scheme: WoS
 Gesamtanzahl: 270 Journale

Rank	Full Journal Title	Total Cites	Journal Impact Factor	Eigenfactor Score
1	NATURE REVIEWS DRUG DISCOVERY	33,154	64.797	0.049170
2	PHARMACOLOGICAL REVIEWS	12,500	17.395	0.010370
3	TRENDS IN PHARMACOLOGICAL SCIENCES	13,034	13.503	0.017780
4	ADVANCED DRUG DELIVERY REVIEWS	36,798	13.300	0.033170
5	Annual Review of Pharmacology and Toxicology	7,812	11.250	0.007970
6	DRUG RESISTANCE UPDATES	3,165	11.000	0.004220
7	PHARMACOLOGY & THERAPEUTICS	16,615	10.557	0.023490
8	MEDICINAL RESEARCH REVIEWS	4,974	9.300	0.005360
9	BRITISH JOURNAL OF PHARMACOLOGY	34,040	7.730	0.031300
10	JOURNAL OF CONTROLLED RELEASE	49,132	7.727	0.051270
11	ALIMENTARY PHARMACOLOGY & THERAPEUTICS	21,233	7.515	0.032840
12	DRUG DISCOVERY TODAY	15,022	7.321	0.020720
13	Acta Pharmaceutica Sinica B	3,560	7.097	0.006580
14	NEUROPSYCHOPHARMACOLOGY	26,281	6.751	0.040680
15	European Heart Journal-Cardiovascular Pharmacotherapy	521	6.696	0.001640
16	CLINICAL PHARMACOLOGY & THERAPEUTICS	16,749	6.565	0.018290
17	DRUGS	11,128	6.189	0.014190
18	Neurotherapeutics	4,998	6.035	0.009520
19	PHARMACOLOGICAL RESEARCH	13,517	5.893	0.019090
20	EXPERT OPINION ON THERAPEUTIC PATENTS	3,350	5.611	0.005090

In vitro and *in vivo* anti-epileptic efficacy of eslicarbazepine acetate in a mouse model of *KCNQ2*-related self-limited epilepsy

Laura Monni^{1,2}  | Larissa Kraus^{1,3} | Matthias Dipper-Wawra^{1,4}  |
Patricio Soares-da-Silva^{5,6,7}  | Nikolaus Maier⁸  | Dietmar Schmitz⁸  |
Martin Holtkamp^{1,4}  | Pawel Fidzinski^{1,2} 

¹Clinical and Experimental Epileptology, Department of Neurology, Charité-Universitätsmedizin Berlin, corporate member of Freie Universität Berlin and Humboldt-Universität zu Berlin, Berlin, Germany

²NeuroCure Clinical Research Centre, Berlin Institute of Health at Charité-Universitätsmedizin Berlin, Berlin, Germany

³Life Sciences Institute, Department of Cellular and Physiological Sciences, University of British Columbia, Vancouver, British Columbia, Canada

⁴Epilepsy-Center Berlin-Brandenburg, Institute for Diagnostics of Epilepsy, Berlin, Germany

⁵Division of Research and Development, BIAL – Portela & CA S. A, da Siderurgia Nacional, São Mamede do Coronado, Portugal

⁶Department of Biomedicine, Unit of Pharmacology and Therapeutics, Faculty of Medicine, University Porto, Porto, Portugal

⁷MedInUP, Centre for Drug Discovery and Innovative Medicines, University Porto, Porto, Portugal

⁸Neuroscience Research Centre, Charité-Universitätsmedizin Berlin, corporate member of Freie Universität Berlin and Humboldt-Universität zu Berlin, Berlin, Germany

Correspondence

Pawel Fidzinski, Clinical and Experimental Epileptology, Department of Neurology, Charité-Universitätsmedizin Berlin, corporate member of Freie Universität Berlin and Humboldt-Universität zu Berlin, Charitéplatz 1, 10117 Berlin, Germany.
Email: pawel.fidzinski@charite.de

Present address

Larissa Kraus, Life Sciences Institute, Department of Cellular and Physiological Sciences, University of British Columbia, Vancouver, British Columbia, Canada

Funding information

Fundação Bial; NeuroCure Exzellenzcluster; NeuroCure Cluster of Excellence, Berlin Institute of Health; BIAL Portela & Ca; Eisai

Background and Purpose: The *KCNQ2* gene encodes for the K_v7.2 subunit of non-inactivating potassium channels. *KCNQ2*-related diseases range from autosomal dominant neonatal self-limited epilepsy, often caused by *KCNQ2* haploinsufficiency, to severe encephalopathies caused by *KCNQ2* missense variants. *In vivo* and *in vitro* effects of the sodium channel blocker eslicarbazepine acetate (ESL) and eslicarbazepine metabolite (S-Lic) in a mouse model of self-limited neonatal epilepsy as a first attempt to assess the utility of ESL in the *KCNQ2* disease spectrum was investigated.

Experimental Approach: Effects of S-Lic on *in vitro* physiological and pathological hippocampal neuronal activity in slices from mice carrying a heterozygous deletion of *Kcnq2* (*Kcnq2*^{+/-}) and *Kcnq2*^{+/+} mice were investigated. ESL *in vivo* efficacy was investigated in the 6-Hz psychomotor seizure model in both *Kcnq2*^{+/-} and *Kcnq2*^{+/+} mice.

Key Results: S-Lic increased the amplitude and decreased the incidence of physiological sharp wave-ripples in a concentration-dependent manner and slightly decreased

Abbreviations: 4-AP, 4-aminopyridine; aCSF, artificial cerebrospinal fluid; BFNE, self-limited familial neonatal epilepsy; CA1–3, cornu ammonis hippocampal regions 1 and 3; ESL, eslicarbazepine acetate; fEPSP, field excitatory postsynaptic potential; KCNQ, potassium channel, voltage-gated, KQT-like subfamily; S-Lic, eslicarbazepine active metabolite; SPW-R, sharp wave-ripple.

This is an open access article under the terms of the Creative Commons Attribution-NonCommercial-NoDerivs License, which permits use and distribution in any medium, provided the original work is properly cited, the use is non-commercial and no modifications or adaptations are made.

© 2021 The Authors. *British Journal of Pharmacology* published by John Wiley & Sons Ltd on behalf of British Pharmacological Society.

gamma oscillations frequency. 4-Aminopyridine-evoked seizure-like events were blocked at high S-Lic concentrations and substantially reduced in incidence at lower concentrations. These results were not different in *Kcnq2*^{+/+} and *Kcnq2*^{+/-} mice, although the EC₅₀ estimation implicated higher efficacy in *Kcnq2*^{+/-} animals. *In vivo*, *Kcnq2*^{+/-} mice had a lower seizure threshold than *Kcnq2*^{+/+} mice. In both genotypes, ESL dose-dependently displayed protection against seizures.

Conclusions and Implications: S-Lic slightly modulates hippocampal oscillations and blocks epileptic activity *in vitro* and *in vivo*. Our results suggest that the increased excitability in *Kcnq2*^{+/-} mice is effectively targeted by S-Lic high concentrations, presumably by blocking diverse sodium channel subtypes.

KEYWORDS

acute seizures models, encephalopathy, eslicarbazepine acetate, hippocampal oscillations, mouse, seizure-like event

1 | INTRODUCTION

Epilepsy is one of the most frequent neurological disorders affecting up to 1% of the population, with a lifetime prevalence of 7.6 per 1000 individuals (Fiest et al., 2017; Hirtz et al., 2007; Ngugi et al., 2010). The incidence (>60 per 100,000 individuals) of epilepsy is highest in children and at age >60 years (Fiest et al., 2017; Symonds et al., 2019). One of the major causes of childhood-onset epilepsy, and of the often associated developmental and intellectual comorbidities is the presence of mutations in the genes that control excitability and disrupt normal brain development, for example, *SCN1A* (Dravet syndrome) or *KCNQ2* (López-Rivera et al., 2020; Wheless et al., 2020). In this study, we have focused on *KCNQ2*-related diseases. The *KCNQ2* gene encodes for the **K_v7.2** subunit of **voltage-gated potassium channels**, which are expressed in various neuronal subtypes and are localized in different cell compartments (Devaux et al., 2004; Fidzinski et al., 2015; Jentsch, 2000). Homo- or heterotetrameric assemblies of K_v7.2, **K_v7.3**, and **K_v7.5** subunits form the functional channel that mediates the non-inactivating, so-called M-current (Brown & Passmore, 2009; Wang et al., 1998). The M-current is activated upon membrane depolarization and dampens neuronal excitability (Brown & Adams, 1980; Delmas & Brown, 2005; Jentsch, 2000). The clinical spectrum of *KCNQ2*-related diseases ranges from self-limited familial neonatal epilepsy (BFNE) to severe *KCNQ2* epileptic encephalopathy. BFNE is characterized by seizures occurring between days 4 and 7 of life, usually resolving within 4–6 months, with normal neurological and cognitive development (International League Against Epilepsy, ILAE; *EpilepsyDiagnosis.org*), while *KCNQ2* encephalopathy is characterized by pharmaco-resistant epilepsy and mild to profound cognitive, intellectual, and developmental impairment (Kato et al., 2013). This broad range of clinical manifestations seems to reflect different degrees of functional impairment caused by distinct variants of the *KCNQ2* gene (Goto et al., 2019; Miceli et al., 2013; Weckhuysen et al., 2012; reviewed by Nappi

What is already known

- In paediatric patients, *KCNQ2*-related diseases range from self-limited epilepsy to severe encephalopathy with pharmaco-resistant seizures.
- Eslicarbazepine acetate has good tolerability and anti-epileptic efficacy in adult forms of epilepsy.

What this study adds

- Eslicarbazepine alters hippocampal oscillations and seizure-like events in a *Kcnq2*^{+/-} mouse model of self-limited epilepsy.
- *In vivo*, eslicarbazepine acetate showed anti-epileptic efficacy also in the increased hyperexcitability *Kcnq2*^{+/-} mice phenotype.

What is the clinical significance

- Eslicarbazepine effects on hippocampal oscillations may clarify the mechanisms underlying the side effects on cognition.
- Eslicarbazepine acetate efficacy in *Kcnq2*^{+/-} mice represents the beginning of alternative treatments for childhood epilepsies.

et al., 2020). According to literature, BFNE is mostly caused by stop-gain mutations with the primary pathogenic mechanism relying on haploinsufficiency (Goto et al., 2019; Miceli et al., 2013). In contrast, *KCNQ2* epileptic encephalopathy is mostly caused by *de novo* *KCNQ2* missense variants (Goto et al., 2019; Kato et al., 2013) resulting in a dominant-negative M-current suppression (Jentsch, 2000; Miceli et al., 2013).

At onset, patients suffering from the mild BFNE phenotype are effectively treated with anti-epileptic drugs (AEDs) such as **phenobarbital** or **carbamazepine**, and in the further course of the disease, seizure remission occurs regardless of treatment (Grinton et al., 2015; Sands et al., 2016). On the other hand, most patients with KCNQ2 encephalopathy continue to suffer from pharmaco-resistant epilepsy and accompanying neurodevelopmental impairments (Goto et al., 2019; Miceli et al., 2013; Weckhuysen et al., 2012; reviewed by Nappi et al., 2020). The anti-epileptic potential of sodium channel blockers such as carbamazepine and **phenytoin** is well known (Beckonert et al., 2018; Doeser et al., 2015; Pisano et al., 2015; Sands et al., 2016). Within the sodium channel blocker family of anti-epileptic drugs, **eslicarbazepine acetate (ESL)** is a rather novel anti-epileptic drug, which, together with carbamazepine and **oxcarbazepine**, belongs to the dibenzoazepine family (Benes et al., 1999; Soares-da-Silva et al., 2015). The principal mechanism of ESL is to block the **voltage-gated sodium channels** by prolonging their slow inactivation state (Hebeisen et al., 2015; Soares-da-Silva et al., 2015). ESL is currently approved as adjunctive and monotherapy in adults with focal-onset seizures by the European Medicines Agency (EMA), the Food and Drug Administration (FDA) and Health Canada (Trinka et al., 2018). Recently, a phase-II trial has shown positive effects of ESL as adjunctive treatment in children and adolescents aged 6–16 years, reducing seizure frequency without negative effects on neurocognitive and behavioural functions (Jóźwiak et al., 2018).

Given good tolerability and the positive therapeutic potential of ESL, we aimed to investigate ESL efficacy in the KCNQ2 disease spectrum. Here, we choose to use a well-characterized and available loss-of-function mouse model of KCNQ2-related self-limited epilepsy, as a first step towards assessment of ESL efficacy in KCNQ2 loss-of-function related diseases including severe KCNQ2 encephalopathies.

The chosen model carries a deletion in the *Kcnq2* gene that leads to a lack of expression of the KCNQ2 protein (Watanabe et al., 2000). Homozygous (*Kcnq2*^{-/-}) mice die shortly after birth due to pulmonary atelectasis, while their heterozygous littermates (*Kcnq2*^{+/-}) show a normal lifespan, no significant behavioural abnormalities and no spontaneous epileptic seizures. However, the reduced expression of the KCNQ2 protein in *Kcnq2*^{+/-} mice results in an increased vulnerability to epileptogenic stimuli, either chemically or electrically induced, such as the pentylenetetrazol (PTZ) or 6-Hz corneal stimulation model, respectively (Otto et al., 2009; Watanabe et al., 2000). We hypothesize that inhibition of sodium channels by ESL might be effective in reducing an increased excitability underlying seizures in KCNQ2-related epilepsy. Specifically, we employed the *Kcnq2*^{+/-} mouse model to investigate *in vitro* effects of S-Lic, eslicarbazepine active metabolite, on physiological hippocampal network oscillations such as sharp wave-ripple complexes (SPW-Rs), gamma oscillations and pathological seizure-like events. In addition, we exploited the 6-Hz psychomotor seizure *in vivo* model to test the anti-seizure efficacy of ESL in *Kcnq2*^{+/-} and *Kcnq2*^{+/+} mice.

2 | METHODS

2.1 | Animals

All experimental procedures were conducted in accordance with the European Directive 2010/63/EU and the German Animal Welfare Act for animal experiments and were approved by the Institutional Animal Welfare Officer and the responsible local authorities (Landesamt für Gesundheit und Soziales Berlin, licence numbers: T0265/17, G0078/18). Particular attention was paid in order to reduce the number of animals used and their suffering. Heterozygous (*Kcnq2*^{+/-}) mice with C57BL/6J background (RRID:IMSR_HAR:2000) and carrying a deletion in *Kcnq2* gene from position 418 to 535 were crossed with wild-type (*Kcnq2*^{+/+}) mice to avoid the birth of *Kcnq2*^{-/-} animals that die around perinatal age (Watanabe et al., 2000). Wild-type littermates were used as control for all *in vitro* and *in vivo* experiments. Mice were maintained under controlled environmental enriched conditions, with 12-h light/dark cycle (6:00 h/18:00 h), on wooden litter with *ad libitum* access to food and water. Up to nine animals of the same sex were kept in the same individually ventilated cage. Animal studies are reported in compliance with the ARRIVE v2.0 guidelines (Percie du Sert et al., 2020) and with the recommendations made by the *British Journal of Pharmacology* (Lilley et al., 2020).

2.2 | Hippocampal slice preparation

All *in vitro* experiments were performed in hippocampal slices from juvenile (P28–32) *Kcnq2*^{+/+} and *Kcnq2*^{+/-} mice (20–25 g). Slice preparation was conducted as previously described (Heuzeroth et al., 2019) with minimal modifications. Briefly, mice were anaesthetised with isoflurane and decapitated, and the brain was quickly removed and kept in ice cold (1–4°C) artificial cerebrospinal fluid (aCSF), continuously carbogenated (95% O₂, 5% CO₂). aCSF contained in mM: NaCl 125.0, KCl 2.0, MgCl₂ 1.0, CaCl₂ 2.0, NaH₂PO₄ 1.25, NaHCO₃ 25.0, and glucose 10.0 (pH 7.4, 300 ± 10 mOsm). The cerebellum was then removed and the hemispheres separated and glued to a vibratome chamber. 400-µm-thick horizontal brain slices were cut from both hemispheres with a vibratome (Leica VT1200S, Wetzlar, Germany) and contained the entorhinal cortex (EC), the subiculum (SUB), the dentate gyrus (DG), and the cornu ammonis regions 1, 2, and 3 (CA1, CA2, and CA3). Before starting of the electrophysiological recording, slices were allowed to recover for at least 1 h in an Haas-type interface chamber (Haas et al., 1979), continuously perfused with prewarmed (35°C) and carbogenated aCSF at 1.6 ml·min⁻¹.

2.3 | Local field potential recordings

Spontaneous sharp wave-ripples (SPW-Rs), kainate-induced gamma oscillations and seizure-like events evoked by 4-AP were all recorded via extracellular local field potential recordings. Borosilicate pipettes

(Science Products, Hofheim, Germany; 1.5 mm outer diameter) were pulled with a vertical puller (PC-10, Narishige, Tokyo, Japan; electrode resistance 1–2 M Ω) and filled with 154-mM NaCl.

SPW-R activity was recorded from CA1 pyramidal layer of ventral hippocampal slices perfused with prewarmed ($\sim 35 \pm 0.5^\circ\text{C}$) and carbogenated aCSF (Kubota et al., 2003; Maier et al., 2003, 2009; Papatheodoropoulos & Kostopoulos, 2002). The recordings were performed in a modified submerged-type recording chamber with high flow rate (10 ml·min⁻¹) (Hill & Greenfield, 2011; Kraus et al., 2020). The signal was sampled at 20 kHz, low-pass filtered at 2 kHz, and digitized by a Digidata1550 interface and processed by PClamp10 software (Molecular Devices, Sunnyvale, CA, USA, RRID:SCR_011323). Baseline activity was recorded for ≥ 30 min (SPW-R incidence ~ 1 Hz). Eslicarbazepine metabolite (S-Lic) was added at a concentration of 0 (0.12% DMSO as vehicle control), 10, 30, 100, and 300 μM , respectively, randomly assigned to one slice per mouse each. During drug application, SPW-R activity was recorded for ≥ 30 min; thereafter, the drug was washed out, and the activity recorded for further ≥ 30 min.

Gamma oscillations were induced by adding kainate (100 nM) (Schneider et al., 2015; Wójtowicz et al., 2009). These recordings were performed from CA3 and CA1 pyramidal layers in an interface chamber in which slices were placed on a transparent membrane (culture plate inserts 0.4 μm Millicell; Millipore, Bedford, MA, United States). Signals were sampled at 10 kHz and acquired by custom-made amplifiers (10 \times) connected to an AD converter (Micro 1401 mk II, Cambridge Electronic Design Limited, Cambridge, UK). Data were processed with Spike2 and Signal (versions 7.00 and 3.07, respectively; Cambridge Electronic Design Limited, Cambridge, UK, RRID:SCR_000903 and SCR_014276, respectively). Baseline was recorded for ≥ 60 min, and S-Lic was then added to aCSF at a concentration of 0 (0.12% DMSO as vehicle control) and 300 μM , randomly assigned to one slice per mouse each. S-Lic was applied and the activity was recorded for ≥ 30 min. Finally, the drug was washed out and activity recorded for further ≥ 40 min.

Input/output (I/O) curves and field excitatory postsynaptic potentials (fEPSP)/population spike coupling were measured in submerged conditions in the presence of 300- μM S-Lic to evaluate effects of S-Lic on synaptic transmission and intrinsic excitability, respectively. A bipolar stimulating electrode (1–2 M Ω) placed in the stratum (st.) radiatum was used to evoke fEPSPs recorded from st. radiatum at more distal CA1 location. Stimulus intensity was increased and adjusted progressively and three independent measurements were done for each stimulus in order to get the desired amplitude of the fibre volley (Fidzinski et al., 2015). In all I/O curve experiments, we examined fEPSPs slope (20–80% of the maximum) in order to minimize contamination by the PS. For fEPSP/PS coupling, two recording electrodes placed in the pyramidal cell layer and the dendritic layer of CA1 were used. Stimulation intensity was adjusted to achieve the maximal fEPSP slope (approx. 1.6–2 mV·ms⁻¹). fEPSP slopes were determined 1 ms prior to the population spike, while population spike amplitude was defined as the absolute difference between population spike peak and anti-peak.

Seizure-like events were recorded in submerged conditions as previously reported, with some modifications (Heuzeroth et al., 2019). Epileptiform activity was induced by application of 4-AP (100 μM), a non-selective potassium channel blocker (Avoli et al., 1993; Perreault & Avoli, 1992), and field potentials were recorded from the entorhinal cortex (Lopantsev & Avoli, 1998). Typically, an *in vitro* seizure-like event evoked with 4-AP appears as a negative field potential shift characterized by the presence of low-amplitude gamma-activity. This activity is then followed by sustained tonic events and terminates with rhythmic bursting that slows down in frequency while increasing in amplitude (Avoli et al., 1993). Here, seizure-like events were identified with the following electrographic features: (1) duration of the negative field potential shift ≥ 10 s; (2) field potential decrease of ≥ 0.5 mV; (3) a seizure-like event starts with a single spike preceding the negative shift and ends with the termination of the rhythmic bursting. The signal was sampled at 10 kHz, low-pass filtered at 2 kHz by a Digidata 1550, and processed by PClamp10 software. Baseline activity was recorded for ≥ 30 min. Then S-Lic was added to the epileptogenic aCSF at a concentration of 0 (0.12% DMSO as vehicle control), 30, 100, and 300 μM , randomly assigned to one slice per mouse, and activity was recorded for ≥ 30 min, followed by a wash-out of ≥ 30 min.

For all *in vitro* experiments, blinding of the experimenter was not possible due to technical reasons, though statistical analysis explained in the last section of methods was conducted in a blinded fashion.

2.4 | 6-Hz psychomotor seizure model

The 6-Hz psychomotor seizure model is employed to induce *in vivo* acute seizures in rodents, which are thought to resemble pharmacoresistant seizures (Barton et al., 2001; Brown et al., 1953). *Kcnq2*^{+/+} and *Kcnq2*^{+/-} mice (P21–P28) were employed to test the effect of ESL on seizures evoked by 6-Hz corneal stimulation. All animals were acclimated to the experimenter 1 week before stimulation and to the experiment room for ≥ 1 h before the experiment started. A topical anaesthetic (0.4% **oxybuprocaine hydrochloride**, Omnivision GmbH, Puchheim, Germany) was applied to both eyes of the mouse to provide local anaesthesia 3 min before corneal stimulation (0.2-ms duration of rectangular pulses for 3 s at 6 Hz). The stimulation was applied via corneal electrodes connected to a constant current pulse generator (ECT Unit 5780, Ugo Basile, Comerio, Italy). The electrodes were wetted with 0.9% saline before each stimulation in order to secure a good electrical contact. Before investigating ESL effects, a total of 40 animals (four subgroups with 10 animals each: male *Kcnq2*^{+/+}, male *Kcnq2*^{+/-}, female *Kcnq2*^{+/+}, female *Kcnq2*^{+/-}) was used to determine the CC₅₀ and CC₉₇ for seizure induction by using the staircase technique previously described by Barton et al. (2001). Briefly, mice were stimulated two or three times every 48 h with increasing current intensities ranging between 8 and 24 mA. Stimulations were excluded from probit analysis when it was not possible to determine the presence of a clear seizure, either because of failure in the electrode conductance detection by

the pulse generator or no clear response from the animal. After determination of the CC_{97} for the two genotypes, the effects of ESL was tested in 20 $Kcnq2^{+/+}$ and 40 $Kcnq2^{+/-}$ male mice (20 mice stimulated with 1.5-fold $Kcnq2^{+/-}$ - CC_{97} and 20 mice stimulated with 1.5-fold $Kcnq2^{+/+}$ - CC_{97}). Sample size was estimated according to previous studies demonstrating a minimum of five to nine animals for sufficient statistic certainty (probability of type II errors <20%) and to reduce animal number to a minimum following 3Rs approach (Vittinghoff & McCulloch, 2007). Each animal was stimulated twice every 72 h, during which the general animal welfare and potential signs of stress were monitored every day. ESL dose (0, 10, 30, and 100 $mg \cdot kg^{-1}$) was randomly administrated via oral gavage (administration volume 10 $ml \cdot kg^{-1}$) approximately 60 min before stimulation. Immediately after stimulation, mice were placed in an open small cage (dimensions: 25 × 20 × 14 cm) for observation. Seizure intensity was scored by using a modified Racine's scale: 0, no behavioural changes; 1, sudden arrest with orofacial automatism; 2, sudden arrest with head nodding; 3, forelimb clonus; 4, forelimb clonus with rearing and possibly falling; 5, generalized tonic-clonic activity with loss of postural tone and sporadic wild jumping (Ihara et al., 2016; Racine, 1972). Experimenters were blinded for mice genotype during the whole experiment and for mice genotypes and ESL doses during follow-up scoring process. All mice were sacrificed at the end of the experiment by decapitation under isoflurane anaesthesia. Whole brain and plasma were collected and frozen at $-80^{\circ}C$ for the analysis of S-Lic concentration.

2.5 | Rotarod test

The rotarod test was used as a preliminary screening for a possible ESL toxicity on motor coordination (Dunham & Miya, 1957). Sixty minutes after ESL oral administration, mice were placed on a rotating rod (Ugo Basile, model 47600) for a maximum of 2 min at a constant speed of 15 rpm. Two trials were done for each mouse, interrupted by a 5-min break. The trial was considered failed if the mouse was not able to maintain its balance for at least 10 s, and it was placed back on the rod for a maximum of three times. The time that a mouse was able to rotate without falling or rotating by grasping onto the drum was recorded.

2.6 | Analyses of the S-Lic metabolite in plasma, whole brain and hippocampal slices

S-Lic concentrations in plasma and tissue (whole brain and hippocampal slices) were determined using a validated enantioselective LC-MS/MS assay (6470, Triple Quad LC-MS Agilent Technologies, Santa Clara, CA, USA) as previously described (Loureiro et al., 2011). In brief, plasma samples (50 μl) were thawed at $4^{\circ}C$, added to 100 μl of internal standard working solution (ISTD; 2000 $ng \cdot ml^{-1}$ of 10,11-dihydrocarbamazepine in phosphate buffer pH 5.6) and

processed by extraction of solid phase. Samples were agitated by using a vortex and centrifuged for 10 min at 20,000 g. Finally, the supernatant was transferred to HPLC vials/plates to be injected into the LC-MS/MS. Whole brain samples (without cerebellum) and hippocampal slices were thawed at $4^{\circ}C$ and weighed. Water was added to obtain a tissue concentration of 0.1 $g \cdot ml^{-1}$. Subsequently, samples were homogenized by using a Heidolph DIAX 900 mixer and transferred to 1.5-ml Eppendorf tubes. Samples were centrifuged for 30 min at 10,000 g at $4^{\circ}C$, and 50 μl of supernatant was added to 100- μl ISTD working solution and then processed by extraction of solid phase. In the same manner as for plasma, brain tissue samples were agitated with a vortex and centrifuged for 10 min at 20,000 g. Finally, the supernatant was filtered and transferred HPLC vials/plates to be injected into the LC-MS/MS. The samples were quantified with the analytical calibration range of 10.0 to 5000.0 $ng \cdot ml^{-1}$, both for plasma and brain tissues. The limit of quantification was 10.0 $ng \cdot ml^{-1}$.

2.7 | Data processing and statistical analyses

The data and statistical analysis comply with the recommendations and requirements on experimental design and analysis in pharmacology (Curtis et al., 2018). SPW-Rs, gamma oscillations, and seizure-like events raw data were analysed with custom-written MATLAB scripts (R2014b, R2016b, MathWorks, Natick, MA, USA, RRID:SCR_001622). For SPW-Rs and gamma oscillations, the last 10 and 5 min of each condition were examined, respectively. For seizure-like events, the last 25 min of each condition were considered for statistical analysis. The different frequency components of SPW-Rs were addressed separately. The slower sharp wave component was detected by low-pass filtering the raw local field potential recording at 50 Hz, and a threshold was set at 3.5 times the standard deviation of baseline free of events. The faster ripple component was detected by filtering the raw data at 80–600 Hz, and a threshold was fixed at 3.5 times the standard deviation of the filtered and smoothed data. Analysed parameters were incidence (events s^{-1}) and amplitude (mV) of sharp waves and ripples. Finally, for CA1 SPW-Rs, the peak amplitudes of sharp waves and ripples were carried out. The correlation coefficients were then calculated for each sharp wave and ripple amplitude pair.

Gamma frequency (Hz) and power spectral density (PSD, $\mu V^2 \cdot Hz^{-1}$) were calculated by first dividing the raw data vector into 10-s bins, obtaining the spectrogram by using Chronux toolbox functions (<http://chronux.org/>, RRID:SCR_005547; Bokil et al., 2010; Mitra & Bokil, 2008). Data were then processed with Welch's based fast Fourier transform for the calculation of power spectra in the 30–48 Hz frequency band. The temporal relationship between CA3 and CA1 regions during gamma oscillation activity was analysed by investigating the gamma phase, cross-correlation, and time lag. To this end, the last 5 min of each condition (baseline, treatment, and washout) from CA3 and CA1 recordings were first notch-filtered at 50 Hz in the frequency domain. Data were then down-sampled to 5 kHz and band-pass filtered (1–100 Hz). Stretches of 5 s were

cross-correlated by using MATLAB “xcorr” function, and the resulting cross-correlation functions were normalized such that the auto-correlations at zero lag were equivalent to 1, and finally averaged. The averaged cross-correlation peaks, along with their lags, were compared across the experimental conditions.

Data obtained from *in vivo* staircase test used to assess the CC₉₇ and their 95% confidence intervals for the 6-Hz psychomotor seizure model were calculated using the probit analysis (Finney, 1971). For the *in vivo* seizure scoring process, two experimenters blindly gave a

score to each mouse response to the current stimulus, and the average of the two scores was considered for the statistical analysis. Correlation analysis was performed to investigate the relationship between seizure score and S-Lic concentration in plasma and whole brain. Simple linear regression analysis was used to investigate differences between the coefficient of determination (r^2) of *in vitro* and *in vivo* data of follow-up measurements of S-Lic concentration in brain tissue. EC₅₀ values were calculated with AAT Bioquest web software (EC50 Calculator|AAT Bioquest).

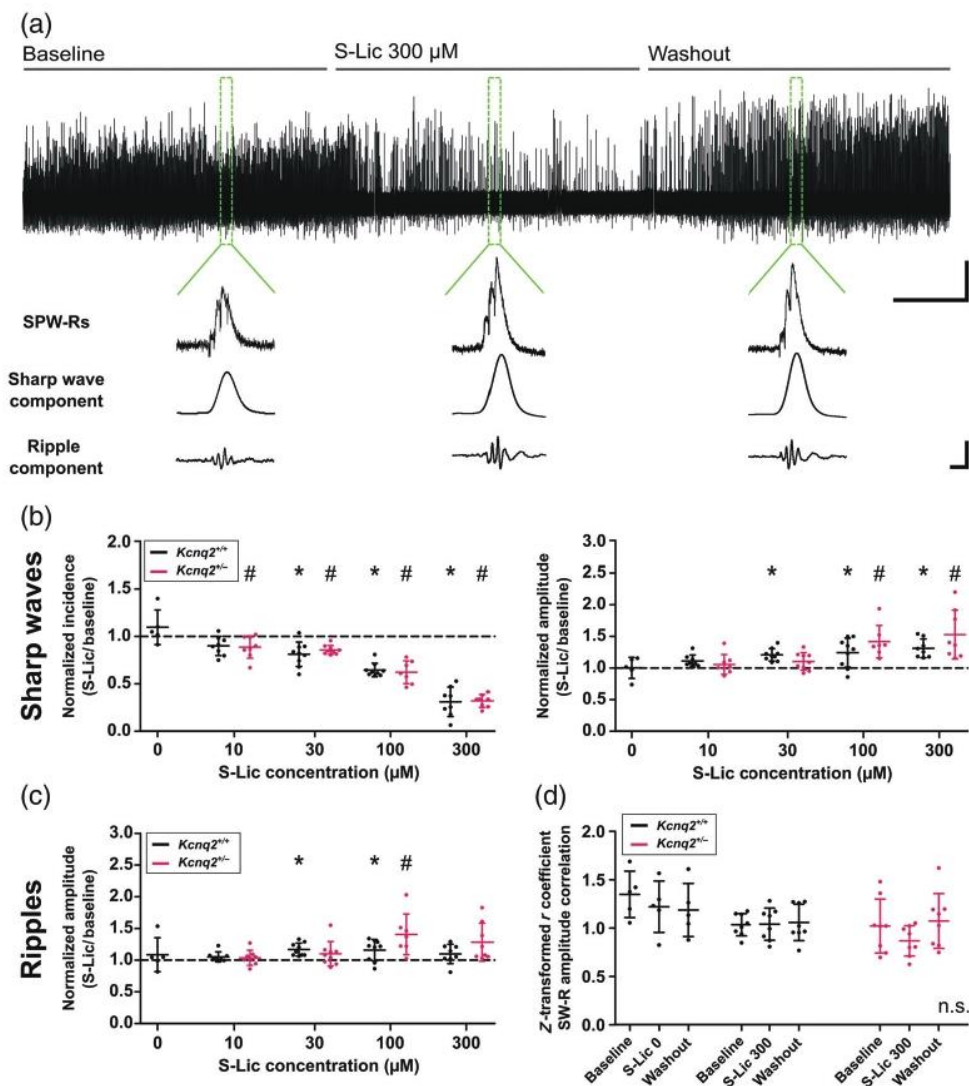


FIGURE 1 S-Lic effects on sharp wave-ripples (SPW-Rs) *in vitro* in the CA1 region. (a) Top: Representative extracellular recording from CA1 pyramidal layer. Bottom: Examples of single SPW-R events including low-pass (30 Hz; sharp wave component) and band pass (80–250 Hz; ripple component) filtered traces during baseline, S-Lic 300 μ M and washout, respectively. Scale bars: 5 min, 0.2 mV; 20 ms, 0.2 mV. (b,c) Scatter plots showing incidence (left panel) and amplitude (right panel) of sharp waves component (b) and ripples component amplitude (c). In each graph, vehicle controls (S-Lic 0) and four different S-Lic concentrations are displayed. (d) Scatter plots showing the z-transformed coefficients of correlation between the amplitude of ripples and sharp waves, during baseline and upon application of vehicle control or S-Lic 300 μ M, respectively, and washout. Each dot refers to one slice obtained from one animal, data are shown as mean \pm standard deviation. Data in (b) and (c) are normalized to the baseline. Asterisks and number signs mark statistically significant differences between treatment and correspondent baseline as assessed by one-way ANOVA or Friedman test and Tukey's or Dunnett's post hoc test for multiple comparisons, respectively (P value \leq 0.05). $Kcnq2^{+/+}$: $n = 5, 8, 9, 9,$ and 8 , for vehicle control and four S-Lic concentrations, respectively; $Kcnq2^{-/-}$: $n = 8, 9, 7,$ and 8 , for four S-Lic concentrations, respectively

Statistical analysis was conducted for experiment group sizes of $n \geq 5$ independent values, referred to biological samples. *In vitro* experiments were designed to be conducted in groups of equal size ranging 5–10 independent samples. In some cases, group size was unequal due to the necessity to evoke stable events such as SPW-Rs, gamma oscillations, or seizure-like events throughout the recording. With the exception of the analysis of the CA3-CA1 temporal relationship during gamma oscillations presented in Figure S2, all power calculations were performed a priori. Sample size was estimated in order to reach a power of 80% with an effect size of 20–25%. In case of the CA3-CA1 temporal relationship, the statistical power calculation was performed a posteriori and revealed that these experiments are underpowered and that a slightly higher number of replicates would have been required. All data were analysed with GraphPad Prism 5 (GraphPad Software Inc., San Diego, CA, USA, RRID: SCR_002798). Prior to statistical evaluation, all data were subjected to D'Agostino and Pearson omnibus normality test or Kolmogorov–Smirnov normality test (when $n < 8$) and further analysed accordingly. Correlation and cross-correlation coefficients of sharp wave and ripple amplitudes and gamma oscillations, respectively, were transformed with the Fisher z-transformation to generate a Gaussian-distributed dataset. The results were expressed as z-transformed r coefficient and z-transformed CrossCorr, respectively. For normally distributed data, statistical analysis was carried out using repeated measurements (for electrophysiological data) one-way analysis of variance (ANOVA) and post hoc Tukey's test for multiple comparisons. Two-way ANOVA and post hoc Bonferroni's test were used to compare data across genotypes. Post hoc tests were run only if ANOVA F value attained the required level of statistical significance, and there was no significant inhomogeneity in variance tested with the Bartlett's test for equal variances. The Pearson coefficient was applied for correlation analysis of normally distributed data. In case the normality test was not passed, the Friedman non-parametric test for repeated measurements or the Kruskal–Wallis test were used, with post hoc Dunnett's multiple comparison of individual groups. The Spearman coefficient was applied for correlation analysis of non-normally distributed data. Circular statistics was used to analyse gamma oscillation phase data with NCSS Statistical Software (2021, NCSS, LLC, Kaysville, Utah, USA, ncss.com/software/ncss). Data of gamma phase from both $Kcna2^{+/+}$ and $Kcna2^{+/-}$ mice showed unequal Von Mises concentration factor (κ); therefore, data were analysed with the nonparametric Uniform Score test.

A P value ≤ 0.05 was considered as statistically significant for all analyses. Normally distributed and normalized data to control for unwanted sources of variation are shown as mean \pm standard deviation (SD). Data of SPW-Rs and seizure-like events are shown as normalized to baseline (Figures 1b,c and 4b, respectively) only for illustrative purposes. Normalized data were expressed as ratio between treatment and baseline. We excluded one data point from the gamma oscillations time lag analysis due to technical reasons, namely, the presence of positive spikes that precluded the correct detection needed for calculating time lag.

2.8 | Materials

Eslicarbazepine acetate [(-)-(S)-10-acetoxy-10,11-dihydro-5H-dibenzo**b,f**/azepine-5-carboxamide] and its metabolite eslicarbazepine (referred also to as [S]-licarbazepine, S-Lic) [(+)-(S)-10,11-dihydro-10-hydroxy-5H-dibenzo**b,f**/azepine-5-carboxamide] were synthesized and tested by BIAL Portela & Ca, S.A., with purities $>99.5\%$. **Kainic acid (kainate)** was employed to evoke *in vitro* gamma oscillations and was purchased from Cayman Chemical Company, Ann Arbor, MI, USA. **4-Aminopyridine (4-AP)**, a non-selective potassium channel blocker, was used to induce *in vitro* seizure-like events and was obtained from Sigma, Munich, Germany. The vehicle used to dissolve eslicarbazepine acetate for *in vivo* oral administration was 0.2% hydroxypropylmethylcellulose (HPMC) dissolved in distilled water, while dimethyl sulfoxide (DMSO, max concentration 0.12%) was used to dissolve the metabolite eslicarbazepine to a stock concentration of 250 mM for *in vitro* experiments. Both HPMC and DMSO were obtained from Sigma.

2.9 | Nomenclature of targets and ligands

Key protein targets and ligands in this article are hyperlinked to corresponding entries in the IUPHAR/BPS Guide to PHARMACOLOGY <http://www.guidetopharmacology.org> and are permanently archived in the Concise Guide to PHARMACOLOGY 2020/21 (Alexander et al., 2021).

3 | RESULTS

3.1 | S-Lic reduces sharp wave incidence and increases SPW-R amplitude

Sharp wave–ripple complexes (SPW-Rs) consist of high frequency (~ 200 Hz) “ripple” oscillations superimposed on slow (~ 5 –10 Hz) waves (sharp waves). *In vivo*, SPW-Rs are observed during slow wave sleep and immobility and are thought to play an important role in a variety of cognitive functions (including memory consolidation) (Buzsáki, 1986; for review, see Buzsáki, 2015, and Maier & Kempter, 2017). Previous studies have established *in vitro* models of SPW-Rs facilitating the investigation of synaptic mechanisms underlying these events (Kubota et al., 2003; Maier et al., 2003; Papatheodoropoulos & Kostopoulos, 2002). Here, we applied SPW-Rs as a readout parameter to assess the effect of S-Lic on functional synchronization in hippocampal networks. SPW-Rs were recorded from CA1 pyramidal layer (Figure 1a). The application of S-Lic significantly and reversibly reduced SPW-R incidence in a concentration-dependent manner (Figure 1b, left panel) in both $Kcna2^{+/+}$ and $Kcna2^{+/-}$ mice. In addition, S-Lic increased SPW-R amplitude (Figure 1b, right panel, and Figure 1c). Control experiments with 0.12% DMSO left SPW-Rs unaffected. The amplitude of sharp waves and ripples recorded in CA1

pyramidal layer were strongly and positively correlated in both $Kcnq2^{+/+}$ and $Kcnq2^{+/-}$ mice. Moreover, the comparison between z-transformed correlation coefficients revealed analogous correlation of sharp waves and ripples amplitude, even upon application of the highest S-Lic concentration (Figure 1d).

3.2 | S-Lic alters properties of hippocampal gamma oscillations

Gamma oscillations occur in the frequency range of 30–90 Hz (Buzsáki & Wang, 2012; Freeman, 2007). They are implicated in many different cognitive functions, for example, episodic memory retrieval and exploratory behaviour (Csicsvari et al., 2003; Montgomery & Buzsáki, 2007). In our study, gamma oscillations *in vitro* in

hippocampal CA3 and CA1 area were evoked via activation of **ionotropic glutamate receptors** with kainate (Figure 2a-1) (Buhl et al., 1998). Application of 300- μ M S-Lic reduced the mean oscillation frequency in CA3 and CA1 both in $Kcnq2^{+/+}$ and in $Kcnq2^{+/-}$ mice (Figure 2c). We did not find any systematic change in gamma spectral power upon application of S-Lic (Figure S1).

We then analysed S-Lic effects on the synchronization and temporal relationship between CA3 and CA1 during gamma oscillations *in vitro* and found that the gamma phase was largely unaffected by S-Lic (Figure S2A), while cross-correlation between CA3 and CA1 decreased during application of S-Lic (Figure S2B). Similarly, the time lag between CA3 and CA1 significantly increased in the presence of the drug (Figure S2C). We have to note, however, that this post hoc analysis was slightly underpowered as detailed in the Methods section.

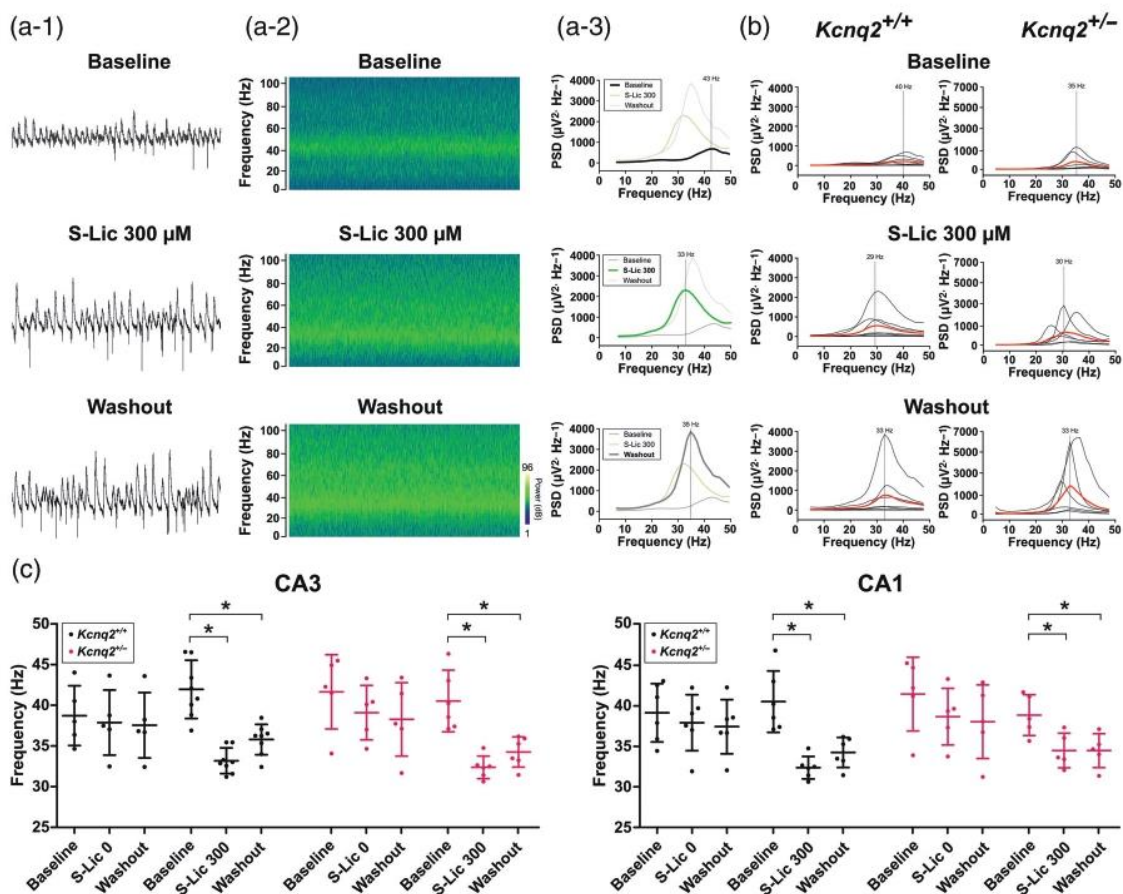


FIGURE 2 S-Lic effects on gamma oscillations *in vitro* in the CA3 region. (a-1) Representative traces of kainate-induced gamma oscillations recorded from pyramidal layer of CA3 mouse hippocampal slice. Top: baseline; middle: S-Lic 300 μ M, bottom: washout. Scale bar: 100 ms, 0.5 mV. (a-2) Wavelet spectrograms of the same example trace depicted in a-1. Scale bar: 1 min. Lighter colours represent higher power. (a-3) Power spectra for the example traces depicted in a-1. Vertical lines denote mean peak of gamma frequency. (b) Power spectra for all experiments recorded from CA3 (each line represents one experiment) obtained during baseline (top), application of S-Lic 300 μ M (middle) and washout (bottom) from $Kcnq2^{+/+}$ (left) and $Kcnq2^{+/-}$ (right) slices. Thicker red lines represent mean of all experiments for a given condition. Vertical lines denote mean peak of gamma frequency. (c) Scatter plots showing the frequency of gamma oscillations recorded from CA3 (left panel) and CA1 (right panel), upon application of vehicle control (S-Lic 0) and S-Lic 300 μ M. $Kcnq2^{+/+}$: S-Lic 300 $n = 8$, S-Lic 0 $n = 5$; $Kcnq2^{+/-}$ S-Lic 300 $n = 6$, S-Lic 0 $n = 5$

3.3 | S-Lic does not affect input/output behaviour and intrinsic excitability in the CA1 area

Interplay between synaptic inhibition and excitation is critical for the network synchronization during hippocampal population activity such as SPW-Rs and gamma rhythm (Atallah & Scanziani, 2009; Buzsáki, 2015; Kubota et al., 2003; Maier et al., 2003). Recording of input/output (I/O) and fEPSP/population spike coupling relationships provide insights in basal properties of synaptic transmission and excitation-to-inhibition coupling in the region of interest, respectively. Therefore, to gain insight into possible target mechanisms underlying the effect of S-Lic on neuronal oscillations, we firstly conducted extracellular I/O recordings in the CA1 area in the absence and presence of S-Lic. Post-synaptic fEPSP slopes at given fibre volley amplitudes (Figure 3a) were not different between wild-type and heterozygous *Kcnc2* mice. Likewise, application of S-Lic did not affect synaptic input behaviour in either genotype (Figure 3a-1,a-2).

We also performed fEPSP/population spike coupling experiments to assess S-Lic effects on intrinsic excitability (Figure 3b). Similar to I/O recordings, S-Lic did not alter population spike amplitude in neither genotype. Of note, also no differences were detected between genotypes (Figure 3b-1,b-2).

3.4 | S-Lic reduces *in vitro* seizure-like events frequency in a concentration-dependent manner

A well-established model to study synaptic foundations of pathological network synchronization is the 4-AP acute model of epileptiform activity (Avoli et al., 1993; Losi et al., 2016; Perreault & Avoli, 1992; Rudy, 1988). Upon exposure to 100- μ M 4-AP, local field potential recordings from entorhinal cortex exhibited stable seizure-like events in brain slices from both *Kcnc2*^{+/+} and *Kcnc2*^{+/-} mice (Figure 4a). As depicted in Figure 4b, S-Lic effectively and concentration-

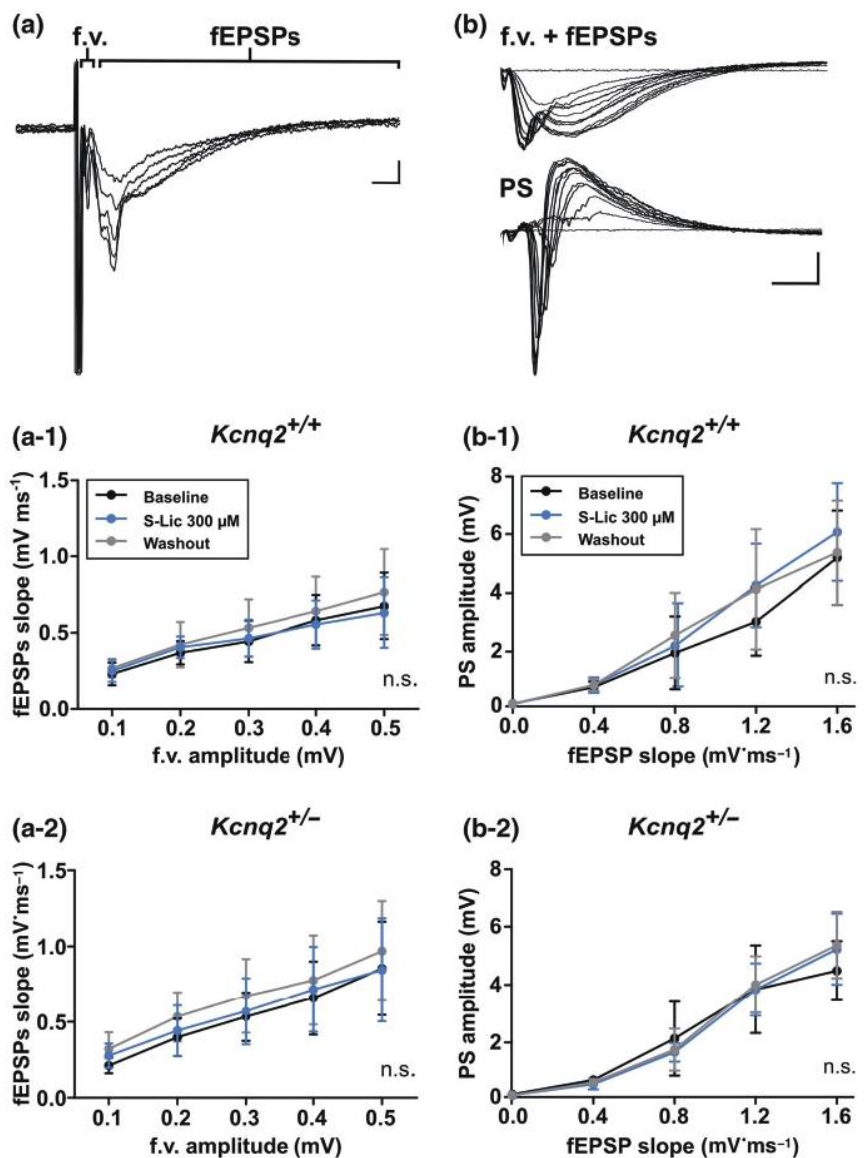


FIGURE 3 S-Lic does not affect I/O properties and intrinsic excitability in the CA1 region *in vitro*. (a) Example recording of fibre volley (f.v.) and the consequent field excitatory postsynaptic potential (fEPSP) responses recorded from the CA1 st. radiatum at five different stimulation intensities. Scale bar: 5 ms, 0.2 mV. (a-1, a-2) Line graphs showing recorded fEPSPs slopes in relation to f.v. amplitudes during baseline, S-Lic and washout in *Kcnc2*^{+/+} (a-1) and *Kcnc2*^{+/-} (a-2). Dots and lines represent mean fEPSPs slopes \pm standard deviation for a given f.v. amplitude. n.s. = not significant difference between the groups ($n = 8$) as assessed by two-way ANOVA. (b) Example recordings showing fibre volleys (f.v.) with consequent fEPSPs from the CA1 st. radiatum of hippocampal slices (top) and the corresponding population spikes (PS) recorded from CA1 pyramidal cell layer (bottom). Scale bar: 5 ms, 1 mV. (b-1, b-2) Line graphs displaying changes of PS amplitude in relation to fEPSPs slopes during baseline, S-Lic and washout in *Kcnc2*^{+/+} (b-1) and *Kcnc2*^{+/-} (b-2). Dots and lines represent mean PS amplitudes \pm standard deviation for a given fEPSPs slope. n.s. = not significant difference between the groups ($n = 5$) as assessed by two-way ANOVA

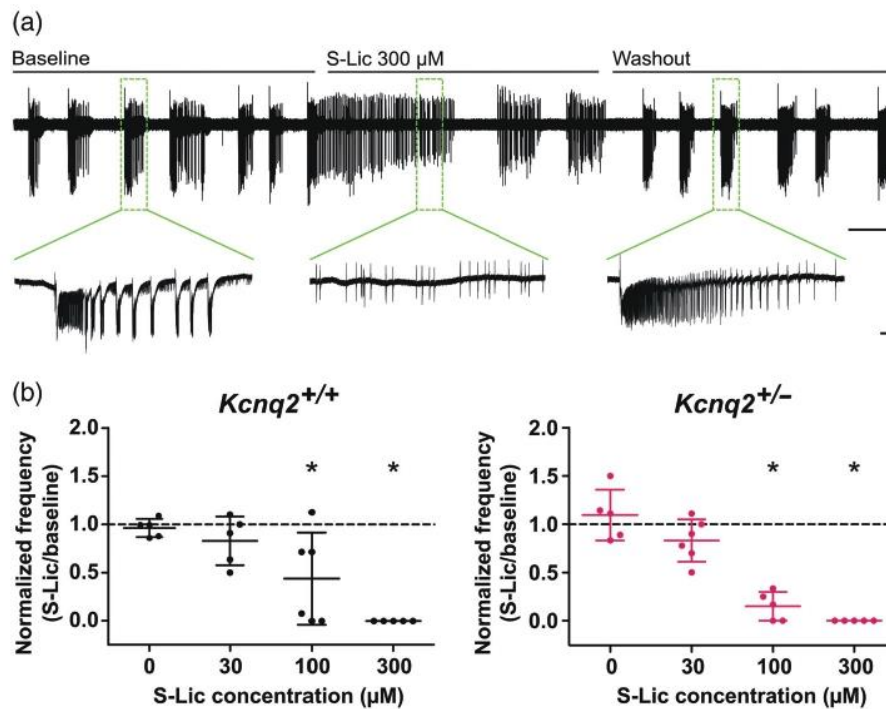


FIGURE 4 S-Lic effects on 4-AP induced seizure-like events *in vitro*. (a) Top: Representative high-pass-filtered recording showing seizure-like events (SLEs) induced by 4-AP from the entorhinal cortex. Bottom: SLE example during baseline (left), near-complete absence of SLEs during application of S-Lic (middle) and reappearance during washout (right). Scale bars: 5 min, 0.5 mV; 10 s, 0.5 mV. (b) Scatter plots showing normalized frequency of SLEs subjected to vehicle control (S-Lic 0) and three different concentrations of S-Lic for *Kcnq2*^{+/+} (left) and *Kcnq2*^{+/-} (right) slices. Each dot refers to one slice obtained from one animal; data are shown as mean ± standard deviation. Asterisks mark statistically significant differences between treatment and correspondent baseline as assessed by one-way ANOVA or Friedman test and Tukey's or Dunnett's post hoc test for multiple comparisons, respectively (*P* value ≤ 0.05). *Kcnq2*^{+/+}: *n* = 5, 5, 6, and 5, respectively, *Kcnq2*^{+/-}: *n* = 5, 6, 5, and 5, respectively

TABLE 1 S-Lic EC₅₀ and ED₅₀ values calculated from *in vitro* and *in vivo* experiments

	<i>In vitro</i>		<i>In vivo</i>	
	Experiment S-Lic EC ₅₀ (μM)	Follow-up S-Lic EC ₅₀ (μg·ml ⁻¹)	Experiment ESL ED ₅₀ (μM)	Follow-up S-Lic EC ₅₀ (μg·ml ⁻¹)
<i>Kcnq2</i> ^{+/+}	73.8	10.42 (41 μM)	33.0	0.94 (4 μM)
<i>Kcnq2</i> ^{+/-}	55.3	10.52 (41 μM)	67.4	1.53 (6 μM)

Note: EC₅₀ and ED₅₀ values calculated from experiments data are depicted in the first column (*in vitro* experiments) and third column (*in vivo* experiments). EC₅₀ values obtained from follow-up measurements of the drug metabolite concentration in brain tissue are shown in the second column (hippocampal slice tissue from *in vitro* experiments) and in the fourth column (whole brain from *in vivo* experiments).

independently blocked seizure-like event activity in both genotypes. Of note, 100-μM S-Lic effectively reduced seizure-like event incidence in all slices from *Kcnq2*^{+/-} mice but only in 50% of slices from *Kcnq2*^{+/+} mice. Consistently, calculation S-Lic EC₅₀ revealed a lower value for *Kcnq2*^{+/-} when compared to *Kcnq2*^{+/+} mice (Table 1, first column).

3.5 | Decreased seizure threshold in *Kcnq2*^{+/-} mice in the 6-Hz psychomotor seizure model

As S-Lic was effective in suppressing seizure-like events *in vitro* and as the results suggested a slightly higher efficacy on *Kcnq2*

heterozygous mice, we extended our investigation to an *in vivo* approach. To this end, we applied the 6-Hz psychomotor seizure model, considered as a model of pharmaco-resistant seizures (Barker-Haliski et al., 2018; Barton et al., 2001). This model was previously used to demonstrate a reduced seizure threshold in *Kcnq2*^{+/-} mice compared to *Kcnq2*^{+/+} littermates when using 1.5- to 2-fold amplitude of the CC₉₇ convulsive current. Using the staircase method described by Barton et al. (2001), mice from both sexes and both genotypes were stimulated with increasing current intensities (8–24 mA). Subsequent probit analysis confirmed previous results by revealing decreased seizure threshold for male *Kcnq2*^{+/-} mice (*Kcnq2*^{+/+}: CC₅₀ = 17.1 mA, 95% CI 16.2–17.9 mA; *Kcnq2*^{+/-}:

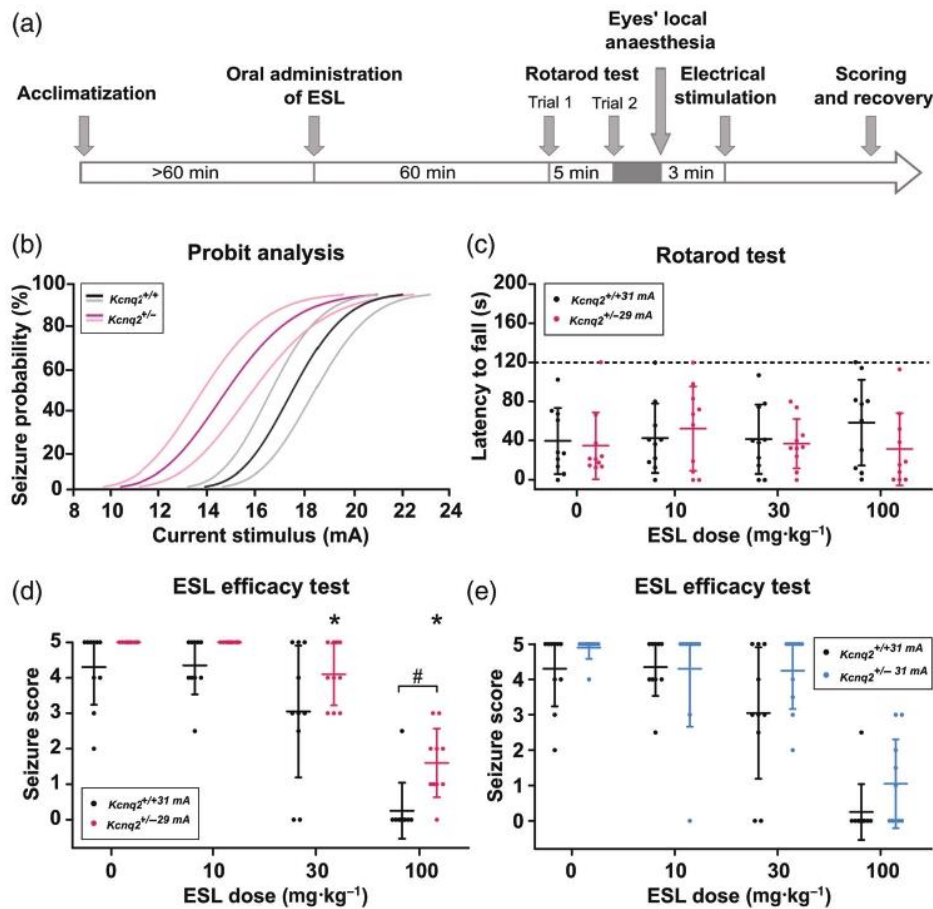


FIGURE 5 Efficacy of ESL in the 6-Hz psychomotor seizure model *in vivo*. (a) Graphical visualization of the time line employed for the 6-Hz psychomotor seizure *in vivo* experiments. Arrows indicate time points. (b) Seizure probability in dependence from stimulation intensity shown as line graphs calculated with the probit analysis. Black/grey and red/pink lines represent mean data \pm 95% confidence interval from *Kcnq2*^{+/+} and *Kcnq2*^{+/-} mice, respectively ($n = 23$; $n = 16$ respectively). (c) Rotarod test results expressed as time to fall and shown as scatter plots with data from different ESL doses including vehicle control ($n = 10$). Each dot represents the mean of two trials. (d, e) Seizure scores (0–5) at different ESL doses. (d) Seizure scores for genotype-specific CC_{97} . (e) Comparison of ESL effect on seizure score in both genotypes stimulated with $1.5 \times CC_{97}$ of *Kcnq2*^{+/+} (same *Kcnq2*^{+/+} group in d and e). Each dot refers to the mean of the scores given to one stimulated animal observed by two experimenters during follow-up blinded seizure scoring process. Data are shown as mean \pm standard deviation ($n = 10$). Asterisks mark statistically significant differences between ESL doses of each genotype assessed by one-way ANOVA and Dunnett's post hoc test for multiple comparisons. Number signs mark statistically significant differences between genotypes assessed by two-way ANOVA and Bonferroni's post hoc test (P value ≤ 0.05)

$CC_{50} = 14.5$ mA, 95% CI 13.6–15.5 mA) (Figure 5b). In female mice, probit analysis was not possible due to high variability of responses in the *Kcnq2*^{+/+} group (data not shown). Subsequent investigation of ESL effects was performed exclusively in male animals.

3.6 | ESL protects against acute seizures *in vivo* without affecting motor coordination

The anti-epileptic effects of ESL *in vivo* were tested in the 6-Hz psychomotor seizure model using 1.5-fold CC_{97} stimulation intensity, which has been proved to be adequate for the screening of anti-epileptic drug efficacy (Barker-Haliski et al., 2018; Barton et al., 2001); 1.5-fold CC_{97} was calculated from the staircase procedure separately

for each genotype: 31 mA for *Kcnq2*^{+/+} and 29 mA for *Kcnq2*^{+/-} mice. Sixty minutes after drug administration and shortly before stimulation, the Rotarod test was employed as screening for motor coordination. No difference in latency to fall was detected between mice that received ESL and mice that received the vehicle control (Figure 5c). Likewise, no difference was detected between *Kcnq2*^{+/+} and *Kcnq2*^{+/-} genotypes. ESL exerted anti-epileptic effects in a dose-dependent manner in both genotypes (Figure 5d). Upon administration of $100 \text{ mg} \cdot \text{kg}^{-1}$ ESL, 9 out of 10 tested *Kcnq2*^{+/+} mice did not display seizures (seizure score = 0) and the remaining animal showed a sudden arrest (seizure score = 2.5). In contrast, in the *Kcnq2*^{+/-} group, only 1 out of 10 animals remained seizure-free while the remaining 9 individuals displayed seizure in a score range 1–3. Of note, in the control group that received only vehicle, we observed a

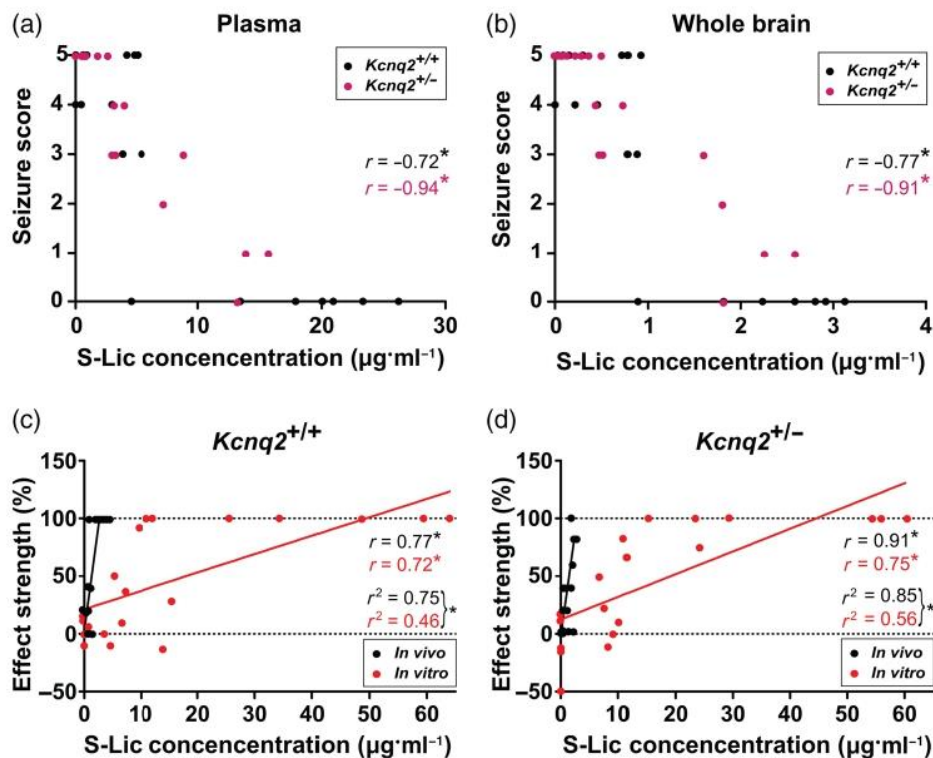


FIGURE 6 S-Lic concentration in plasma and whole brain and comparison between *in vitro* and *in vivo* correlation. (a, b) Dot plots displaying the relationship between seizure score assessed during 6 Hz psychomotor seizure model and S-Lic concentration in plasma (a) and whole brain tissue (b). Each dot refers to one plasma or whole brain sample obtained from one animal ($n = 20$). r : corresponding colour-coded correlation coefficients. Asterisks mark statistical significance assessed by correlation analysis (P value ≤ 0.05). (c, d) Correlation of anti-epileptic effect strength and S-Lic concentration *in vitro* and *in vivo*, for Kcnq2^{+/+} (c) and Kcnq2^{+/-} (d) mice. Dot plots display relationship between S-Lic concentration and anti-epileptic effect strength given in %. r and r^2 : corresponding colour-coded correlation coefficients and coefficients of determination for each group, respectively. Each dot refers to one hippocampal slice ($n = 20$) or whole brain ($n = 20$) sample obtained from one animal. Asterisks mark statistical significance assessed by correlation analysis (P value ≤ 0.05). Statistically significant differences between black and red best-fit lines slope assessed by linear regression analysis: $F(1, 36) = 30.6$, $P \leq 0.05$ (Kcnq2^{+/+}); $F(1, 36) = 22.3$, $P \leq 0.05$ (Kcnq2^{+/-})

tendency of Kcnq2^{+/-} mice to display a higher seizure score. Moreover, ED₅₀ for Kcnq2^{+/-} mice was higher than Kcnq2^{+/+} mice (Table 1, third column). To exclude that these effects were due to different stimulation intensities (genotype-specific CC₉₇), we repeated the experiment in an additional group of Kcnq2^{+/-} mice using the same stimulation intensity that was applied in Kcnq2^{+/+} animals (31 mA). Here, we found that the seizure score difference remained unaltered (Figure 5e). Taken together, our results confirmed that Kcnq2^{+/-} mice displayed a lower seizure threshold and demonstrated that ESL is effective in these animals.

3.7 | S-Lic concentration correlates with efficacy *in vivo* and *in vitro*

Correlation analysis was applied to investigate the relationship between S-Lic concentration in plasma and whole brain and the seizure scores of mice exposed to 6-Hz stimulation. In line with the expected anti-seizure efficacy of ESL, S-Lic concentration in

both plasma and brain was significantly and negatively correlated to the seizure score in either genotype (Figure 6a,b). Statistical analysis was then applied to compare S-Lic concentrations in brain tissue from *in vitro* and *in vivo* experiments with the respective effect strength (Figure 6c,d). Effect strength was determined separately for each hippocampal slice or investigated animal as the relative drug efficacy in suppressing seizure-like or seizure activity. For *in vitro* experiments, effect strength was calculated as $[(1 - \text{seizure-like event frequency drug} / \text{seizure-like event frequency baseline}) \times 100]$. For *in vivo* experiments, the seizure scores were considered equivalent to effect strength of: 5 = 0%; 4 = 20%; 3 = 40%; 2 = 60%; 1 = 80%; 0 = 100%. In either genotype, S-Lic concentration was positively correlated with its effect strength both *in vitro* and *in vivo* (Figure 6c,d). Linear regression analysis showed a statistically significant difference between the best-fit lines of *in vitro* and *in vivo* data from both genotypes (Figure 6c,d). In addition, EC₅₀ values revealed that substantially higher concentrations of S-Lic are required *in vitro* (Table 1, second and fourth columns).

4 | DISCUSSION

In the present study, we investigated the effects of the anti-epileptic drug ESL and its major active metabolite S-Lic in a mouse model of KCNQ2-related childhood epilepsy (Watanabe et al., 2000). In both *Kcnq2*^{+/+} and *Kcnq2*^{+/-} slice preparations, (1) S-Lic modified SPW-Rs complexes and (2), to a lesser degree also gamma oscillations, (3) S-Lic did not affect input/output properties or fEPSP/population spike coupling in CA1, but (4) effectively reduced 4-AP induced seizure-like events. *In vivo*, (5) ESL reduced seizure incidence and score in the 6 Hz psychomotor seizure model. Also, (6) *Kcnq2*^{+/-} mice displayed a decreased seizure threshold and decreased sensitivity to ESL, while (7) no effects of ESL on motor coordination were detected. Finally, (8) S-Lic concentrations negatively correlated with seizure score *in vivo* and revealed (9) differences between effective S-Lic concentrations *in vitro* and *in vivo*.

4.1 | Eslicarbazepine effects on hippocampal oscillations

SPW-Rs and gamma oscillations play critical roles in a variety of cognitive functions. While SPW-Rs are involved in consolidation of long-term memory, gamma oscillations are considered to coordinate neuronal activity in the CA3 and CA1 regions and modulate higher cognitive functions (Csicsvari et al., 2003; Montgomery & Buzsáki, 2007).

The decreased incidence and increased amplitude of SPW-R in the CA1 region in both genotypes indicate an impact of S-Lic on rhythm generators. S-Lic did not alter synaptic or intrinsic properties in field recordings, which is in line with previous findings (Booker et al., 2015). At the single cell level, S-Lic modulates the slow inactivation of **Na_v1.2** and **Na_v1.6** sodium channels (Booker et al., 2015; Holtkamp et al., 2018). However, these effects might be too subtle to be detected at the level of field potential recordings.

S-Lic decreased gamma frequency without affecting its power and likely decreased the cross-correlation between CA3 and CA1 without affecting the gamma phase. Previous studies point to gamma generators in the entorhinal cortex and the CA3 area inducing high- and low-frequency gamma oscillations, respectively (Bragin et al., 1995; Colgin et al., 2009). Although slightly underpowered, our supplemental data on cross-correlation and time lag between CA3 and CA1 point to a downtrend impact of S-Lic on their temporal relationship, potentially due to less precise neuronal spiking. Mechanistically, S-Lic mediated inhibition of sodium channels likely affects feedback regulation between principal neurons and interneurons, critical for synchronization of gamma oscillations (Fisahn et al., 1998). The lacking wash-out effect (Figures 2c and S1) is possibly due to enhanced synaptic activity induced by gamma oscillations in excitatory synapses, leading to enlarged presence of SPW-Rs after wash-out of kainate or **carbachol** (Zarnadze et al., 2016). Persistent gamma activity might lead to a boost of gamma power itself and a decrease of the gamma frequency. In our study, the gamma power continuously increased also in long-term (2 h) control experiments.

Effects of S-Lic on neuronal oscillations are possibly associated with cognitive side effects observed with high doses of eslicarbazepine acetate. Of note, therapeutic S-Lic concentrations in plasma samples from patients are lower (by a magnitude of ~10) than what was used in our *in vitro* experiments (Hebeisen et al., 2015). Despite the fact that the M-current is implicated in hippocampal network synchronization underlying SPW-Rs, gamma and theta oscillations (Cooper et al., 2001), our *in vitro* experiments did not reveal differences between the two investigated genotypes. The K_v7.2 subunit is highly expressed in hippocampal interneurons, which modulate excitability and synchronization during oscillations (Cooper et al., 2001). In a recent study, K_v7.2/7.3 channel inhibition was shown to increase SPW-Rs incidence (Trompoukis et al., 2020). Also, K_v7.5 channels have been demonstrated to control excitability through modulation of synaptic activity and loss of *Kcnq5* gene expression caused a reduction in gamma oscillations and ripples *in vivo* (Fidzinski et al., 2015). The lack of differences between genotypes in our study is possibly due to a compensatory increase in K_v7.2 expression, a phenomenon that was observed before in adult mice heterozygous for the *Kcnq2* gene (Robbins et al., 2013). Although we employed juvenile mice (≤4 weeks), which are more susceptible to epileptogenic stimuli *in vivo* (Watanabe et al., 2000), it is possible that this “compensatory” mechanism was already taking place, which might explain the absence of clear differences between the genotypes seen throughout the application of S-Lic during SPW-Rs and gamma oscillations. This slow, age-dependent recurrence of the M-current might have also impacted pathological seizure-like events *in vitro*, though to a lower extent.

4.2 | S-Lic reduces *in vitro* seizure like-events in both genotypes

In contrast to mild S-Lic effects on physiological oscillations *in vitro*, S-Lic massively reduced the incidence of seizure-like events. Interestingly, at submaximal concentrations (100 μM), S-Lic was more effective in *Kcnq2*^{+/-} mice when compared to *Kcnq2*^{+/+} littermates. The spike threshold in *Kcnq2*^{+/-} mice is lower (Otto et al., 2009; Watanabe et al., 2000), and it might have been effectively counteracted by sodium channel inhibition by S-Lic. It is unclear whether the increased efficacy of S-Lic in slices from affected animals is specific—we did not test S-Lic in other *in vitro* models such as high potassium or low magnesium (Mody et al., 1987; Traynelis & Dingledine, 1988) due to their long-term instability. The 4-AP *in vitro* model of acute seizure-like events used in our study leads to stable activity over hours and is sensitive to a variety of anti-epileptic drugs (Heuzeroth et al., 2019). However, application of 4-AP presents a massive pro-epileptic stimulus, which might also explain differences of S-Lic EC₅₀ between *in vivo* (4–6 μM) and *in vitro* (41 μM) conditions. Finally, an important limitation of an *in vitro* acute model of seizure-like events in contrast to epileptic animals is the lack of a genuine epileptic network (Heuzeroth et al., 2019)—*in vitro* seizure-like events reflect electrographic features but not seizures.

4.3 | ESL is effective against acute seizures in the 6-Hz psychomotor seizure model

In line with previous studies (Otto et al., 2009; Watanabe et al., 2000), we confirmed a decreased seizure threshold in *Kcnq2*^{+/-} male mice. Results from female mice were variable and precluded proper staircase/probit analysis, possibly due to hormonal cycle influence on neuronal excitability and seizure threshold (Scharfman & MacLusky, 2006). In males, ESL protected mice of both genotypes against acute seizures evoked by 1.5-fold CC₉₇ in a dose-dependent manner. ESL efficacy at the highest dose (100 mg·kg⁻¹) was more robust in *Kcnq2*^{+/+} than in *Kcnq2*^{+/-} mice. This difference prevailed also when *Kcnq2*^{+/-} mice were stimulated with 1.5-fold CC₉₇ of *Kcnq2*^{+/+} animals. The results point to a genotype-dependent ESL efficacy and further confirm that seizure threshold is decreased in *Kcnq2*^{+/-} mice.

ESL doses in the present work were chosen according to previous studies (Booker et al., 2015; Hebeisen et al., 2015). Using 2xCC₉₇ (44 mA), the mentioned studies revealed an ED₅₀ in the range of 12–16 mg·kg⁻¹. Taking into account the limited number of doses employed, we estimated an ED₅₀ of 33 and 67.4 mg·kg⁻¹ for *Kcnq2*^{+/+} and *Kcnq2*^{+/-} mice, respectively, indicating a lower relative ESL efficacy in *Kcnq2*^{+/-} animals. We did not test ESL doses >100 mg·kg⁻¹. Our results confirm that ESL has a strong anti-convulsant effect in the 6-Hz psychomotor seizure model and indicates increased drug resistance in *Kcnq2*^{+/-} mice. As reported previously by others, ESL doses employed in our study did not affect motor coordination (Doeser et al., 2015; Hebeisen et al., 2015).

In the 6-Hz psychomotor seizure model, widely used to assess anti-convulsant effects of different anti-epileptic drugs (Barton et al., 2001; Hebeisen et al., 2015; Leclercq & Kaminski, 2015), the genetic background can strongly influence the seizure score and resistance to drugs (Barker-Haliski et al., 2018). The mice employed in our study had a C57Bl/6J background, while Leclercq and Kaminski, as well as Hebeisen et al., used NMRI mice. These two mouse lines have been reported to have a comparable seizure threshold but a different level of seizure resistance to phenytoin and **levetiracetam** (Leclercq & Kaminski, 2015). The higher seizure scores in *Kcnq2*^{+/-} compared to *Kcnq2*^{+/+} mice are in line with increased neuronal excitability in *Kcnq2*^{+/-} mice that apparently is easier to detect *in vivo*. Potentially, preserved connectivity in the brain *in vivo* might be required for the full manifestation of network effects derived from the reduced expression of channels containing K_v7.2 subunits (Otto et al., 2009).

4.4 | Comparison of S-Lic efficacy in *in vitro* and *in vivo* experiments

The effective S-Lic concentration in brain tissue is ~10× lower *in vivo* than in experiments conducted *in vitro* (Figure 6 and Table 1), which is in line with previous studies showing (1) a low brain/plasma ratio due to low capability of S-Lic in crossing the blood-

brain barrier (Alves et al., 2008) and (2) plasma/tissue distribution in *in vitro* experiments (Hebeisen et al., 2015). S-Lic has a half-life of 13–20 h and peaks at 1–3 h (Almeida et al., 2008). Since whole brains were sampled ~60 min after oral administration, we can exclude that the metabolite was already subjected to clearance. Therefore, even if the EC₅₀/ED₅₀ values in this study are estimations that could not be statistically analysed according to pharmacological standards (Jiang & Kopp-Schneider, 2015), they point to differences of substance efficacy between *in vitro* and *in vivo* preparations.

In previous studies, ESL was effective at comparable concentrations to those applied in our work. *In vivo*, ESL 100 mg·kg⁻¹ prevented acute seizures and epilepsy in the latrunculin A mouse model and prevented paroxysmal activity in EEG recordings, indicating a possible anti-epileptogenic effect (Sierra-Paredes et al., 2014). In a **pilocarpine** rat model, Doeser et al. postulated a protective effect of ESL (150–300 mg·kg⁻¹) against chronically induced epileptic activity and development of repetitive seizures *in vitro* and *in vivo* (Doeser et al., 2015). ESL (30–100 mg·kg⁻¹) anti-seizure efficacy was also demonstrated in corneal and amygdala kindling models of focal-onset seizures (Potschka et al., 2014). Hebeisen and colleagues investigated *in vitro* anti-seizure activity of S-Lic at 30, 100, and 300 μM in hippocampal slices from wild-type mice and revealed ESL (50, 100, and 150 mg·kg⁻¹) efficacy in the MES and 6-Hz psychomotor models *in vivo*. Further, the analysis of ESL metabolites in whole brain tissue and plasma revealed comparable concentrations between tissue S-Lic concentration and ESL doses used in *in vivo* experiments (Hebeisen et al., 2015). In our work, we have additionally provided a demonstration of the expected effective concentrations in *in vitro* experiments and the difference reported in *in vivo* conditions.

4.5 | Limitations of the *Kcnq2* mouse model

In our study, we used juvenile animals in order to apply the 6-Hz model that is not established for neonates. The chosen age presents a limitation as the use of animals shortly after birth would have better reflected the early disease onset in KCNQ2-related disorders in patients. Overall, acute epilepsy models present a limitation per se—chronic models with spontaneous recurrent seizures are more adequate. Peters and colleagues developed a mouse model with a conditional dominant negative *Kcnq2* transgene, which causes the suppression of the M-current and spontaneous seizures (2005), but these mice showed features inconsistent with the human phenotype. In other *Kcnq2* mutations such as A306T, adult seizures occur in 16% of patients, but this mutation has been characterized only for some BFNE families (Singh et al., 2008). The *Kcnq2* heterozygous mouse model developed by Watanabe and colleagues was advantageous in terms of similarities in network features underlying KCNQ2-related epilepsy (Otto et al., 2009; Watanabe et al., 2000). Therefore, by choosing to investigate *in vitro* and *in vivo* ESL effects in a model of BFNE, we sought to provide first preclinical data for a

possible choice of this compound as anti-seizure treatment also for the more severe *KCNQ2* epilepsy phenotypes. In 2020, in a novel model for *KCNQ2* encephalopathy generated by introducing the p. (Thr274Met) variant in C57Bl/6N mice, most of the pathophysiological features of the human disease have been successfully reproduced (Milh et al., 2020). Future studies on S-Lic efficacy on the *Kcnq2*^{p.(Thr274Met)/+} mouse model would therefore represent a helpful add-on.

4.6 | Potential role of eslicarbazepine acetate for the treatment of *KCNQ2*-related epilepsy

Currently, a disease-specific therapy against *KCNQ2*-related epilepsy does not exist, although in a clinical trial, the efficacy and tolerability of the K_v7 channel modulator **XEN496** (retigabine) are being tested (ClinicalTrials.gov, Identifier: NCT04639310; Millichap et al., 2016). Current treatments for *KCNQ2*-related epilepsies are based on administration of anti-epileptic drugs including sodium channel inhibitors, such as phenytoin or carbamazepine. While BFNE outcomes are mostly positive, patients suffering from *KCNQ2*-related severe encephalopathy often remain refractory to treatment (Kuersten et al., 2020). ESL has shown improved tolerability and safety compared to other dibenzoazepine family members both in children and in adults (Almeida et al., 2008; Galiana et al., 2017; Rocamora, 2015). Moreover, multiple clinical trials have shown ESL to be effective in patients in whom other sodium channel blockers had failed (Ben-Menachem et al., 2010; Elger et al., 2009; Halász et al., 2010). The mechanisms for the improved efficacy of ESL include a lower affinity for the resting state of voltage-gated sodium channels and the ability to increase their slow, rather than fast, inactivation (Doeser et al., 2015; Hebeisen et al., 2015; Patrício Soares-da-Silva et al., 2015). These observations suggest a possibly enhanced efficacy of ESL to prevent seizures in paediatric and adult patients suffering from epilepsy refractory to standard treatment.

5 | CONCLUSIONS

Here, we investigated *in vitro* effects and *in vivo* efficacy of the novel anti-epileptic drug eslicarbazepine acetate in a *Kcnq2* mouse model of *KCNQ2*-related self-limited epilepsy. Our results indicate that hyperexcitability caused by a potassium channel mutation can be effectively targeted by an anti-seizure drug acting mainly on sodium channels. Our work confirms the anti-seizure efficacy of eslicarbazepine acetate in an *in vivo* mouse model of childhood epilepsy and furthermore points to important differences between *in vitro* and *in vivo* investigations in seizure and epilepsy models.

ACKNOWLEDGEMENTS

This work was supported by Eisai and BIAL Portela & Ca. LM and PF were partially funded by NeuroCure Cluster of Excellence, Berlin

Institute of Health. We would like to thank Mandy Marbler-Pötter for excellent technical assistance and Imandra Kempe for her contribution to the *in vitro* seizure-like events experiments.

AUTHOR CONTRIBUTIONS

PF, MH, MDW, and PSdS conceived the presented project idea. LM designed and performed *in vitro* and *in vivo* experiments and analysed the data. LK assisted with *in vivo* experiments and analyses. NM, MDW, and PF assisted with MATLAB analysis of *in vitro* experiments and interpretation. PSdS carried out ESL metabolite extraction. LM and PF wrote the manuscript and designed the figures. DS contributed to critical manuscript revision and supervision of data analysis. All authors discussed the results and commented on the manuscript.

CONFLICT OF INTEREST

Martin Holtkamp received speaker's honoraria and/or consultancy fees from Arvelle, Bial, Desitin, Eisai, GW Pharmaceuticals, UCB, and Zogenix within the last 3 years. The other authors declare no conflict of interest.

DECLARATION OF TRANSPARENCY AND SCIENTIFIC RIGOUR

This Declaration acknowledges that this paper adheres to the principles for transparent reporting and scientific rigour of preclinical research as stated in the *British Journal of Pharmacology* guidelines for [Design and Analysis](#) and [Animal Experimentation](#), and as recommended by funding agencies, publishers and other organisations engaged with supporting research.

DATA AVAILABILITY STATEMENT

The data that supports the findings of this study are also available from the corresponding author upon reasonable request.

ORCID

Laura Monni  <https://orcid.org/0000-0002-9513-6378>

Matthias Dipper-Wawra  <https://orcid.org/0000-0002-7311-1823>

Patrício Soares-da-Silva  <https://orcid.org/0000-0002-2446-5078>

Nikolaus Maier  <https://orcid.org/0000-0001-5203-0736>

Dietmar Schmitz  <https://orcid.org/0000-0003-2741-5241>

Martin Holtkamp  <https://orcid.org/0000-0003-2258-1670>

Pawel Fidzinski  <https://orcid.org/0000-0001-6373-4763>

REFERENCES

- Alexander, S. P., Mathie, A., Peters, J. A., Veale, E. L., Striessnig, J., Kelly, E., Armstrong, J. F., Faccenda, E., Harding, S. D., Pawson, A. J., Southan, C., Davies, J. A., Aldrich, R. W., Attali, B., Baggetta, A. M., Becirovic, E., Biel, M., Bill, R. M., Catterall, W. A., ... Zhu, M. (2021). The Concise Guide to PHARMACOLOGY 2021/22: Ion channels. *British Journal of Pharmacology*, 178(S1), S157–S245. <https://doi.org/10.1111/bph.15539>
- Almeida, L., Minciu, I., Nunes, T., Butoianu, N., Falcão, A., Magureanu, S.-A., & Soares-Da-Silva, P. (2008). Pharmacokinetics, efficacy, and tolerability of eslicarbazepine acetate in children and adolescents with epilepsy. *Journal of Clinical Pharmacology*, 48(8), 966–977. <https://doi.org/10.1177/0091270008319706>

- Alves, G., Figueiredo, I., Castel-Branco, M., Lourenço, N., Falcão, A., Caramona, M., & Soares-da-Silva, P. (2008). Disposition of eslicarbazepine acetate in the mouse after oral administration. *Fundamental & Clinical Pharmacology*, 22(5), 529–536. <https://doi.org/10.1111/j.1472-8206.2008.00617.x>
- Atallah, B. V., & Scanziani, M. (2009). Instantaneous modulation of gamma oscillation frequency by balancing excitation with inhibition. *Neuron*, 62(4), 566–577. <https://doi.org/10.1016/j.neuron.2009.04.027>
- Avoli, M., Psarropoulou, C., Tancredi, V., & Fueta, Y. (1993). On the synchronous activity induced by 4-aminopyridine in the CA3 subfield of juvenile rat hippocampus. *Journal of Neurophysiology*, 70(3), 1018–1029. <https://doi.org/10.1152/jn.1993.70.3.1018>
- Barker-Haliski, M., Löscher, W., Xiao, B., Brandt, C., Ravizza, T., Smolders, I., Xiao, B., Brandt, C., Löscher, W., & Harte-Hargrove, L. C. (2018). A companion to the preclinical common data elements for pharmacologic studies in animal models of seizures and epilepsy. A report of the TASK3 Pharmacology Working Group of the ILAE/AES Joint Translational Task Force. *Epilepsia Open*, 3, 53–68. <https://doi.org/10.1002/epi4.12254>
- Barton, M. E., Klein, B. D., Wolf, H. H., & White, H. S. (2001). Pharmacological characterization of the 6 Hz psychomotor seizure model of partial epilepsy. *Epilepsy Research*, 47(3), 217–227. [https://doi.org/10.1016/S0920-1211\(01\)00302-3](https://doi.org/10.1016/S0920-1211(01)00302-3)
- Beckonert, N. M., Opitz, T., Pitsch, X., da Silva, P. S., & Beck, H. (2018). Polyamine modulation of anticonvulsant drug response: A potential mechanism contributing to pharmacoresistance in chronic epilepsy. *Journal of Neuroscience*, 38(24), 5596–5605. <https://doi.org/10.1523/JNEUROSCI.0640-18.2018>
- Benes, J., Parada, A., Figueiredo, A. A., Alves, P. C., Freitas, A. P., Learmonth, D. A., Cunha, R. A., Garrett, J., & Soares-Da-Silva, P. (1999). Anticonvulsant and Sodium Channel-blocking properties of novel 10,11-dihydro-5H-dibenz[b,f]azepine-5-carboxamide derivatives. *Journal of Medicinal Chemistry*, 42(14), 2582–2587. <https://doi.org/10.1021/jm980627g>
- Ben-Menachem, E., Gabbai, A. A., Hufnagel, A., Maia, J., Almeida, L., & Soares-da-Silva, P. (2010). Eslicarbazepine acetate as adjunctive therapy in adult patients with partial epilepsy. *Epilepsy Research*, 89(2–3), 278–285. <https://doi.org/10.1016/j.eplepsyres.2010.01.014>
- Bokil, H., Andrews, P., Kulkarni, J. E., Mehta, S., & Mitra, P. P. (2010). Chronux: A platform for analyzing neural signals. *Journal of Neuroscience Methods*, 192(1), 146–151. <https://doi.org/10.1016/j.jneumeth.2010.06.020>
- Booker, S. A., Pires, N., Cobb, S., Soares-Da-Silva, P., & Vida, I. (2015). Carbamazepine and oxcarbazepine, but not eslicarbazepine, enhance excitatory synaptic transmission onto hippocampal CA1 pyramidal cells through an antagonistic action at adenosine A1 receptors. *Neuropharmacology*, 93, 103–115. <https://doi.org/10.1016/j.neuropharm.2015.01.019>
- Bragin, A., Jando, G., Nadasdy, Z., Hetke, J., Wise, K., & Buzsáki, G. (1995). Gamma (40–100 Hz) oscillation in the hippocampus of the behaving rat. *Journal of Neuroscience*, 15(11), 47–60. <https://doi.org/10.1523/jneurosci.15-01-00047.1995>
- Brown, D. A., & Adams, P. R. (1980). Muscarinic suppression of a novel voltage-sensitive K⁺ current in a vertebrate neurone. *Nature*, 283(5748), 673–676. <http://www.ncbi.nlm.nih.gov/pubmed/6965523>, <https://doi.org/10.1038/283673a0>
- Brown, D. A., & Passmore, G. M. (2009). REVIEW neural KCNQ (Kv7) channels. *British Journal of Pharmacology*, 156, 1185–1195. <https://doi.org/10.1111/j.1476-5381.2009.00111.x>
- Brown, W. C., Schiffman, D. O., Swinyard, E. A., & Goodman, L. S. (1953). Comparative assay of an antiepileptic drugs by psychomotor seizure test and minimal electroshock threshold test. *The Journal of Pharmacology and Experimental Therapeutics*, 107(3), 273–283. <http://www.ncbi.nlm.nih.gov/pubmed/13035666>
- Buhl, E. H., Tamás, G., & Fisahn, A. (1998). Cholinergic activation and tonic excitation induce persistent gamma oscillations in mouse somatosensory cortex in vitro. *Journal of Physiology*, 513(1), 117–126. <https://doi.org/10.1111/j.1469-7793.1998.117by.x>
- Buzsáki, G. (1986). Hippocampal sharp waves: Their origin and significance. *Brain Research*, 398(2), 242–252. [https://doi.org/10.1016/0006-8993\(86\)91483-6](https://doi.org/10.1016/0006-8993(86)91483-6)
- Buzsáki, G. (2015). Hippocampal sharp wave-ripple: A cognitive biomarker for episodic memory and planning. *Hippocampus*, 25(10), 1073–1188. <https://doi.org/10.1002/hipo.22488>
- Buzsáki, G., & Wang, X.-J. (2012). Mechanisms of gamma oscillations. *Annual Review of Neuroscience*, 35(1), 203–225. <https://doi.org/10.1146/annurev-neuro-062111-150444>
- Colgin, L. L., Denninger, T., Fyhn, M., Hafting, T., Bonnevie, T., Jensen, O., Moser, M.-B., & Moser, E. I. (2009). Frequency of gamma oscillations routes flow of information in the hippocampus. *Nature*, 462(7271), 353–357. <https://doi.org/10.1038/nature08573>
- Cooper, E. C., Harrington, E., Jan, Y. N., & Jan, L. Y. (2001). M channel KCNQ2 subunits are localized to key sites for control of neuronal network oscillations and synchronization in mouse brain. *Journal of Neuroscience*, 21(24), 9529–9540. <https://doi.org/10.1523/jneurosci.21-24-09529.2001>
- Csicsvari, J., Jamieson, B., Wise, K. D., & Buzsáki, G. (2003). Mechanisms of gamma oscillations in the hippocampus of the behaving rat. *Neuron*, 37(2), 311–322. [https://doi.org/10.1016/S0896-6273\(02\)01169-8](https://doi.org/10.1016/S0896-6273(02)01169-8)
- Curtis, M. J., Alexander, S., Cirino, G., Docherty, J. R., George, C. H., Giembycz, M. A., Hoyer, D., Insel, P. A., Izzo, A. A., Ji, Y., MacEwan, D. J., Sobey, C. G., Stanford, S. C., Teixeira, M. M., Wonnacott, S., & Ahluwalia, A. (2018). Experimental design and analysis and their reporting II: Updated and simplified guidance for authors and peer reviewers. *British Journal of Pharmacology*, 175, 987–993. John Wiley and Sons Inc. <https://doi.org/10.1111/bph.14153>
- Delmas, P., & Brown, D. A. (2005). Pathways modulating neural KCNQ/M (Kv7) potassium channels. *Nature Reviews*, 6, 850–862. <https://doi.org/10.1038/nrn1785>
- Devaux, J. J., Kleopa, K. A., Cooper, E. C., & Scherer, S. S. (2004). KCNQ2 is a nodal K⁺ channel. *Journal of Neuroscience*, 24(5), 1236–1244. <https://doi.org/10.1523/JNEUROSCI.4512-03.2004>
- Doerer, A., Dickhof, G., Reitze, M., Uebachs, M., Schaub, C., Pires, N. M., Bonifácio, M. J., Soares-da-Silva, P., & Beck, H. (2015). Targeting pharmacoresistant epilepsy and epileptogenesis with a dual-purpose antiepileptic drug. *Brain*, 138(2), 371–387. <https://doi.org/10.1093/brain/awu339>
- Dunham, N. W., & Miya, T. S. (1957). A note on a simple apparatus for detecting neurological deficit in rats and mice**College of Pharmacy, University of Nebraska, Lincoln 8. *Journal of the American Pharmaceutical Association (Scientific Ed.)*, 46(3), 208–209. <https://doi.org/10.1002/jps.3030460322>
- EC50 Calculator|AAT Bioquest. Retrieved November 24, 2020, from <https://www.aatbio.com/tools/ec50-calculator>
- Elger, C., Halász, P., Maia, J., Almeida, L., & Soares-Da-Silva, P. (2009). Efficacy and safety of eslicarbazepine acetate as adjunctive treatment in adults with refractory partial-onset seizures: A randomized, double-blind, placebo-controlled, parallel-group phase III study. *Epilepsia*, 50(3), 454–463. <https://doi.org/10.1111/j.1528-1167.2008.01946.x>
- EpilepsyDiagnosis.org. Retrieved April 28, 2021, from <https://www.epilepsydiagnosis.org/>
- Fidzinski, P., Korotkova, T., Heidenreich, M., Maier, N., Schuetze, S., Kobler, O., Zuschratter, W., Schmitz, D., Ponomarenko, A., & Jentsch, T. J. (2015). KCNQ5 K⁺ channels control hippocampal synaptic inhibition and fast network oscillations. *Nature Communications*, 6, 6254. <https://doi.org/10.1038/ncomms7254>
- Fiest, K. M., Sauro, K. M., Wiebe, S., Patten, S. B., Kwon, C. S., Dykeman, J., Pringsheim, T., Lorenzetti, D. L., & Jetté, N. (2017). Prevalence and incidence of epilepsy. *Neurology Lippincott Williams*

- and Wilkins, 88, 296–303. <https://doi.org/10.1212/WNL.0000000000003509>
- Finney, D. J. (1971). Probit analysis. *Journal of Pharmaceutical Sciences*, 60(9), 1432. <https://doi.org/10.1002/jps.2600600940>
- Fisahn, A., Pike, F. G., Buhl, E. H., & Paulsen, O. (1998). Cholinergic induction of network oscillations at 40 Hz in the hippocampus in vitro. *Nature*, 394(6689), 186–189. <https://doi.org/10.1038/28179>
- Freeman, W. J. (2007). Definitions of state variables and state space for brain-computer interface: Part 1. Multiple hierarchical levels of brain function. *Cognitive Neurodynamics*, 1(1), 3–14. <https://doi.org/10.1007/s11571-006-9001-x>
- Galiana, G. L., Gauthier, A. C., & Mattson, R. H. (2017). Eslicarbazepine acetate: A new improvement on a classic drug family for the treatment of partial-onset seizures. *Drugs in R&D* Springer International Publishing, 17, 329–339. <https://doi.org/10.1007/s40268-017-0197-5>
- Goto, A., Ishii, A., Shibata, M., Ihara, Y., Cooper, E. C., & Hirose, S. (2019). Characteristics of KCNQ2 variants causing either benign neonatal epilepsy or developmental and epileptic encephalopathy. *Epilepsia*, 60(9), 1870–1880. <https://doi.org/10.1111/epi.16314>
- Grinton, B. E., Heron, S. E., Pelekanos, J. T., Zuberi, S. M., Kivity, S., Afawi, Z., Williams, T. C., Casalaz, D. M., Yendle, S., Linder, I., Lev, D., Lerman-Sagie, T., Malone, S., Bassan, H., Goldberg-Stern, H., Stanley, T., Hayman, M., Calvert, S., Korczyn, A. D., ... Berkovic, S. F. (2015). Familial neonatal seizures in 36 families: Clinical and genetic features correlate with outcome. *Epilepsia*, 56(7), 1071–1080. <https://doi.org/10.1111/epi.13020>
- Haas, H. L., Schaerer, B., & Vosmansky, M. (1979). A simple perfusion chamber for the study of nervous tissue slices in vitro. *Journal of Neuroscience Methods*, 1(4), 323–325. [https://doi.org/10.1016/0165-0270\(79\)90021-9](https://doi.org/10.1016/0165-0270(79)90021-9)
- Halász, P., Cramer, J. A., Hodoba, D., Członkowska, A., Guekht, A., Maia, J., Elger, C., Almeida, L., Soares-da-Silva, P., & BIA-2093-301 Study Group. (2010). Long-term efficacy and safety of eslicarbazepine acetate: Results of a 1-year open-label extension study in partial-onset seizures in adults with epilepsy. *Epilepsia*, 51(10), 1963–1969. <https://doi.org/10.1111/j.1528-1167.2010.02660.x>
- Hebeisen, S., Pires, N., Loureiro, A. I., Bonifácio, M. J., Palma, N., Whyment, A., Spanswick, D., & Soares-Da-Silva, P. (2015). Eslicarbazepine and the enhancement of slow inactivation of voltage-gated sodium channels: A comparison with carbamazepine, oxcarbazepine and lacosamide. *Neuropharmacology*, 89, 122–135. <https://doi.org/10.1016/j.neuropharm.2014.09.008>
- Heuzeroth, H., Wawra, M., Fidzinski, P., Dag, R., & Holtkamp, M. (2019). The 4-aminopyridine model of acute seizures in vitro elucidates efficacy of new antiepileptic drugs. *Frontiers in Neuroscience*, 13(JUN), 1–12. <https://doi.org/10.3389/fnins.2019.00677>
- Hill, M. R. H., & Greenfield, S. A. (2011). The membrane chamber: A new type of in vitro recording chamber. *Journal of Neuroscience Methods*, 195(1), 15–23. <https://doi.org/10.1016/j.jneumeth.2010.10.024>
- Hirtz, D., Thurman, D. J., Gwinn-Hardy, K., Mohamed, M., Chaudhuri, A. R., & Zalutsky, R. (2007). How common are the “common” neurologic disorders? *Neurology*, 68(5), 326–337. <https://doi.org/10.1212/01.wnl.0000252807.38124.a3>
- Holtkamp, D., Opitz, T., Hebeisen, S., Soares-da-Silva, P., & Beck, H. (2018). Effects of eslicarbazepine on slow inactivation processes of sodium channels in dentate gyrus granule cells. *Epilepsia*, 59(8), 1492–1506. <https://doi.org/10.1111/epi.14504>
- Ihara, Y., Tomonoh, Y., Deshimaru, M., Zhang, B., Uchida, T., Ishii, A., & Hirose, S. (2016). Retigabine, a Kv7.2/Kv7.3-channel opener, attenuates drug-induced seizures in knock-in mice harboring Kcnq2 mutations. *PLoS ONE*, 11(2), e0150095. <https://doi.org/10.1371/journal.pone.0150095>
- Jentsch, T. J. (2000). Neuronal KCNQ potassium channels: Physiology and role in disease. *Nature Reviews Neuroscience*, 1(October), 21–30. <https://doi.org/10.1038/35036198>
- Jiang, X., & Kopp-Schneider, A. (2015). Statistical strategies for averaging EC50 from multiple dose–response experiments. *Archives of Toxicology*, 89(11), 2119–2127. <https://doi.org/10.1007/s00204-014-1350-3>
- Józwiak, S., Veggiotti, P., Moreira, J., Gama, H., Rocha, F., & Soares-da-Silva, P. (2018). Effects of adjunctive eslicarbazepine acetate on neurocognitive functioning in children with refractory focal-onset seizures. *Epilepsy and Behavior*, 81, 1–11. <https://doi.org/10.1016/j.yebeh.2018.01.029>
- Kato, M., Yamagata, T., Kubota, M., Arai, H., Yamashita, S., Nakagawa, T., Fujii, T., Sugai, K., Imai, K., Uster, T., Chitayat, D., Weiss, S., Kashii, H., Kusano, R., Matsumoto, A., Nakamura, K., Oyazato, Y., Maeno, M., Nishiyama, K., ... Saitsu, H. (2013). Clinical spectrum of early onset epileptic encephalopathies caused by KCNQ2 mutation. *Epilepsia*, 54(7), 1282–1287. <https://doi.org/10.1111/epi.12200>
- Kraus, L., Monni, L., Schneider, U. C., Onken, J., Spindler, P., Holtkamp, M., & Fidzinski, P. (2020). Preparation of acute human hippocampal slices for electrophysiological recordings. *Journal of Visualized Experiments*, 159, 61085. <https://doi.org/10.3791/61085>
- Kubota, D., Colgin, L. L., Casale, M., Brucher, F. A., & Lynch, G. (2003). Endogenous waves in hippocampal slices. *Journal of Neurophysiology*, 89(1), 81–89. <https://doi.org/10.1152/jn.00542.2002>
- Kuersten, M., Tacke, M., Gerstl, L., Hoelz, H., Stülpnagel, C. V., & Borggraefe, I. (2020). Antiepileptic therapy approaches in KCNQ2 related epilepsy: A systematic review. *European Journal of Medical Genetics* Elsevier Masson SAS, 10.1016/j.ejmg.2019.02.001 63, 103628.
- Leclercq, K., & Kaminski, R. M. (2015). Genetic background of mice strongly influences treatment resistance in the 6 Hz seizure model. *Epilepsia*, 56(2), 310–318. <https://doi.org/10.1111/epi.12893>
- Lilley, E., Stanford, S. C., Kendall, D. E., Alexander, S. P. H., Cirino, G., Docherty, J. R., George, C. H., Insel, P. A., Izzo, A. A., Ji, Y., Panettieri, R. A., Sobey, C. G., Stefanska, B., Stephens, G., Teixeira, M., & Ahluwalia, A. (2020). ARRIVE 2.0 and the British Journal of Pharmacology: Updated guidance for 2020. *British Journal of Pharmacology*, 177(16), 3611–3616. <https://doi.org/10.1111/BPH.15178>
- Lopantsev, V., & Avoli, M. (1998). Laminar organization of epileptiform discharges in the rat entorhinal cortex in vitro. *Journal of Physiology*, 509(3), 785–796. <https://doi.org/10.1111/j.1469-7793.1998.785bm.x>
- López-Rivera, J. A., Pérez-Palma, E., Symonds, J., Lindy, A. S., McKnight, D. A., Leu, C., Zuberi, S., Brunklaus, A., Møller, R. S., & Lal, D. (2020). A catalogue of new incidence estimates of monogenic neurodevelopmental disorders caused by de novo variants. *Brain*, 143, 1099–1105. <https://doi.org/10.1093/brain/awaa051>
- Losi, G., Marcon, I., Mariotti, L., Sessolo, M., Chiavegato, A., & Carnignoto, G. (2016). A brain slice experimental model to study the generation and the propagation of focally-induced epileptiform activity. *Journal of Neuroscience Methods*, 260, 125–131. <https://doi.org/10.1016/j.jneumeth.2015.04.001>
- Loureiro, A. I., Fernandes-Lopes, C., Wright, L. C., & Soares-da-Silva, P. (2011). Development and validation of an enantioselective liquid-chromatography/tandem mass spectrometry method for the separation and quantification of eslicarbazepine acetate, eslicarbazepine, R-licarbazepine and oxcarbazepine in human plasma. *Journal of Chromatography B: Analytical Technologies in the Biomedical and Life Sciences*, 879(25), 2611–2618. <https://doi.org/10.1016/j.jchromb.2011.07.019>
- Maier, N., & Kempter, R. (2017). Hippocampal sharp wave/ripple complexes—Physiology and mechanisms. *Cognitive neuroscience of memory consolidation*. Studies in neuroscience, psychology and behavioral

- economics (pp. 227–249). Springer. https://doi.org/10.1007/978-3-319-45066-7_14
- Maier, N., Morris, G., Johanning, F. W., & Schmitz, D. (2009). An approach for reliably investigating hippocampal sharpwave-ripples in vitro. *PLoS ONE*, 4(9), e6925. <https://doi.org/10.1371/journal.pone.0006925>
- Maier, N., Nimrich, V., & Draguhn, A. (2003). Cellular and network mechanisms underlying spontaneous sharp wave-ripple complexes in mouse hippocampal slices. *The Journal of Physiology*, 550(Pt 3), 873–887. <https://doi.org/10.1113/jphysiol.2003.044602>
- Miceli, F., Soldovieri, M. V., Ambrosino, P., Barrese, V., Migliore, M., Cilio, M. R., & Tagliatela, M. (2013). Genotype-phenotype correlations in neonatal epilepsies caused by mutations in the voltage sensor of K v 7.2 potassium channel subunits. *Proceedings of the National Academy of Sciences*, 110, 4386–4391. <https://doi.org/10.1073/pnas.1216867110>
- Milh, M., Roubertoux, P., Biba, N., Chavany, J., Spiga Ghata, A., Fulachier, C., Collins, S. C., Wagner, C., Roux, J. C., Yalcin, B., Félix, M. S., Molinari, F., Lenck-Santini, P. P., & Villard, L. (2020). A knock-in mouse model for KCNQ2-related epileptic encephalopathy displays spontaneous generalized seizures and cognitive impairment. *Epilepsia*, 61, (5), 868–878. <https://doi.org/10.1111/epi.16494>
- Millichap, J. J., Park, K. L., Tsuchida, T., Ben-Zeev, B., Carmant, L., Flamini, R., Joshi, N., Levisohn, P. M., Marsh, E., Nangia, S., Narayanan, V., Ortiz-Gonzalez, X. R., Patterson, M. C., Pearl, P. L., Porter, B., Ramsey, K., McGinnis, E. L., Tagliatela, M., Tracy, M., ... Cooper, E. C. (2016). KCNQ2 encephalopathy: Features, mutational hot spots, and ezogabine treatment of 11 patients. *Neurology: Genetics*, 2(5), e96. <https://doi.org/10.1212/NXG.0000000000000096>
- Mitra, P., & Bokil, H. (2008). *Observed Brain Dynamics*. Oxford University Press. <https://doi.org/10.1093/acprof:oso/9780195178081.001.0001>
- Mody, I., Lambert, J. D. C., & Heinemann, U. (1987). Low extracellular magnesium induces epileptiform activity and spreading depression in rat hippocampal slices. *Journal of Neurophysiology*, 57(3), 869–888. <https://doi.org/10.1152/jn.1987.57.3.869>
- Montgomery, S. M., & Buzsáki, G. (2007). Gamma oscillations dynamically couple hippocampal CA3 and CA1 regions during memory task performance. *Proceedings of the National Academy of Sciences of the United States of America*, 104(36), 14495–14500. <https://doi.org/10.1073/pnas.0701826104>
- Nappi, P., Miceli, F., Soldovieri, M. V., Ambrosino, P., Barrese, V., & Tagliatela, M. (2020). Epileptic channelopathies caused by neuronal Kv7 (KCNQ) channel dysfunction. *Pflügers Archiv / European Journal of Physiology* Springer, 472, 881–898. <https://doi.org/10.1007/s00424-020-02404-2>
- Ngugi, A. K., Bottomley, C., Kleinschmidt, I., Sander, J. W., & Newton, C. R. (2010). Estimation of the burden of active and life-time epilepsy: A meta-analytic approach. *Epilepsia*, 51(5), 883–890. <https://doi.org/10.1111/j.1528-1167.2009.02481.x>
- Otto, J. F., Singh, N. A., Dahle, E. J., Leppert, M. F., Pappas, C. M., Pruess, T. H., Wilcox, K. S., & White, H. S. (2009). Electroconvulsive seizure thresholds and kindling acquisition rates are altered in mouse models of human KCNQ2 and KCNQ3 mutations for benign familial neonatal convulsions. *Epilepsia*, 50(7), 1752–1759. <https://doi.org/10.1111/j.1528-1167.2009.02100.x>
- Papathodoropoulos, C., & Kostopoulos, G. (2002). Spontaneous, low frequency (~2–3 Hz) field activity generated in rat ventral hippocampal slices perfused with normal medium. *Brain Research Bulletin*, 57(2), 187–193. [https://doi.org/10.1016/S0361-9230\(01\)00738-9](https://doi.org/10.1016/S0361-9230(01)00738-9)
- Percie du Sert, N., Hurst, V., Ahluwalia, A., Alam, S., Avey, M. T., Baker, M., Browne, W. J., Clark, A., Cuthill, I. C., Dimagli, U., Emerson, M., Garner, P., Holgate, S. T., Howells, D. W., Karp, N. A., Lázic, S. E., Lidster, K., MacCallum, C. J., Macleod, M., ... Würbel, H. (2020). The ARRIVE guidelines 2.0: Updated guidelines for reporting animal research. *Experimental Physiology*, 105(9), 1459–1466. <https://doi.org/10.1113/EP088870>
- Perreault, P., & Avoli, M. (1992). 4-Aminopyridine-induced epileptiform activity and a GABA-mediated long-lasting depolarization in the rat hippocampus. *Journal of Neuroscience*, 12(1), 104–115. <https://doi.org/10.1523/jneurosci.12-01-00104.1992>
- Pisano, T., Numis, A. L., Heavin, S. B., Weckhuysen, S., Angriman, M., Suls, A., Podesta, B., Thibert, R. L., Shapiro, K. A., Guerrini, R., Scheffer, I. E., Marini, C., & Cilio, M. R. (2015). Early and effective treatment of KCNQ2 encephalopathy. *Epilepsia*, 56(5), 685–691. <https://doi.org/10.1111/epi.12984>
- Potschka, H., Soerensen, J., Pekcec, A., Loureiro, A., & Soares-da-Silva, P. (2014). Effect of eslicarbazepine acetate in the corneal kindling progression and the amygdala kindling model of temporal lobe epilepsy. *Epilepsy Research*, 108(2), 212–222. <https://doi.org/10.1016/j.eplepsyres.2013.11.017>
- Racine, R. J. (1972). Modification of seizure activity by electrical stimulation: II. Motor seizure. *Electroencephalography and Clinical Neurophysiology*, 32(3), 281–294. [https://doi.org/10.1016/0013-4694\(72\)90177-0](https://doi.org/10.1016/0013-4694(72)90177-0)
- Robbins, J., Passmore, G. M., Abogadie, F. C., Reilly, J. M., & Brown, D. A. (2013). Effects of KCNQ2 gene truncation on M-type Kv7 potassium currents. *PLoS ONE*, 8(8), 1–6. <https://doi.org/10.1371/journal.pone.0071809>
- Rocamora, R. (2015). A review of the efficacy and safety of eslicarbazepine acetate in the management of partial-onset seizures. *Therapeutic Advances in Neurological Disorders* SAGE Publications, 8, 178–186. <https://doi.org/10.1177/1756285615589711>
- Rudy, B. (1988). Diversity and ubiquity of K channels. *Neuroscience*, 25(3), 729–749. [https://doi.org/10.1016/0306-4522\(88\)90033-4](https://doi.org/10.1016/0306-4522(88)90033-4)
- Sands, T. T., Balestri, M., Bellini, G., Mulkey, S. B., Danhaive, O., Bakken, E. H., Tagliatela, M., Oldham, M. S., Vigeveno, F., Holmes, G. L., & Cilio, M. R. (2016). Rapid and safe response to low-dose carbamazepine in neonatal epilepsy. *Epilepsia*, 57(12), 2019–2030. <https://doi.org/10.1111/epi.13596>
- Scharfman, H. E., & MacLusky, N. J. (2006). The influence of gonadal hormones on neuronal excitability, seizures, and epilepsy in the female. *Epilepsia NIH Public Access*, 47, 1423–1440. <https://doi.org/10.1111/j.1528-1167.2006.00672.x>
- Schneider, J., Lewen, A., Ta, T. T., Galow, L. V., Isola, R., Papageorgiou, I. E., & Kann, O. (2015). A reliable model for gamma oscillations in hippocampal tissue. *Journal of Neuroscience Research*, 93(7), 1067–1078. <https://doi.org/10.1002/jnr.23590>
- Sierra-Paredes, G., Loureiro, A. I., Wright, L. C., Sierra-Marcuño, G., & Soares-da-Silva, P. (2014). Effects of eslicarbazepine acetate on acute and chronic latrunculin A-induced seizures and extracellular amino acid levels in the mouse hippocampus. *BMC Neuroscience*, 15(1), 134. <https://doi.org/10.1186/s12868-014-0134-2>
- Singh, N. A., Otto, J. F., Jill Dahle, E., Pappas, C., Leslie, J. D., Leslie, J. D., Vilaythong, A., Noebels, J. L., White, H. S., Wilcox, K. S., & Leppert, M. F. (2008). Mouse models of human KCNQ2 and KCNQ3 mutations for benign familial neonatal convulsions show seizures and neuronal plasticity without synaptic reorganization. *Journal of Physiology*, 586(14), 3405–3423. <https://doi.org/10.1113/jphysiol.2008.154971>
- Soares-da-Silva, P., Pires, N., Bonifácio, M. J., Loureiro, A. I., Palma, N., & Wright, L. C. (2015). Eslicarbazepine acetate for the treatment of focal epilepsy: An update on its proposed mechanisms of action. *Pharmacology Research & Perspectives*, 3(2), e00124. <https://doi.org/10.1002/prp2.124>
- Symonds, J. D., Zuberi, S. M., Stewart, K., McLellan, A., O'Regan, M., MacLeod, S., Jollands, A., Joss, S., Kirkpatrick, M., Brunklaus, A., Pilz, D. T., Shetty, J., Dorris, L., Abu-Arafeh, I., Andrew, J., Brink, P., Callaghan, M., Cruden, J., Diver, L. A., ... Wilson, M. (2019). Incidence and phenotypes of childhood-onset genetic epilepsies: A prospective population-based national cohort. *Brain: A Journal of Neurology*, 142(8), 2303–2318. <https://doi.org/10.1093/brain/awz195>

- Traynelis, S. F., & Dingledine, R. (1988). Potassium-induced spontaneous electrographic seizures in the rat hippocampal slice. *Journal of Neurophysiology*, 59(1), 259–276. <https://doi.org/10.1152/jn.1988.59.1.259>
- Trinka, E., Ben-Menachem, E., Kowacs, P. A., Elger, C., Keller, B., Löffler, K., Rocha, J. F., & Soares-da-Silva, P. (2018). Efficacy and safety of eslicarbazepine acetate versus controlled-release carbamazepine monotherapy in newly diagnosed epilepsy: A phase III double-blind, randomized, parallel-group, multicenter study. *Epilepsia*, 59(2), 479–491. <https://doi.org/10.1111/epi.13993>
- Trompoukis, G., Rigas, P., Leontiadis, L. J., & Papatheodoropoulos, C. (2020). Ih, GIRK, and KCNQ/Kv7 channels differently modulate sharp wave-ripples in the dorsal and ventral hippocampus. *Molecular and Cellular Neuroscience*, 107, 103531. <https://doi.org/10.1016/j.mcn.2020.103531>
- Vittinghoff, E., & McCulloch, C. E. (2007). Relaxing the rule of ten events per variable in logistic and cox regression. *American Journal of Epidemiology*, 165(6), 710–718. <https://doi.org/10.1093/aje/kwk052>
- Wang, H. S., Pan, Z., Shi, W., Brown, B. S., Wymore, R. S., Cohen, I. S., Dixon, J. E., & McKinnon, D. (1998). KCNQ2 and KCNQ3 potassium channel subunits: Molecular correlates of the M-channel. *Science*, 282(5395), 1890–1893. <https://doi.org/10.1126/science.282.5395.1890>
- Watanabe, H., Nagata, E., Kosakai, A., Nakamura, M., Yokoyama, M., Tanaka, K., & Sasai, H. (2000). Disruption of the epilepsy KCNQ2 gene results in neural hyperexcitability. *Journal of Neurochemistry*, 75(1), 28–33. <https://doi.org/10.1046/j.1471-4159.2000.0750028.x>
- Weckhuysen, S., Mandelstam, S., Suls, A., Audenaert, D., Deconinck, T., Claes, L. R. F., Deprez, L., Smets, K., Hristova, D., Yordanova, I., Jordanova, A., Ceulemans, B., Jansen, A., Hasaerts, D., Roelens, F., Lagae, L., Yendle, S., Stanley, T., Heron, S. E., ... De Jonghe, P. (2012). KCNQ2 encephalopathy: Emerging phenotype of a neonatal epileptic encephalopathy. *Annals of Neurology*, 71(1), 15–25. <https://doi.org/10.1002/ana.22644>
- Wheless, J. W., Fulton, S. P., & Mudigoudar, B. D. (2020). Dravet syndrome: A review of current management. *Pediatric Neurology Elsevier Inc*, 107, 28–40. <https://doi.org/10.1016/j.pediatrneurol.2020.01.005>
- Wójtowicz, A. M., van den Boom, L., Chakrabarty, A., Maggio, N., Haq, R. U., Behrens, C. J., & Heinemann, U. (2009). Monoamines block kainate- and carbachol-induced γ -oscillations but augment stimulus-induced γ -oscillations in rat hippocampus in vitro. *Hippocampus*, 19(3), 273–288. <https://doi.org/10.1002/hipo.20508>
- XEN496 (Ezogabine) in children with KCNQ2 developmental and epileptic encephalopathy—Full text view—ClinicalTrials.gov. Retrieved May 17, 2021, from <https://clinicaltrials.gov/ct2/show/study/NCT04639310>
- Zamadze, S., Bäuerle, P., Santos-Torres, J., Böhm, C., Schmitz, D., Geiger, J. R., Dugladze, T., & Gloveli, T. (2016). Cell-specific synaptic plasticity induced by network oscillations. *eLife*, 5(MAY2016), e14912. <https://doi.org/10.7554/eLife.14912>

SUPPORTING INFORMATION

Additional supporting information may be found in the online version of the article at the publisher's website.

How to cite this article: Monni, L., Kraus, L., Dipper-Wawra, M., Soares-da-Silva, P., Maier, N., Schmitz, D., Holtkamp, M., & Fidzinski, P. (2021). *In vitro* and *in vivo* anti-epileptic efficacy of eslicarbazepine acetate in a mouse model of KCNQ2-related self-limited epilepsy. *British Journal of Pharmacology*, 1–19. <https://doi.org/10.1111/bph.15689>

14. Curriculum Vitae

My curriculum vitae does not appear in the electronic version of my work for reasons of data protection.

15. Complete list of own publications

1. **Monni L.**, Kraus L., Dipper-Wawra M., Soares-da-Silva P., Maier N., Schmitz D., Holtkamp M., Fidzinski P. (2022). In vitro and in vivo antiepileptic efficacy of eslicarbazepine acetate in a mouse model of KCNQ2-related self-limited epilepsy. *British Journal of Pharmacology*, 179(1), 84–102. <https://doi.org/10.1111/BPH.15689> (first published online: 2021 Oct 4). Impact Factor 2021: 9.473.
2. Schlabit S., **Monni L.**, Ragot A., Dipper-Wawra M., Onken J., Holtkamp M., Fidzinski P., (2021). Spatiotemporal Correlation of Epileptiform Activity and Gene Expression in vitro. *Frontiers in molecular neuroscience*, 14, 643763. doi: 10.3389/fnmol.2021.643763. Impact Factor 2021: 6.261.
3. Kraus L., **Monni L.**, Schneider U.C., Onken J., Spindler P., Holtkamp M., Fidzinski P., (2020). Preparation of Acute Human Hippocampal Slices for Electrophysiological Recordings. *Journal of visualized experiments: JoVE*, (159). doi: 10.3791/61085. Impact Factor 2021: 1.424.
4. Ghezzi F., **Monni L.**, Nistri A., (2018). Functional up-regulation of the M-current by retigabine contrasts hyperexcitability and excitotoxicity on rat hypoglossal motoneurons. *The Journal of physiology*, 596(13), 2611–2629. doi: 10.1113/JP275906. Impact Factor 2021: 6.228.
5. Ghezzi F.*, **Monni L.***, Corsini S., Rauti R., Nistri A., (2017). Propofol protects rat hypoglossal motoneurons in an in vitro model of excitotoxicity by boosting GABAergic inhibition and reducing oxidative stress. *Neuroscience*, 367, 15–33. doi: 10.1016/j.neuroscience.2017.10.019. Impact Factor 2021: 3.708.
6. **Monni L.***, Ghezzi F.*, Corsini S., Nistri A., (2017). Neurotoxicity of propofol on rat hypoglossal motoneurons in vitro. *Neuroscience letters*, 655, 95–100. doi: 10.1016/j.neulet.2017.06.040. Impact Factor 2021: 3.197.

16. Acknowledgments

I would like to thank my supervisors, who gave me the opportunity to run this conceptually and technically very interesting project for my PhD work and experience. I would like to thank Martin (Holtkamp) for his constant positive support and for the opportunity to work in the epileptology group, giving me the chance also to get to know closer the clinical aspects of neurology.

A big thank to Pawel (Fidzinski), who has been simply an excellent supervisor for me. During these years, I really grew up also thanks to his support, giving me the chance to work independently but with the feeling of having always an eye on me. Thanks for always trusting me, but also for being there to teach me both theoretical concepts and lab tricks!

Thanks to Matthias (Dipper-Wawra) for his precious advices on statistics and IT help with Matlab.

I would like then to thank the people of the lab: Mandy, for the technical, bureaucratic and personal support to be able to even start doing my experiments! Thanks to Marie and Alice, who in the last year have been always there, thank you both for the laughs in the lab and outside, including our language tandem lessons! A big thank to my “at the beginning colleague” but by now one of my dearest friends, Larissa. Thanks for all our never-ending discussions, loud laughs and supporting sessions.

I deeply thank my family: mom, dad and my brother Seba, who are all my best friends and the main constant in my life. Everything becomes easier when I share it with you, maybe in front of a glass of good wine!

A huge thank to Daniele, who infinitely supports me in every aspect of life and helped me to discover and love this city as no one else could. Berlin immediately became Home with you and these years would not have been the same without you.

Last but not least, I thank all my Berlin-friends! Camila, another of my dearest friends known in this city. We grew up together here, sharing the same work and “life style”, in short: thanks for your constant presence and your positive attitude. I would like to thank every one of my friends who made and is making my life here full of familiar support, fun and love.